CONTROLLED RELEASE OF AN ANTIFOULING AGENT FROM MICROCAPSULES WITH ENHANCED MECHANICAL AND THERMAL PROPERTIES

by

Xiaotong Zhang

A thesis submitted to the University of Birmingham for the degree of

MASTER OF PHILOSOPHY

School of Chemical Engineering

The University of Birmingham

January 2020

UNIVERSITY OF
BIRMINGHAM

University of Birmingham Research Archive

e-theses repository

This unpublished thesis/dissertation is copyright of the author and/or third parties. The intellectual property rights of the author or third parties in respect of this work are as defined by The Copyright Designs and Patents Act 1988 or as modified by any successor legislation.

Any use made of information contained in this thesis/dissertation must be in accordance with that legislation and must be properly acknowledged. Further distribution or reproduction in any format is prohibited without the permission of the copyright holder.

ABSTRACT

It is well known that wind energy is abundant at sea so many offshore wind power generators have been installed and used. However, there are a few factors affecting the efficiency and reliability of wind turbines. Biofouling caused by a complex marine environment is one of the problems influencing the state of power generation systems in seawater. Therefore antifouling coatings have to be developed and applied to their surfaces. Microcapsules, which can be incorporated into certain coating materials, are an ideal micro-carrier of antifouling agent to achieve its sustained release. This project aimed to prepare microcapsules with an antifouling agent, which can have a high payload, be mechanically strong, have good thermal conductivity, and can achieve sustained release of the active ingredient. The long-term objectives are to achieve the long-term sustained release of the active ingredient in marine environment and antifouling performance, after the microcapsules are incorporated into marine coating that will then be applied to metal surfaces.

In this project, microcapsules consisting of N-Vanillylnonanamide (capsaicin synthetic) in the core, which is an antifouling agent, and cellulose acetate butyrate (CAB) as the shell material have been prepared by solvent evaporation method, based on oil in water (O/W) emulsification in a stirred tank. The effects of formulation and processing conditions on the morphology, size, mechanical properties, thermal properties of microcapsules, release rate of the active ingredient in model liquid have been investigated. The formulation and processing conditions included type of emulsifier, emulsifier concentration, agitation speed, core/shell ratio, metallic coating on the CAB microcapsules with capsaicin synthetic. A range of experimental techniques have been used to characterise the microcapsules, including optical microscopy, Scanning Electron Microscopy (SEM) with Energy Dispersive Spectroscopy

(EDS), Malvern particle sizing, micromanipulation, UV-VIS spectrophotometry and laser flash analysis.

It has been found that the prepared microcapsules had a matrix structure with multiple cores. Based on the experimental conditions and experimental results, using an emulsifier of polyvinyl alcohol (PVA) with concentration of 0.5%, and agitation speed of 1000 rpm to generate the O/W emulsion produced the microcapsules smaller than 60μm for potentially being incorporated into the coatings, an encapsulation efficiency and the payload reached 80.7% and 16.5%, respectively, which is desirable. As for the mechanical properties, the microcapsules showed elastic and plastic deformations under compression, but not rupture for the experimental conditions investigated due to their matrix structure. The Young's modulus value of microcapsules, calculated by the Hertz model, decreased significantly with increasing the ratio of core/shell material from 0 to 1/2, w/w, and were all in Mega Pascal scale, which are stiffer compared with many different microcapsules prepared by other researchers. Moreover, cyclohexane was used for accelerating the release of capsaicin synthetic from microcapsules and was found to enable to predict the release profile in water by considering the solubility of capsaicin synthetic in each liquid. Ritger-Peppas Model with $n = 0.43$ was demonstrated to describe the release kinetics of capsaicin synthetic from the microcapsules well, and it is concluded that the release from the matrix microcapsules was driven by Fickian diffusion.

In addition, metallic coating of the microcapsules on their surface were achieved successfully by electroless plating copper after generating a layer of polydopamine based on its self-polymerisation of dopamine. The microcapsules with copper were proved much stiffer than those without any metallic composition. The thermal conductivities were enhanced up to 7

times by incorporating copper and prolonging the time of both self-polymerising PDA and suspending microcapsules.

Thus, the microcapsules with an antifouling agent have been successfully prepared, which showed its sustained release over a few months. And the microcapsules with metal on their surface were prepared by electroless plating copper after generating a layer of polydopamine based on its self-polymerisation of dopamine, achieving the aim of enhancing thermal conductivity of the antifouling microcapsules.

ACKNOWLEDGEMENTS

Firstly I would like to express my deepest appreciation to my supervisors Prof. Zhibing Zhang and Prof. Jon Preece for their excellent supervisions, invaluable guidance, encouragement and endless patience and kindness to me, without whom I could not have done this project. During these years studying here, I learned a lot from my supervisors, not only the way of doing research but also many other transferable skills such as problem-solving skill, critical and logical thinking. Words could not express how thankful I am.

Then I would like to thank all other members of the Group of Micromanipulation and Microencapsulation. I am very thankful to Prof. Colin Thomas for his great guidance, to Dr. Fideline Tchuenbou-Magaia for her kind help and guidance in the early stage of my study and to Dr. Sen Liu for his excellent detailed trainings and generous help to me. I appreciate these very much. My gratitude also goes to Dr. Yan Zhang for his expertise, experience and insight into the research, which help me a lot, and for all his support as a good friend. And many thanks to other excellent and lovely colleagues formerly and currently in the group for their hands-on help: Jianfeng Hu, Mingming Du, Lei Xing, Bingyu Zhuo, Mariana Cardoso, Andrew Grey, Tom Simons, Hongdi Wang, Juliette Delarue, Gilmore Wellio, Daniele Baiocco, Abdullah Mustapha, Fanqianhui Yu, etc.

Besides I would like to thank the School of Chemical Engineering, University of Birmingham, for providing various administrative and technical supports and as well as Guangzhou Goaland Energy Conservation Tech Co., Ltd for the financial support.

Ultimately I would like to say thank you so much to my beloved family and friends. Even though they are living all over the world, they are always turning up anytime when I need

them and giving me endless supports no matter how many time zones there are between us. Without them, I could not have done the work, either.

I am very grateful to everyone I met, even though some are not acquainted for long time, it is all of them who enrich my life. Whether they bring me happiness or sadness, I would appreciate it as a gift of the life.

Table of Contents

LIST OF FIGURES

LIST OF TABLES

NOMENCLATURE

Symbols	Definitions	Units
A	Absorbance	[-]
b	Amount of burst release	mg
CAB	Cellulose acetate butyrate	
Com	Compliance of the force transducer	µm/mN
c	Concentration of the component in the solution	mg/mL
c_p	Molar heat capacity at constant pressure	J/(g·K)
D	Displacement of the transducer probe travelling downwards	µm
DSC	Differential Scanning Calorimetry	
E	Young's modulus	MPa
EDS	Energy Dispersive Spectroscopy	
e	Electron	
F	Force	mN
I	Intensity of light	[-]

LFA	Laser Flash Apparatus	
l	Thickness of sample for LFA	mm
M^0	Metal	
M^+	Metal ion	
M_t	Mass of the active ingredient released at t time	mg
M_∞	Initial mass of the active in the tablet	mg
n	Release exponent	
Ox	Oxidised product	
P	Bear load of obstacle	μN
PDA	Polydopamine	
PVA	Polyvinyl alcohol	
R	Radius of the microcapsule	μm
Red	Reducing agent	
SEM	Scanning Electron Microscopy	
Sen	Sensitivity of the specific transducer	mN/V
T	Temperature	℃

T_l	Transmittance of the light	
TRIS	Tris(hydroxymethyl)aminomethane	
t	Time	s
V	Voltage	V

Greek Symbols	Definitions	Units
a	Thermal diffusivity	mm^2/s
ϵ	Strain of the material	[-]
ε	Extinction coefficient	$L \cdot g^{-1} \cdot mm^{-1}$
Δ	Diametric compressive displacement	µm
δ	Deformation/displacement of the material	µm
ι	Path length of the light	mm
K	Release constant	[-]
k	The constant of stiffness	N/m
λ	Thermal conductivity	W/(m·K)
ρ	Density	g/cm^3
σ	Stress applied to the material	MPa
υ	Travelling speed of the probe	µm/s
ν	Poisson's ratio	[-]

CHAPTER 1 INTRODUCTION

1.1 Background

Nowadays wind power has become a significantly important energy to generate electricity and the development of it is growing fast. Wind power is an environmental-friendly, clean and reliable energy source, and it will not produce greenhouse gases and not cause air pollution (Barton and Infield, 2004; Kempton et al., 2005). The need of renewable sources has been increasing, among which wind power is more appealing compared with other energy sources (Barbier, 2002). The efficiency of utilizing wind power depends on the speed of wind (Barton and Infield, 2004). It is widely known that wind source is adequate at sea so there are many offshore wind power generators. Some countries have adopted policies in order to develop the offshore wind energy on a large scale (Bahaj, 2011). With sufficient wind source, wind power could cost less than other sources (Sherif et al., 2005). Thus, with a variety of benefits offshore wind power has enormous value and great potential.

However, there are a few factors affecting the efficiency and reliability of wind turbine. Biofouling caused by a complex marine environment is a problem influencing the state of power generation systems in seawater, which can be defined as the attachment and the undesirable accumulation of marine biological organisms on the surface of metal under seawater (Deng et al., 2016; Kochkodan and Hilal, 2015; Yebra et al., 2004). There are plenty of marine microorganisms floating freely in seawater, such as barnacles, ascidiacea, hydra and serpulidae, and they can attach on the surfaces of equipment and accumulate gradually (Huang and Peng, 2004; Zhou et al., 2011). Marine biofouling can cause the corrosion of metal, high consumption of energy, low heat transfer efficiency of the equipment in seawater and high cost of maintenance, which will affect the performance of the offshore power

generation systems. As the microorganisms can grow and relocate on the surface, it is necessary and important to reduce the effects of biofouling on the equipment. Therefore, antifouling coatings have to be developed and applied to their surfaces.

Coatings have been widely used to protect corrosion and fouling on steel surfaces, the bottoms of ships, marine power generators and marine platforms (Carteau et al., 2014; Gittens et al., 2013). Marine antifouling systems traditionally contained inorganic heavy metals such as copper and zinc compounds (Singh and Turner, 2009). Tributyltin was also introduced as a biocide into the antifouling coatings applied to marine area (Champ, 2000). Those antifouling agents are toxic and not environmental friendly, therefore it is necessary to develop non-toxic and natural active ingredient to be used in marine antifouling coatings. Currently on the market there are a few alternative antifouling coatings containing hybrid fluorine copolymer, silicone oils, hybrid and hydrogel silicone, etc (Dafforn et al., 2011; Li et al., 2014). As a natural antifouling alternative, capsaicin has been identified to be an effective antifouling and antiseptic agent (Turgud et al., 2004; Wang et al., 2014; Watts, 1995; Xu et al., 2013). Capsaicin is a natural active hydrophobic component extracted from chilli pepper, and capsaicin and its derivatives have strong pungency which can cause irritation to microorganisms (Shi and Wang, 2006). Unlike other antifouling agents which can contain heavy metal elements, it has been proved that capsaicin has a low environmental impact as an antifouling and antiseptic substance (Shi and Wang, 2006; Wang et al., 2014). Therefore, capsaicin incorporated in coatings can be used as an environmental-friendly antifouling agent in marine environment.

Nevertheless, coatings without antifouling and antiseptic effects have to be frequently applied to the surfaces exposed to seawater, which is not desirable due to high maintenance cost. In

order to address this challenge, an effective method may be to encapsulate capsaicin with a micro-carrier which can be incorporated into certain coating materials to achieve its sustained release. Consequently, the microcapsules containing capsaicin in coatings will deliver a long-term effective protection against biofouling for offshore energy generators. Currently, the release of the active ingredient can be achieved over a few days to a few weeks (Ma et al., 2012; Olsen et al., 2010; Weisman et al., 1992). However, this is still not long enough for the equipment in marine environment. It is more desirable to achieve sustained release over a few months or even years.

1.2 Objectives

The aim of this project is to prepare antifouling microcapsules containing capsaicin with enhanced thermal properties for potential applications in coatings to achieve its sustained release in marine environment, which can prevent the adhesion of the microbial organisms on the surface of equipment. The specific objectives are to encapsulate capsaicin in microcapsules with high payload, sufficient mechanical stability, sustainable release rate in water environment and high heat conductivity.

1.3 Thesis layout

Chapter 2 provides the basic knowledge of microencapsulation of antifouling agent. First of all, the antifouling agents including capsaicin are introduced. Secondly, the method of microencapsulation by solvent evaporation is reviewed. Thirdly, the electroless plating is reviewed, especially the self-polymerisation of dopamine which introduces amine onto the

microcapsule before electroless plating. Finally, the characterisation methods of microcapsules are reviewed, including the techniques to characterise mechanical properties, thermal properties of microcapsules and the release rate of active ingredient from them.

Chapter 3 reports materials and methods used to prepare antifouling microcapsules and the techniques used to characterise the microcapsules.

Chapter 4 describes the encapsulation of capsaicin using solvent evaporation with cellulose acetate butyrate (CAB) as the shell material. The formulation and processing conditions are detailed in this chapter. The effects of each parameter on the morphology, the size distribution, the encapsulation efficiency, the payload, mechanical properties and the release rate are investigated using various characterisation techniques.

Chapter 5 focuses on incorporating metallic compound into the microcapsules with enhanced thermal property. Firstly, aluminium oxide was added into the process of emulsification, the microcapsules containing aluminium oxide were obtained and characterised. Secondly, copper oxide was mixed with a suspension of the microcapsules and a commercial bonding material, and a spray dryer was used to achieve the microcapsules with metal coating. Finally, electroless plating of copper was chosen to introduce the metal onto the surface of microcapsules, and polydopamine (PDA) was used to modify the CAB capsules before plating copper on their surface. The microcapsules with copper on the surface were obtained and characterised.

Chapter 6 presents overall conclusions of the project and recommendations for future work.

CHAPTER 2 LITERATURE REVIEW

This project aims to prepare microcapsules with an antifouling agent, which can have a high payload, be mechanically strong, have good thermal conductivity, and can achieve sustained release of the active ingredient to prevent the adhesion of microbial organisms on the surface of equipment. In this chapter, the basic antifouling agents are described, as well as the principles and processes to encapsulate active ingredient by solvent evaporation. Moreover, different approaches to produce metallic coating of polymeric microcapsules using the electroless plating are reviewed, as well as the self-polymerisation of dopamine which can introduce amine onto the microcapsule to assist electroless plating. And the characterisation methods of microcapsules are reviewed, including the techniques to characterise the mechanical properties, thermal properties of microcapsules and the release rate of active ingredient from them.

2.1 Antifouling agent

Biofouling is a problem influencing the efficacy and lifetime of equipment in marine environments. It is a phenomenon of the attachment and the undesirable accumulation of marine biological organisms growing on the surface of substrate under seawater (Deng et al., 2016; Kochkodan and Hilal, 2015; Yebra et al., 2004). Marine biofouling can cause a series of problems to the equipment working in seawater, including the corrosion of metal, high consumption of energy, low efficiency of the equipment in seawater and high cost of maintenance, all of which will affect the performance of the offshore systems. As the microorganisms can grow and relocate on their surface, it is extremely important to reduce the

effects of biofouling. In order to prevent these negative effects on the systems, antifouling coatings have to be developed and applied to their surfaces.

Coatings have been widely used to protect corrosion and prevent fouling on steel surfaces, the bottoms of ships, marine power generators and marine platforms (Carteau et al., 2014; Gittens et al., 2013). Traditionally inorganic heavy metals such as copper and zinc compounds were incorporated into marine antifouling coatings, as well as organic compounds such as tributyltin (TBT) which has been banned by some countries in the last century (Champ, 2000; Singh and Turner, 2009). Those antifouling agents are toxic and not environmental friendly, therefore it is necessary to develop non-toxic and natural active ingredient to be used in marine antifouling coatings. Capsaicin, a natural antifouling alternative, has been identified to be an effective antifouling agent (Wang et al., 2014; Watts, 1995; Xu et al., 2013).

Capsaicin is a natural active hydrophobic component extracted from chilli pepper, and capsaicin and its derivatives have strong pungency which have antimicrobial properties (Cichewicz and Thorpe, 1996). Scoville Scale is a measurement of the pungent degree of chilli peppers (Scoville, 1912), and the Scoville Heat Unit (SHU) of pure capsaicin is 16.1 million while SHU of sweet chilli is 0 and the blistering habaneros and bird's eye chilli are between 100,000–300,000 SHU (Berke and Shieh, 2012). N-vanillylnonanamide is a synthetic analogue of capsaicin, which has the similar bioactivity but lower price in commercial compared with the extracted and purified capsaicin from nature. In addition, the toxicity of capsaicin has been tested in a few animals, and the experiments showed neither death nor obvious effects of sub-chronic doses on their behaviours and physiology (Berke and Shieh, 2012). So when capsaicin is added in the antifouling coatings in marine, it will only expel the microorganisms away from the equipment rather than killing them (Shi and Wang,

2006). Thus, n-vanillylnonanamide could be used as an environmental-friendly antifouling agent against the marine biofouling.

2.2 Microencapsulation by solvent evaporation

2.2.1 Microcapsules

Microencapsulation is a process of enclosing solids, liquids or gases by a continuous wall of material (e.g. polymer) to generate microcapsules with the size ranging from 1μm to 1000μm for a variety of applications in wide fields (Jamekhorshid et al., 2014; Lam and Gambari, 2014; Rathore et al., 2013). Microcapsules can provide a better barrier between the entrapped ingredient with desirable properties and the external surroundings to realise its protection and controlled or sustained delivery from the microcapsules (Bile et al., 2015). The ingredient with the desirable properties is called active or core material, and the carrier to protect the core material is shell material accordingly (Jyothi et al., 2010). Generally, the preparation method and the properties of the shell materials determine the morphology of the microcapsules (Bakry et al., 2016). Fig 2.1 shows a few common types of the morphologies of microcapsules. The microcapsules with mononuclear structure could be broken by pressure so that the active ingredient is released from the core, while those with polynuclear or matrix structure contain the active not only dispersed in the carrier but also on their surfaces (Zuidam and Shimoni, 2010).

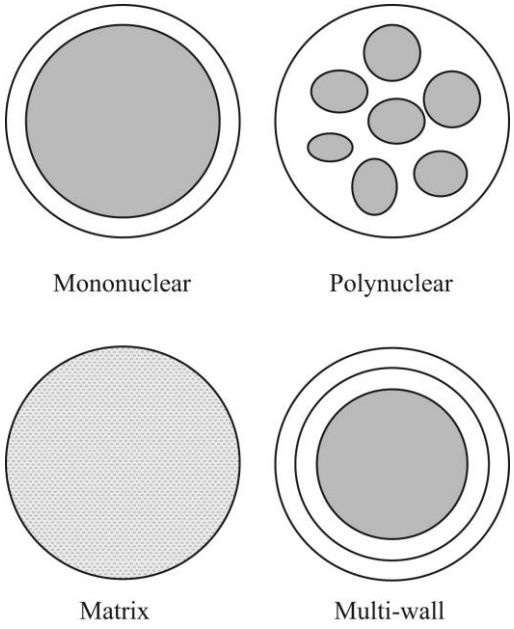

Fig 2.1 The morphologies of microcapsules (Jamekhorshid et al., 2014)

2.2.2 Shell materials

As the carrier and the protector of the core material, the shell material is an important barrier isolating the core from the outer surroundings. There are a large variety of materials that can be used as the shell materials depending on the nature of core materials and the functionalities of the microcapsules. Due to its cheap cost, polymer is commonly used as the shell material, which could be divided into natural polymer such as chitosan and gelatine, synthetic biodegradable polymer such as PLA and PLGA and the acrylic polymer like Eudragit and others (Miladi et al., 2014).

Cellulose acetate butyrate (CAB), one of the derivatives of cellulose ester, is a thermoplastic polymer with excellent properties, such as low toxicity, high stability, forming membrane with enough strength, high compatibility with a large number of the actives and the ability to

form micro-particles (Fundueanu et al., 2005; Wang et al., 2011a). It is well known that cellulose esters are degradable thermally and by hydrolysis in specific environments, which is related to the pH, the temperature and the degrading solution (Badmeier and Chen, 1993; Collins et al., 2017; Xing et al., 2013). CAB is a brittle and transparent material that can be used as a plasticiser for some materials (Tachibana et al., 2010). It can act as a barrier protecting the core materials against erosion in the surroundings with elevated temperature or acid, and enzymatic inactivation of the sensitive ingredients (Wallick, 2014). With these outstanding properties, CAB has become a widely used shell material of microcapsules.

2.2.3 Preparation of microcapsules by solvent evaporation

There are a large number of methods preparing microcapsules, basically they could be divided into three main categories: chemical methods, physico-chemical methods and physical methods (Jamekhorshid et al., 2014). For example, interfacial polymerisation is one of the chemical methods. The hydrophilic and lipophilic monomers polymerise at the interface of the oil in water emulsion with the help of emulsifier (Jamekhorshid et al., 2014). Besides, coacervation is one of the physico-chemical methods, the principle of which is phase separation. The two oppositely charged colloids, one of which is full of polymer, interact and form the coatings around the oil droplets by adjusting pH and reducing the temperature (Kaushik et al., 2015). In addition, spray drying is one of the physical methods. A dispersion of core and shell materials in a solvent is sprayed into a hot chamber, and the shell material is solidified to form microcapsules due to the rapid evaporation of the solvent (Lam and Gambari, 2014). Table 2.1 summarises typical microencapsulation methods.

Table 2.1 Summary of typical microencapsulation methods (Lam and Gambari, 2014)

Category	Microencapsulation method	Particle size (μm)	Stability	Advantages	Disadvantages	Examples
Chemical	Interfacial polymerization	0.5–1000 [91]	Based on the types of polymeric wall materials used [92]	• High drug encapsulation efficiency [93]	• Difficult to control polymerization reactions, loss of water soluble drugs caused by exhaustive washing steps [92]; • More side effects after drug administration due to an involvement of nonbiodegradable wall materials or residual solvents [19]	• Dimethyl-dodecyl-(5-hydroxy-pentyl)-ammonium bromide (antibacterial agent) grafted polyurea microcapsules for topical delivery [94] • Insulin (core drug, peptide) loaded poly(methacrylic acid)/poly(ethylene glycol) microparticles for oral delivery [80–82,95]
	Free radical polymerization	–				
Physico-chemical	Coacervation (phase separation)	2–1200 [91]	An addition of non-solvent forms stable coacervates without causing agglomeration [96]	• Simple and cheap method for drug encapsulation[16]; • High drug encapsulation efficiency and efficient control of the particle size with a narrower size distribution [92]	• Aggregation of microspheres and hard scaling-up for mass production [97]	• Insulin (core drug, peptide) loaded mucin/sodium alginate (wall) microcapsules for oral delivery [98] • Hydrocortisone succinate acid (core drug, steroid hormone)/5-fluorouracil (core drug, anticancer agent)/phyllanthin (core drug, plant bioactive) loaded chitosan (wall) microcapsules for oral and topical deliveries [12,14] • Fucoxanthin (core drug, xanthophyll) loaded fish gelatin–gum arabic (wall) for oral delivery [99]
	Ionotropic gelation	–	Low mechanical strength due to permeable hydrogel membrane of microspheres [92]	• No requirement of organic solvents or elevated temperatures; • Prevention of liable drug damages such as proteins; • Simple, fast and cost-effective method [92]	• Relatively fast release of drug due to the low mechanical strength [92]	• Curcumin-phytosome (core drug, plant bioactive) loaded chitosan (wall) microspheres for oral delivery [100] • Egg yolk immunoglobulin (core drug, antibody) loaded chitosan/alginate (wall) microcapsules for oral delivery [101] • Insulin (core drug, peptide) loaded chitosan/alginate microcapsules for oral delivery [102,103]
Mechanical	Fluid bed coating	20–1500 [91]	Based on the thickness of the coating layers [78,91]	• Total control over the drying temperature; • Lower operation cost [104]	• Relatively longer duration (up to 2 h) involved in the drying process [104]; • Agglomeration/sticking of particles during coating [105]	• Berberine HCl (core drug) loaded hydroxypropyl–methylcellulose microparticles coated with Eudragit E100 (wall) for oral delivery [68] • Diclofenac sodium (core drug, anti-inflammatory agent) loaded Eudragit RS30D (wall) microcapsules for oral delivery [106]
	Solvent evaporation/extraction	0.5–1000 [91]	Microcapsules prepared with solvent extraction result in higher porosities than those produced by solvent evaporation [85]	• Useful method for the delivery of small drug molecules [92]	• Low drug encapsulation efficiency and high cost [92]; • More side effects after drug administration due to an involvement of non biodegradable wall materials or residual solvents [94]	• Cidofovir (core drug, antiviral agent) loaded poly(lactide-co-glycolide) (PLGA) microcapsules for topical delivery [107] • Human recombinant insulin (core drug, peptide) loaded poly(D,L-lactide-co-glycolide) (PLGA) (wall) microcapsules for topical delivery [108] • Carvedilol (core drug, antihypertensive agent) loaded Ordered mesoporous carbon (wall) microparticles for oral delivery [109]
	Spray drying	5–5000 [91]	High stability [110]	• Low operation cost, good stability and retention, and easy scaling-up for mass production [110,111]; • No limitation of polymer choices, high encapsulation efficiency, time-efficiency, useful for heat-sensitive drug entrapment such as proteins or peptides due to an involvement of mild temperatures [112]	• Particle agglomerations and larger sized microcapsules [91]; • Loss of input materials, change of polymorphism of spray-dried drugs, and limited amount of polymer and drugs being encapsulated [92]; • No uniform microcapsules [110]	• Cidofovir (core drug, antiviral agent) loaded poly(lactide-co-glycolide) (PLGA) microcapsules for topical delivery [107] • Ibuprofen (core drug, anti-inflammatory agent) loaded gelatin (wall) microcapsules for oral delivery [113] • Soft mannitol/lecithin agglomerates containing pantoprazole (core drug, proton-pump inhibitor) loaded Eudragit S100 (wall) microparticles for oral delivery [114]

Solvent evaporation is another physical method preparing microcapsules utilising the solubility change of the solvent. It has been applied widely with a lot of advantages including low cost, availability to encapsulate liquid or solid materials which could be soluble or insoluble (Jamekhorshid et al., 2014). It does not require elevated temperature, pH adjustment or phase separation (Freitas et al., 2005). Therefore, solvent evaporation is a mild method preparing microcapsules.

In general, the solvent evaporation method consists of four steps: (1) dispersion of the oil phase as the dispersed phase containing solvent, core and shell materials; (2) emulsification of the oil phase in the aqueous phase as the continuous phase; (3) evaporation or extraction of the solvent to transform the droplets into solid microcapsules; (4) harvest of the microcapsules (Freitas et al., 2005). In the stage (2) of the emulsification, the oil droplets

containing polymer are broken up by the hydrodynamic force produced by agitation, mainly determining the size distribution of the microcapsules (Rosca et al., 2004). The stage (3) of the solvent evaporation or extraction is the most important process during the preparation, which determines the morphology and the encapsulation efficiency, influencing the active release behaviour (Rosca et al., 2004). Raising the temperature and continuously adding aqueous phase solution are needed for promoting the removal of the solvent, which could cause the matrix structure with pores inside the microcapsules (Yang et al., 2000). In addition, the shrinkage of the microcapsules could occur in this stage due to the high volatility of the solvent, the rapid precipitation of the polymer and the incompressibility of the inner droplets (Rosca et al., 2004). Apart from these, there are many factors in this stage influencing the encapsulation, such as the solubility of the solvent in water, the rate of solvent removal and the temperature gradient of the solvent removal (Jeyanthi et al., 1996; Jyothi et al., 2010). In the stage (4) of the harvest and drying, the microcapsules are washed, filtrated and dried, not only removing the non-encapsulated ingredient, the continuous phase liquid and the trace of the solvent on the surfaces of microcapsules but also the liquid from the interior of the microcapsules (Freitas et al., 2005). The basic scheme of the solvent evaporation method is presented in Fig 2.2.

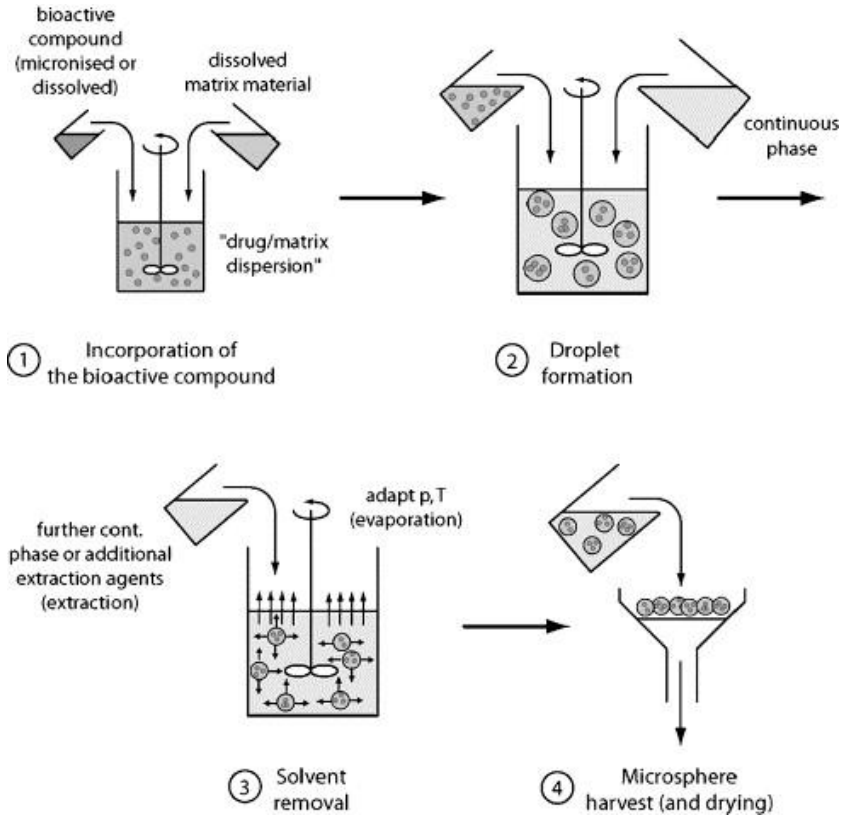

Fig 2.2 Basic scheme of the solvent evaporation method preparing microcapsules (Freitas et al., 2005)

2.3 Electroless plating

It is desirable to incorporate the antifouling microcapsules with enhanced thermal property into the marine coatings, and metal is a good candidate to promote their thermal properties due to its high thermal conductivity. Electroless plating is an effective method to deposit metal on the surface of substance. With the help of polydopamine, the electroless plating may be achievable (Al-Shannaq et al., 2016). In this section, previous methods to achieve self-polymerisation of dopamine and electroless plating are reviewed.

2.3.1 Self-polymerisation of dopamine

Mussels are able to attach to the wet surfaces in marine environment easily and strongly, which has been contributed by 3,4-dihydroxy-L-phenylalanine (DOPA) and lysine amino acids near the plaque-substrate interface (Lee et al., 2007; Liu et al., 2014). Inspired by mussels, polydopamine (PDA), with a similar structure to DOPA, has been found to be able to form on almost all types of organic and inorganic materials due to its adhesive versatility (Lee et al., 2007). In addition, the PDA coating on the substances has been found as a secondary platform for further surface modification by not only polymers but also metals (Lee et al., 2007). It has been reported that microspheres with a layer of PDA could have metal deposited on them by electroless plating (Al-Shannaq et al., 2016; Wang et al., 2011b; Wu et al., 2015). With the help of the rich amount of active catechol and amine groups in its molecular structure, PDA plays a role of binding reagents for various secondary reactions, resulting in a large variety of materials with multi-functional features (Wu et al., 2015).

There are several methods producing PDA. The most well-known method is the solution oxidation method primarily introduced by Lee et al. (2007). Typically dopamine hydrochloride, available commercially, is used in the reaction (Liu et al., 2014). The monomer dopamine is dissolved in 10mM TRIS buffer solution with the concentration of 2mg/mL at pH 8.5, which is a typical marine environment (Lee et al., 2007). The substrate is then simply immersed in the solution, leading to an oxidised deposition of adhesive polymeric layer spontaneously on the substrate. The scheme is shown in Fig 2.3(a). It is also available to polymerise dopamine by the enzymatic oxidation method. The substrate is dispersed in 0.05mol/L acetate buffer solution of pH 6.0 and under vigorous sonication, and successively added by 20mmol/L dopamine and 1mg/mL laccase (Lac), resulting in the entrapment of Lac

in the PDA matrix on the substrate with enzymatic property (Tan et al., 2010). The brief scheme is shown in Fig 2.3(b). Alternatively, polydopamine can be produced by an electropolymerisation method. The PDA could be prepared by performing cyclic voltammetry (−0.5V to 0.5 V) in the 10mmol/L phosphate buffer solution of pH 7.4 containing 5mmol/L dopamine and 5mmol/L nicotine deoxygenated by bubbling with pure N_2 (Liu et al., 2006).

So far the formation of PDA and its mechanism are not fully clear, and there are a few main hypotheses implying the possible pathway of its self-polymerisation. In the early stage, it was believed that the pathway of dopamine polymerisation was similar to the synthesis of melanin (Bernsmann et al., 2011). In contrast to the melanin model, another model of polydopamine was proposed as a supramolecular aggregate of monomers instead of a covalent polymer (Dreyer et al., 2012). Beside these models, it was also proposed that the formation of PDA was a combination of two pathways: covalent bond-forming oxidative polymerisation and physical self-assembly of dopamine and its oxidative product 5,6-dihydroxyindole (DHI) (Hong et al., 2012). Moreover, another model was suggested as a combination of three possible pathways: dimerisation of dopamine, cyclisation to DHI and mixed coupling of the reactions, and the structure of PDA could change with the conditions of preparation (Della Vecchia et al., 2013; Liu et al., 2014).

Despite the pathway of dopamine polymerisation, there are a lot of factors influencing the formation and the thickness of PDA on the substrate. It has been found that the maximum thickness of PDA increases constantly as the concentration of dopamine in TRIS solution increases from 0.1g/L to 5g/L (Ball et al., 2012). Higher temperature, rising from 25℃ to 60℃, also showed a significant positive effect on the deposition of PDA (Zhou et al., 2014). The type of the oxidant may also affect the formation and the thickness, and dopamine could

have a covalent incorporation of the TRIS buffer solution (Bernsmann et al., 2011; Della Vecchia et al., 2013). Besides, the value of pH could affect the deposition of PDA, the thickness of PDA film increased significantly as the pH value rose from 5.0 to 8.5, and when the pH went up to 10.2 the thickness did not change much (Ball et al., 2012). In addition, the vigorous stirring during the preparation resulted in speeding up the rate of PDA deposition compared with static or shake methods (Zhou et al., 2014).

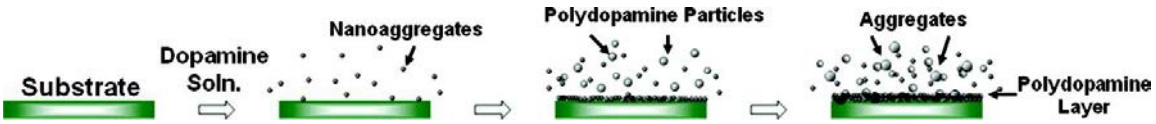

(a) Scheme of self-oxidised polymerisation of dopamine on the substrate (Jiang et al., 2011)

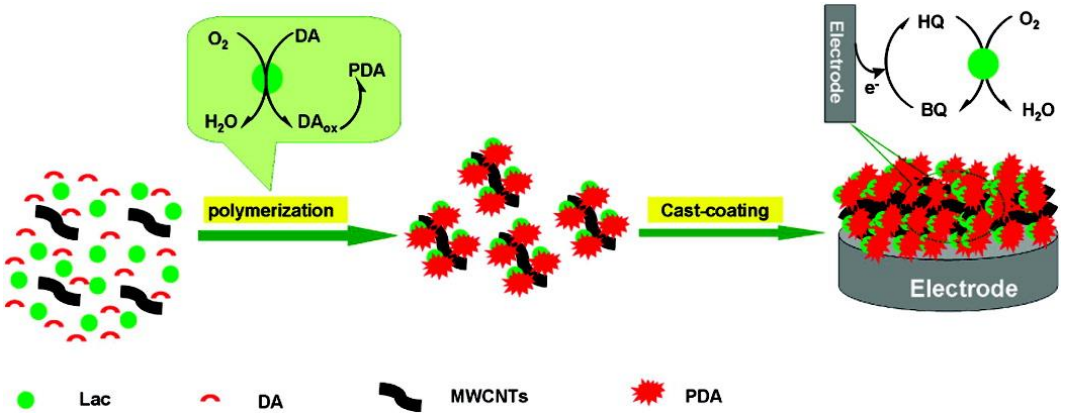

(b) Scheme of Lac-catalysed polydopamine (PDA) on multiwalled carbon nanotubes (MWCNTs) and then deposited on a glassy carbon electrode (Tan et al., 2010)

Fig 2.3 Scheme of two methods of polymerisation of dopamine

2.3.2 Electroless plating of copper

Electroless plating is an autocatalytic process of oxidation-reduction (redox) reaction where the metal ions are reduced chemically on the surface of the inorganic or organic substrates without an external current supplying the electrons (Gudeczaukas, 2007; Kind et al., 1998). The basic reactions are shown as Equation (2.1), and they involve (a) reduction reaction and (b) oxidation reaction in electroless plating. The scheme of the electroless plating is shown in Fig 2.4.

$$M^+ + \text{Red} \rightarrow M^0 + \text{Ox} \quad (2.1)$$

$$\text{Reduction: } M^+ + e \rightarrow M^0 \quad (2.1a)$$

$$\text{Oxidation: } \text{Re} + H_2O \rightarrow \text{Ox} + H^+ + e \quad (2.1b)$$

where M^+ is metal ion, "Red" represents reducing agent, M^0 is metal, Ox represents oxidised product and e is electron.

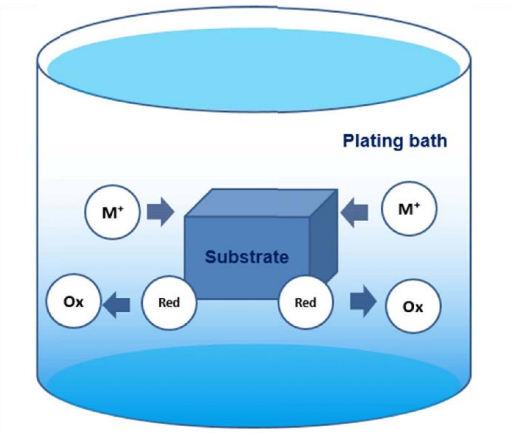

Fig 2.4 Scheme of the electroless plating, where M^+ is the metal ion, "Red" represents the reducing agent and "Ox" represents the oxidised product (Sharma et al., 2016)

Electroless plating has been developed for more than a hundred years and considered an elegant way to deposit metals on the substrates (Sharma et al., 2016; Sharma et al., 2006). Compared with other methods of metal coating, the electroless plating has been utilised most widely because it could be realised simply, fast and suitable for mass production (Mondin et al., 2013). However, it is difficult for metal to be directly deposited on the surface of substrates, therefore a pre-treatment is needed for sensitisation and activation of the electroless plating of metal (Xu et al., 2004). In general, there are two approaches for the nucleation of metals on the surface of the substrates. One is two-step method consisting of sensitisation in $SnCl_2$/HCl solution and activation in Pd^{2+} solution. The mechanism is that the colloid is formed because of the air oxidation and hydrolysis of Sn^{2+} in the solution and then the substrates are washed by water resulting in the rapid change of pH so that $SnCl_2$ precipitates on the surfaces of substrates (Wei and Roper, 2014). Afterwards, the solid $SnCl_2$ reacts with Pd^{2+} in the solution so that it reduces Pd^{2+} to Pd^0 and enhances the absorption of Pd^0 binding to the surfaces (Ang et al., 2000). The other method is one-step activation in a mixed Sn^{2+}-Pd^{2+} solution, which combines the two steps above. The substrate is immersed in the Sn^{2+}-Pd^{2+} solution with the large excess of Sn^{2+} so that Pd^0 is produced and surrounded by Sn^{4+} in the solution, where Sn^{2+} is the reducing agent for Pd^{2+} and Sn^{4+} is the nucleus absorbing Pd^0 growing around it (Cui et al., 2011). The overall reaction of the two methods can be described as Equation (2.2) below, and the schemes of them are shown in Fig 2.5. After the sensitisation and activation, electroless plating of metal takes place with Pd^0 as the catalyst involving the highly complex redox reactions (Kind et al., 1998).

$$Sn^{2+}(s) + Pd^{2+}(aq) \rightarrow Sn^{4+}(s) + Pd^{0}(s) \quad (2.2)$$

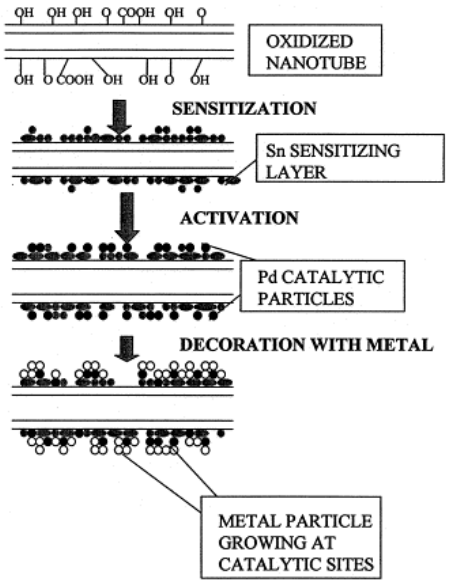

(a) Two-step method of Sn^{2+} sensitisation and Pd^{2+} activation

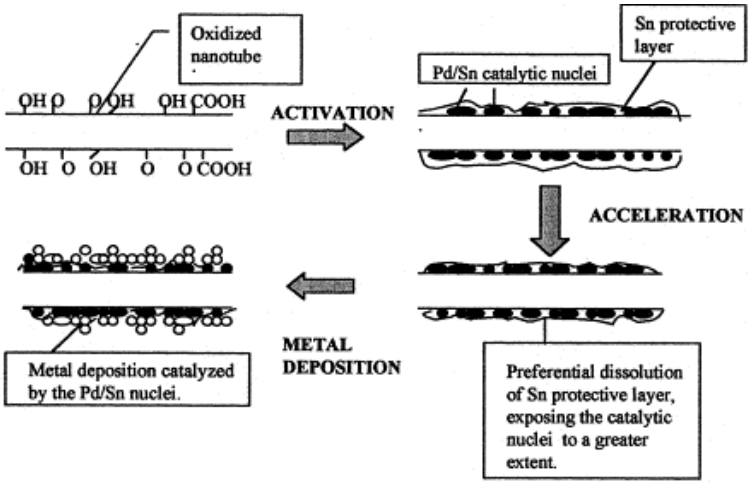

(b) One-step method of Sn^{2+}-Pd^{2+} activation

Fig 2.5 Schemes of two methods pre-treating the electroless plating (Ang et al., 2000)

The aim of the sensitisation and activation is to provide catalytic nuclei (Pd^0 or Pd-Sn alloy) growing on the substrates for the metal ions subsequently depositing on their surfaces by electroless plating (Ang et al., 2000; Xu et al., 2004). Even though there are a number of factors influencing the process of electroless plating, the process of activation is one of the key factors controlling the deposition of metal ions, and it is Pd^0 that can catalyse the electroless reaction instead of Pd^{2+} (Kind et al., 1998; Lee et al., 2003). However, the processes of sensitisation and activation are complicated and $SnCl_2$ is not considered to be environmental-friendly (Xu et al., 2004). Therefore, polydopamine (PDA) has been introduced to eliminate the disadvantages of the sensitisation before the electroless plating of metal due to the amino groups on its molecule reacting with Pd^{2+} (Kind et al., 1998).

Apart from the sensitisation and activation, the composition of the electroless bath is another important factor influencing the process of electroless plating (Sharma et al., 2006). Basically, there are five elements of the metallic bath for electroless plating (Bengston, 2005). A solution of salt is the source providing the metallic ions depositing on the substrate, which could be $NiSO_4$, $CuSO_4$, $FeSO_4$, etc (Dinderman et al., 2006; Mondin et al., 2013; Tsuneyoshi and Ono, 2017). The reducing agent, traditionally and typically formaldehyde in alkaline environment, plays the most important role in electroless plating, reducing the ions to the metal atoms (Sharma et al., 2016). The complexing agent, traditionally EDTA or tartrates, is for preventing the metallic ions from transforming into metallic hydroxides in the alkaline bath, and also stabilising and increasing the life of the bath (Bengston, 2005; Sharma et al., 2016). The stabiliser and the buffering solution can prevent the spontaneous decomposition of the bath and the reduction of metallic ions into atoms, and stabilise the pH of the bath such as NaOH (Bengston, 2005; Sharma et al., 2016). Beside these compositions, other variables such

as temperature and pH also play important roles in the process of electroless plating (Sharma et al., 2006).

The electroless plating can be applied on a variety of materials including plastics, ceramics and non-conducting substrates by deposition of copper, nickel, cobalt, palladium, platinum, gold, silver, etc (Kind et al., 1998; Sharma et al., 2006). Among these metals, copper is considered as an ideal metal for electroless plating due to its electrical conductivity, thermal conductivity and cost effectiveness (Sharma et al., 2006). So electroless plating of copper has been extensively used in many research areas and industries (Sharma et al., 2016). The electrochemical mechanisms of each component in the bath are complicated, and the overall reaction of electroless plating with formaldehyde as the reducing agent in an alkaline Cu^{2+} bath can be shown below (Shacham-Diamand and Dubin, 1997).

$$Cu^{2+} + 2HCHO + 4OH^{-} \rightarrow Cu^{0} + 2HCOO^{-} + 2H_2O + H_2 \quad (2.3)$$

2.4 Characterisation of microcapsules

The characterisations of microcapsules involve the morphology, the shell thickness, the size and size distribution, the encapsulation efficiency, the mechanical properties, the electrical properties, the thermal properties, the release performance, etc. Here the literature review is focused on the mechanical properties, the thermal properties and the release performance of the microcapsules.

2.4.1 Mechanical properties of single microcapsules by micromanipulation technique

2.4.1.1 Compression test by micromanipulation technique

The micromanipulation technique has been developed and used successfully to determine the mechanical properties of single microcapsules (Zhang, 1999; Zhang et al., 1991). Fig 2.6 shows the schematic diagram of the micromanipulation rig and Fig 2.7 presents the actual view when compressing the single microcapsule on the glass slide. Briefly, it is realised by compressing the single microcapsules between two flat surfaces that are the glass probe with the required diameter and the glass slide holding the microcapsules. The probe of transducer is positioned vertically above the single microcapsules. The electrical signal from the probe contacting the single microcapsules is recorded by the electrical box and sent to the computer, while the probe is travelling downwards at a preset constant speed controlled by a motor. The view of compression could be observed from a side-view or a bottom-view camera connected with a TV monitor. The corresponding force of the recorded voltage could be calculated by the sensitivity of the specific transducer as shown in Equation (2.4). The displacement of the probe could be obtained by Equation (2.5). The graph of force versus displacement, therefore, could be drawn. The compliance is defined as the reciprocal of the slope of the linear regression from the force versus displacement graph by compressing the empty slide.

$$F = V \times Sen \tag{2.4}$$

$$D = \upsilon \times t - F \times Com \tag{2.5}$$

where F is the force, mN, V is the voltage recorded, V, Sen represents the sensitivity of the specific transducer, mN/V, D is the displacement of the probe travelling downwards, μm, υ is

the travelling speed of the probe controlled by the motor, μm/s, t is the time, s, and Com represents the compliance of the force transducer, μm/mN.

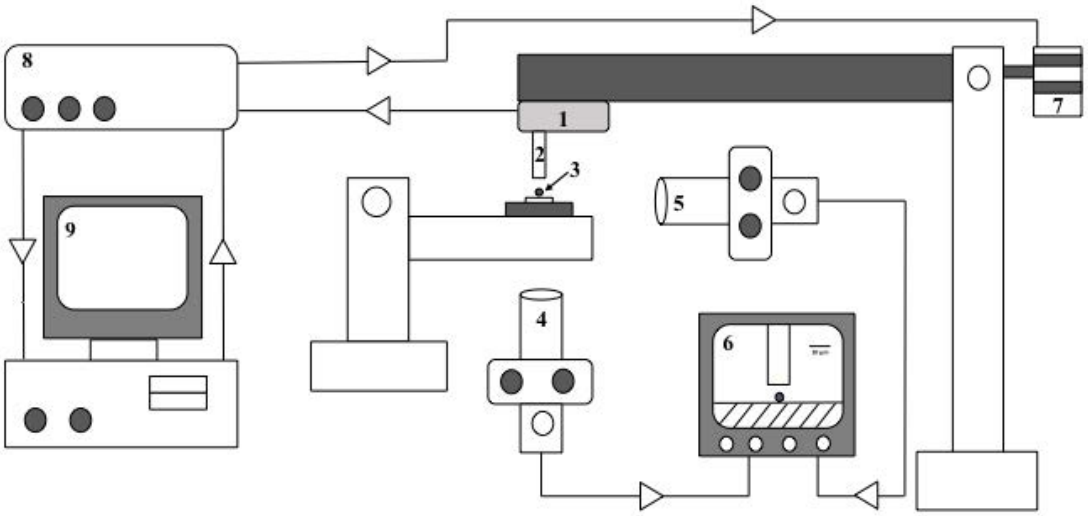

Fig 2.6 Schematic diagram of a micromanipulation rig (1- a force transducer; 2- probe; 3- a single microcapsule; 4- a bottom-view camera; 5- a side-view camera; 6- a TV monitor; 7- motor; 8- electrical box for recording voltage and 9- computer)

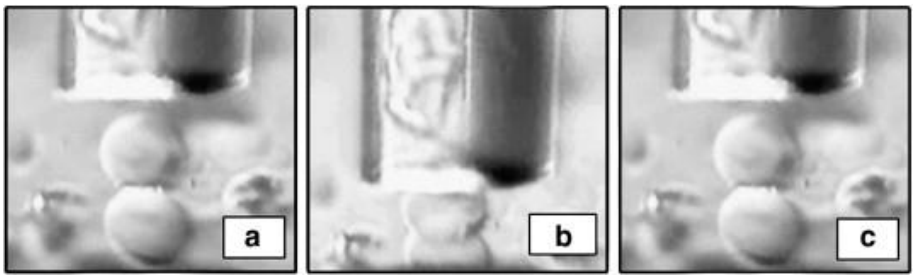

Fig 2.7 Compressing a single agarose microsphere of diameter 35μm by a micromanipulation rig, (a) before compression; (b) during compression; (c) after compression and full recovery (Yan et al., 2009)

Micromanipulation can be used to determine the mechanical properties of a large variety of materials such as microcapsules, microspheres and cells, including the information of rupture force, deformation at rupture, nominal rupture stress and elastic properties in small deformation (Gray et al., 2016; Mercade-Prieto and Zhang, 2012). Fig 2.8 gives a typical curve of the force versus the travelling distance of the probe. The probe starts travelling downwards in the air from the point A', and touches the single microcapsule at the point A. The force increases continuously as the probe is moving. In the region of A to B, the microcapsule shows elastic deformation, which is still recoverable. After the yield point B, the microcapsule deforms irreversibly. At the point C, the microcapsule is ruptured, its core material (oil) starts to release, and the force drops to zero immediately from C to D. When the probe keeps going downwards, it touches the glass slide or the residue of the broken microcapsule at the point E with the force going up rapidly. From the graph of force versus displacement, the mechanical properties of the microcapsule could be obtained accordingly.

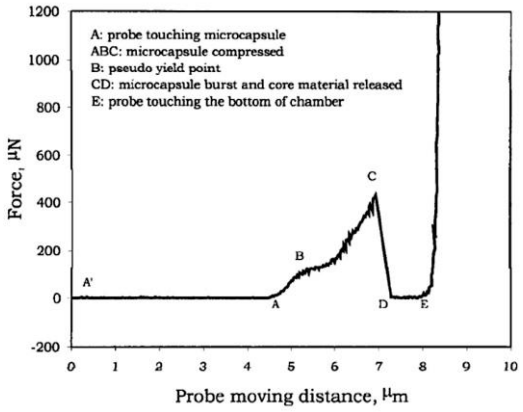

Fig 2.8 A typical curve of the force versus the probe moving distance from compression of a melamine formaldehyde microcapsule (Sun and Zhang, 2001)

2.4.1.2 Elastic properties of microcapsules

Stiffness refers to the load required to cause a deformation of the material, which is usually measured by a small load (Roylance, 2008). Hook's Law describes the linear relation between the stress and the strain of the material when small load is applied to it. It is originally shown as Equation (2.6) and can be written as Equation (2.7), which is suitable for both tension and compression. The material following the Hook's Law is elastic while a small load is applied.

$$P = k\delta \tag{2.6}$$

$$\sigma = E\epsilon \tag{2.7}$$

where P is the bear load, N, δ is the deformation of the material, m, k is the constant of proportionality that is called the stiffness, N/m, σ is the stress applied to the material, MPa, ϵ is the strain of the material and E is called Young's modulus, MPa (Roylance, 2008).

Thus, Young's modulus can be used to describe the stiffness of a material, and the higher value it has, the less deformable the material is (Du et al., 2017). However, Hook's Law could not be used directly for the spherical elastic materials, instead the Hertz model is applied to these materials under compression between two flat rigid surfaces (Muller et al., 2005). There are a few theoretical models analyzing the mechanical properties of polymeric microspheres, including the Hertz model, the Tatara model and models based on finite element analysis (FEA). The Hertz model is normally applied to a nominal strain less than 10%, assuming that the contact area is much smaller than the diameter of the micro-particles (Muller et al., 2005; Zhang et al., 2007). The Tatara model has been presented for large elastic deformations up to 60% nominal strain such as a rubber sphere (Tatara, 1991; Yan et al., 2009). Finite element

modelling is suitable for the analysis of large deformations of micro-particles and the full description of their mechanical properties (Nguyen et al., 2009; Zhang et al., 2007). Therefore, for the small elastic deformation of the microcapsules, the Hertz model can be used to determine the value of Young's modulus of micro-particles including microcapsules.

2.4.2 Thermal properties of microcapsules

Theoretically, most of the properties of materials are temperature-dependent, including mechanical property, electrical property, magnetic property or optical property (Buck and Rudtsch, 2011). Compared with these properties, thermal property mainly reflects the effect of thermal energy treatment on the material (Buck and Rudtsch, 2011). Thermal properties can be characterised as glass transition temperature, thermal stability, thermal expansion coefficient, and thermal conductivity (Vengatesan et al., 2018). Thermal conductivity of materials reflects the ability of thermal conduction where the heat transfers from high temperature to low temperature (Liu and Chen, 2014). It is defined as the amount of heat passing through unit cross-sectional area per unit time for a unit temperature gradient (Varshneya and Mauro, 2019b).

There are a variety of methods measuring the thermal conductivity of materials. Depending on the time dependence of the thermal response, the measurement methods could be classified as steady measurement or dynamic measurement (Abad et al., 2017; Liu and Chen, 2014). The steady measurement is applied with the in-flow method, requiring the temperature not changing and the heat flux kept the same during the measurement, while the dynamic measurement refers to the thermal diffusivity as a function of time (Liu and Chen, 2014). Besides, based on the heating process, the measurement methods could also be divided into

contact-heating method and non-contact heating method (Kumanek and Janas, 2019). The contact method is heating the sample by direct heat, while the non-contact method is usually based on the photo-thermal effect where an absorbed incident radiation produces the heat (Abad et al., 2017).

The laser flash method is a non-contact dynamic measurement for thermal conductivity. It is a simple and fast method determining the thermal conductivity compared with other steady methods (Liu and Chen, 2014). A laser pulse is heating the sample on the one side, and on the other side an IR detector is detecting the temperature change at the same time (Abad et al., 2017; Kumanek and Janas, 2019; Ruoho et al., 2015). The sample is coated with two layers of black paint (such as graphite) on the one side for absorbing the heating laser and on the other side for enhancing emission for IR detector (Abad et al., 2017; Ruoho et al., 2015). The schematic diagram of Laser Flash Apparatus (LFA) is demonstrated in Fig 2.9.

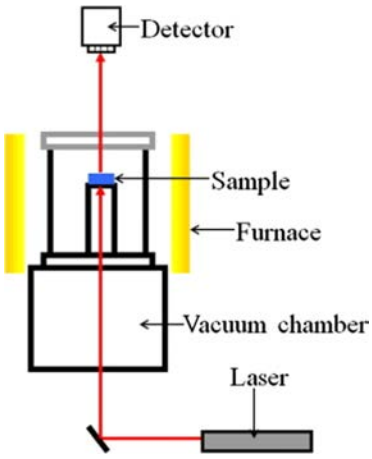

Fig 2.9 Schematic diagram of Laser Flash Apparatus (LFA) (Kumanek and Janas, 2019)

The laser flash method was firstly introduced by Parker et al. (1961), and his half-rise time method can be described as Equation 2.8. The thermal diffusivity is measured and the thermal conductivity can be calculated with the value of heat capacity of the material as shown in Equation (2.9).

$$a = 1.38\frac{l^2}{\pi^2 \cdot t_{0.5}} \tag{2.8}$$

$$\lambda(T) = a(T) \cdot c_p(T) \cdot \rho(T) \tag{2.9}$$

where a represents the thermal diffusivity, mm^2/s; l represents the thickness of the sample, mm; $t_{0.5}$ is the time at 50% of the temperature increase; λ represents the thermal conductivity, W/(m·K); c_p is the molar heat capacity at constant pressure, J/(g·K) and ρ is the density of the material, g/cm^3.

2.4.3 Release of active ingredient from microcapsules and the release models

2.4.3.1 Release of active ingredient

Release of active ingredient is an important process in the application of microcapsules, in which it is able to cross the barrier and then to the release medium (Fu and Kao, 2010). There are a few release mechanisms including diffusion-controlled processes, chemical controlled processes (erosion and reaction), osmosis-controlled processes and swelling controlled processes (Fu and Kao, 2010; Peppas and Narasimhan, 2014). There are several factors influencing the kinetics of the active ingredient release, such as the structure of the microcapsules, the loading of the ingredient, the physiochemical properties of the polymer and the condition of the releasing environment, (Jämsä et al., 2013; Junyaprasert and

Manwiwattanakul, 2008; Shardor, 2013). A summary of the main factors influencing the release kinetics is listed in Fig 2.10.

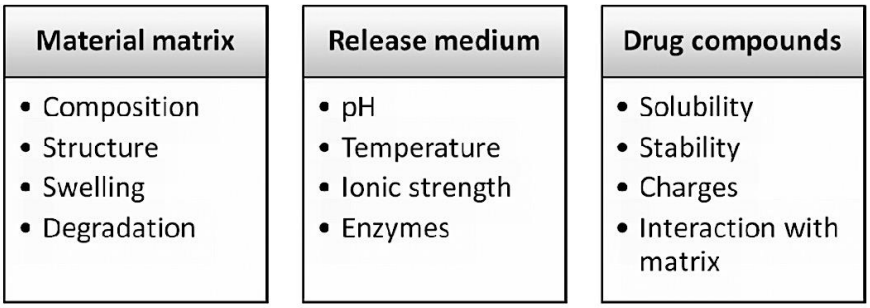

Fig 2.10 Main factors affecting the active ingredient (drug) release kinetics (Fu and Kao, 2010)

It has been stated that the active ingredient release includes multiple processes rather than simple dissolution (Siepmann and Siepmann, 2013). First of all, the microcapsules are exposed in the dissolution liquid. For the solid ingredient in the microcapsules, the liquid would penetrate into the microcapsules and contact the solid active so that part of the active ingredient would be dissolved in the liquid around them. Then the dissolved molecules would diffuse into the liquid outside the microcapsules because of the gradient of the concentration. Finally, the dissolution would reach the equilibrium. During these processes, the polymer may swell or degrade due to its physiochemical properties in the dissolution liquid (Aguiar et al., 2016). Therefore the active release involves not only dissolution but also diffusion. The scheme of the difference between the dissolution and release of an active ingredient is presented as Fig 2.11. Besides, a burst release may occur in short time at the beginning of the release as the scheme shows in Fig 2.12. It has been investigated that there may be a few reasons causing the burst release, such as the morphology and porous structure of the

microspheres, the physical and chemical properties of the materials and the conditions of preparing the materials, etc. (Huang and Brazel, 2001). The burst release is very likely to occur as the microcapsules prepared by solvent evaporation have a matrix structure and involve drying processes (Bile et al., 2015; Yang et al., 2000). There are some molecules of the active ingredient not fully embedded into the microcapsules but remaining on the surface of the microcapsules so that they would easily diffuse into the dissolution liquid once exposed in the liquid (Bile et al., 2015). In addition, the active ingredient release experiment should be carried out under the sink condition. Based on the requirement, the volume of the dissolution liquid must be five to ten times greater than the volume of the saturated solution of the ingredient (Pal et al., 2018). The sink condition is a basic requirement for carrying out the release experiment as the driven force under this is mainly the dissolution (Bruschi, 2015). Otherwise, the release rate would be significantly different compared with those under the sink condition (Pal et al., 2018).

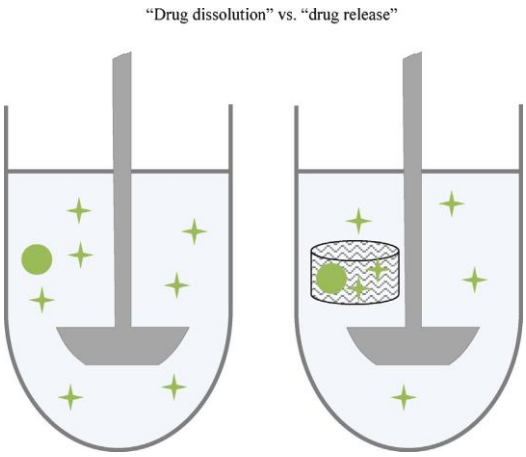

Fig 2.11 Scheme of the active (e.g. drug) dissolution (left) and the active release (right), where the green circles are the active particles and the green stars are the dissolved molecules of the active (Siepmann and Siepmann, 2013)

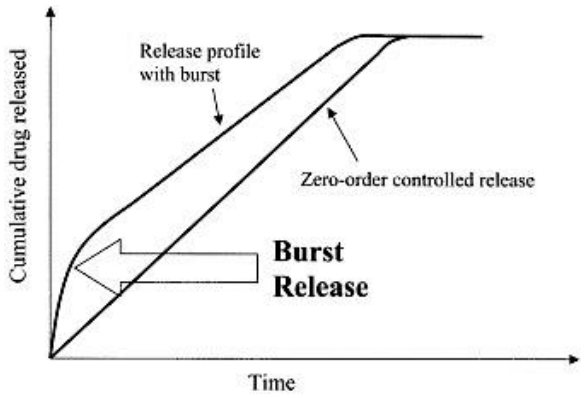

Fig 2.12 Scheme of the burst release in a zero-order release profile (Huang and Brazel, 2001)

2.4.3.2 Release models

The release mechanism of dissolved active ingredient in a polymer as the carrier is more likely to be Fickian diffusion, where it moves from the initial position to the outer surface of the polymer and then to the environment (Langer, 1990). Generally, the release from polymer with matrix structure is related to the gradient of active ingredient concentration, the distance of diffusion and the degree of swelling (Fu and Kao, 2010). There are a number of mathematical models that can be used to describe the release kinetics. They are important to predict the quantitative release of the active ingredients by knowing the mechanisms of mass transport and to evaluate and design the formulations for the new products (Bruschi, 2015). The available models have been demonstrated to be sufficient in describing most of the release systems, which are related to different the mechanisms.

A Zero-order Model (Ranjha et al., 2009) has been widely applied in therapeutic systems releasing the soluble active ingredient constantly over a certain period of time (Bruschi, 2015).

Generally these release kinetics can be generated from a core/shell structure. When the core ingredient contacts with the liquid, it dissolves and makes the core become a saturated reservoir inside the membrane/shell. And then the release occurs at a constant rate by diffusion or osmosis of the core ingredient through the swollen or relaxed polymeric membrane. The Zero-order Model is described as Equation (2.10) (Fu and Kao, 2010).

$$\frac{M_t}{M_\infty} = K_0 t \tag{2.10}$$

where M_t is the amount of the active ingredient released at the time, M_∞ is the initial amount of the active in the tablet added into the liquid, t is the time, K_0 is the release constant of the Zero-order model.

A First-order Model has been used to describe the absorption and/or elimination of a large quantity of the therapeutic ingredients (Bruschi, 2015). For a matrix structure of the therapeutic systems, the quantity of the active released has linear relation with the quantity of the active remaining in the porous matrix. Therefore the model could be described as Equation (2.11) (Bruschi, 2015).

$$lnM_t = lnM_\infty + \frac{K_1 t}{2.303} \tag{2.11}$$

where K_1 is the release constant of the First-order model.

The Higuchi Model has been applied to the solid or semi-solid matrix systems with soluble or insoluble active ingredient (Bruschi, 2015; Ranjha et al., 2009). This model requires that the initial amount of the active in the dissolution liquid should be much higher than its solubility and the polymeric membranes should not swell or dissolve by contacting the dissolution liquid. Based on the Fick's Law, the equation of the Higuchi Model is simplified and

displayed as Equation (2.12) below (Fu and Kao, 2010). The amount released is proportional to the square root of the time.

$$\frac{M_t}{M_\infty} = K_H\sqrt{t} \tag{2.12}$$

where K_H is the release constant of the Higuchi Model.

The Hixson-Crowell Model, which is also called cube-root law, indicates the linear relation between the release time and the cube root of the remaining amount of the active in the tablets and is used in pharmaceutics (Siepmann and Siepmann, 2013). The model is suitable for the dissolution occurring in planes parallel to the surface of the dosage form (Bruschi, 2015). It is supposed that the release is controlled by the rate of the dissolution instead of the diffusion, which could happen through the matrix structure of the polymer. And the dissolving particles remain spherical and intact during the dissolution process (Siepmann and Siepmann, 2013). The simplified model can be written as follows (Bruschi, 2015).

$$\sqrt[3]{1 - \frac{M_t}{M_\infty}} = 1 - K_{HC}t \tag{2.13}$$

where K_{HC} is the release constant of the Hixson-Crowell Model.

The Ritger-Peppas Model, which is also called Power law, is a semi-empirical model specifically for the drug release from a polymeric matrix as Equation (2.14) shows (Bruschi, 2015; Ritger and Peppas, 1987). This model can be used to investigate the release mechanism unknown or driven by more than one type. Based on the model, the mechanisms of the release from polymer can be divided into Fickian model (Case I) and Non-Fickian models that include Case II, Anomalous Case and Super Case II. The detailed explanations of each case are demonstrated in other researchers' work (Bruschi, 2015). As shown in Equation (2.14),

there is a release exponent n indicating the type of the release. When $n = 0.5$, the release is the same as the Fickian model and driven by diffusion. When n is between 0.5 and 1, the release mechanism is anomalous transport and driven by diffusion and the swelling of the polymer. When $n = 1$, the release is Non-Fickian Case II and corresponding to the Zero-order Model. When n is above 1, the model is called Super Case II where the polymer is broken. Besides, by considering the geometry of the release substance, Table 2.2 summarises the application of each value of n. In addition, considering the burst release at the beginning of the release, the equation can be modified as (2.15) shown below. Generally, the cumulative amount $\frac{M_t}{M_\infty}$ less than 60% is suggested.

$$\frac{M_t}{M_\infty} = K_{RP} t^n \tag{2.14}$$

$$\frac{M_t}{M_\infty} = K_{RP} t^n + b \tag{2.15}$$

where, K_{RP} is the release constant of Ritger-Peppas Model, n means the release exponent and b represents the burst effect of the initial release.

Table 2.2 Summary of the exponent value applying to the Ritger-Peppas Model and the corresponding release mechanisms (Bruschi, 2015; Siepmann and Peppas, 2011)

	Planar (thin films)	Cylinders	Spheres	Release mechanism
The value of the release exponent n	0.5	0.45	0.43	Fickian diffusion
	$0.5< n <1.0$	$0.45< n <0.89$	$0.43< n <0.85$	Anomalous transport
	1.0	0.89	0.85	Case II transport
	$n>1$	$n>0.89$	$n>0.85$	Super Case II transport

CHAPTER 3 MATERIALS AND METHODS

3.1 Introduction

The aim of this project is to prepare antifouling microcapsules containing capsaicin synthetic with enhanced thermal properties for potential applications in coatings to achieve its sustained release in marine environment, which can prevent the adhesion of the microbial organisms on the surface of equipment. In this chapter, the materials and the process of preparing antifouling microcapsules with metal on their surface are demonstrated, as well as the techniques and methodology used to characterise the microcapsules. Solvent evaporation method was used to prepare microcapsules, based on oil in water (O/W) emulsification in a stirred vessel with a Rushton turbine. The microcapsules with metal on their surface were prepared by electroless plating copper after generating a layer of polydopamine based on its self-polymerisation of dopamine. The morphology of microcapsules was characterised by optical microscopy and scanning electron microscopy (SEM), and the elements on their surface were analysed by energy dispersive spectroscopy (EDS). The size and size distribution of microcapsules were measured by Malvern particle sizing. UV-VIS spectrophotometry was used to quantify the amount of capsaicin in the microcapsules for measuring the encapsulation efficiency, the payload and the release rate. The mechanical properties of microcapsules were determined by a micromanipulation technique. The thermal conductivity of microcapsules was analysed by laser flash technique. The release performance of capsaicin from microcapsules was carried out in water and cyclohexane to accelerate the release, respectively. The materials used, as well as details of each process and methodology will be described in this chapter.

3.2 Materials

N-vanillylnonanamide (Capsaicin synthetic, ≥ 97%, powder), cellulose acetate butyrate (average Mn~30000), ethyl acetate (anhydrous, 99.8%), polyvinyl alcohol (PVA) (87-89%, hydrolysed, average M. W. 13000-23000), cyclohexane (anhydrous, 99.5%), hydrochloric acid (37%), formaldehyde solution (ACS reagent, 37 wt. % in H_2O) and sodium hydroxide (reagent grade) were purchased from Sigma-Aldrich, Dorset, the UK. Ethanol (HPLC grade) and copper (II) sulfate pentahydrate (≥ 99%) were supplied by Fisher Scientific, Leicestershire, UK. Ethylenediaminetetraacetic acid disodium salt dihydrate (EDTA-Na_2) (≥ 99%), tris(hydroxymethyl)aminomethane (TRIS) (99%) and dopamine hydrochloride (99%) were obtained from Alfa Aesar, Lancaster, UK. Palladium(II) chloride (ReagentPlus, 99%) was purchased from Scientific Laboratory Supplies, North Humberside, UK. Potassium sodium tartrate (>99%) was supplied by Fluka Analytical, UK. Fumed aluminium oxide (Aeroxide® Alu 130) was obtained from Evonik Industries, Staffordshire, UK. All the solutions were made by deionized water.

3.3 Microencapsulation by solvent evaporation

Microcapsules consisting of a core of capsaicin and shell of cellulose acetate butyrate (CAB) were prepared using a solvent evaporation method, based on emulsification of oil in water phase (O/W) in a stirred vessel with a Rushton turbine (IKA laboratory technology, Germany). The Rushton turbine has an impeller of 30mm in diameter. The amount of fluids, the diameter of impeller and the distance between the impeller and the bottom of the vessel met the requirement of standard tank configuration (diameter of the tank 6.5 cm; height of the liquid 6.5 cm; width of baffle 0.7 cm; distance between the impeller and the bottom of the tank 2-3

cm). The vessel was wrapped by aluminium foil during the whole process since the active capsaicin can be degraded by light. First of all, 2g CAB was dissolved in 20mL of solvent which was ethyl acetate. The oil phase was formed after another 10mL ethyl acetate dissolving a specific amount of capsaicin synthetic (the ratio of the active/polymer = 1/8, 1/4 or 1/2 w/w) was added into the former solution, which was mixed by a magnetic stirrer (Stuart, UK) for at least 30 min. Then 150mL of PVA aqueous solution (0.1%, 0.2%, 0.5% or 0.8% w/v) was poured into a vessel with a volume of 250mL, which was stirred by the Rushton turbine at a specific stirring speed. The vessel was a jacketed beaker (Sigma-Aldrich, UK) with four baffles in it to increase turbulence and connected with a refrigerated and heating circulator to maintain a constant temperature. The PVA aqueous solution was pre-saturated with 15mL ethyl acetate in order to prevent the precipitation of CAB into the fibre-like agglomerates from the oil phase (Altshuller and Everson, 1953; Li et al., 2008). The O/W emulsification took place at 10℃ while the oil phase was injected into the water phase, which was agitated continuously at various speed (600 rpm, 800 rpm or 1000rpm). The top of the vessel should be covered to prevent quick solvent evaporation. After a period of the emulsification process, another 50mL of PVA aqueous solution was added into the vessel dropwise (80-90 drops per minute) by a pump (101U, Watson-Marlow, UK) to extract solvent into the continuous phase gradually. The cover on the vessel was removed, and evaporation of the solvent was controlled at 30℃ for overnight. Microcapsules containing capsaicin synthetic were then obtained from the suspension by centrifugation at 3820 ×g (Labnet International, USA) and washed by water for three times at least. Finally the microcapsules were dried in a vacuum dryer (Edwards Ltd, UK) for 24 hours.

3.4 Electroless plating

3.4.1 Self-polymerised dopamine on microcapsules

The polydopamine (PDA) was formed on the surface of microcapsules containing capsaicin synthetic at room temperature (18-23°C). Firstly, 100mg dopamine hydrochloride was added into 50mL 10mM pH8.5 TRIS buffer solution stirred by a magnetic stirrer plate (Stuart, UK) at 300rpm to reach the concentration of 2mg/mL. The self-polymerisation of dopamine began, and after a period of agitation (0min, 30min, 1h, 2h or 24h) 100mg microcapsules were added into the pre-formed PDA solution and kept stirring for 30min, 1h, 2h or 3h. The microcapsules with PDA on their surface were then filtrated and washed by DI-water for three times. The 10mM TRIS buffer solution was prepared by DI-water and adjusted to pH 8.5 by 1M HCl.

3.4.2 Electroless plating copper

The microcapsules containing capsaicin synthetic were coated with copper by electroless plating at room temperature. First of all, the microcapsules with PDA on their surface were suspended in 2mM $NaPdCl_4$ solution for 2 hours to activate the electroless plating process. Then the suspension was filtrated and washed by DI-water. The activated microcapsules were subsequently immersed in the Cu^{2+} electroless plating bath overnight. Eventually, the microcapsules coated by copper were obtained by filtration, washing by DI-water and dried in the vacuum dryer.

The aqueous solution of 2mM $NaPdCl_4$ was prepared with 1mol $PdCl_2$ and 2mol NaCl per litre of DI-water in the ultrasonic surroundings. The composition of the chemical components

in the Cu^{2+} electroless plating bath is shown in Table 3.1. Each component was prepared into solution based on the final concentration in the bath, and mixed one by one in the order listed in the table to prevent precipitation, and potassium sodium tartrate and sodium hydroxide were added dropwise, respectively. The pH value of the bath was adjusted to 12.5 by sodium hydroxide. The final concentration of each solution is shown in the table.

Table 3.1 Composition of the Cu^{2+} electroless plating bath (Zhou et al., 2016)

Component	Chemical Formula	Role in the bath	Concentration
Copper(II) sulfate pentahydrate	$CuSO_4 \cdot 5H_2O$	Metallic ions of plating	16g/L
EDTA-Na_2	$C_{10}H_{14}N_2Na_2O_8 \cdot 2H_2O$	Stabiliser	25g/L
Potassium sodium tartrate	$KNaC_4H_4O_6 \cdot 4H_2O$	Complexing agent	14g/L
Sodium hydroxide	NaOH	Buffering solution	12g/L
Formaldehyde	HCHO	Reducing agent	12mL/L

3.5 Techniques to characterise the microcapsules

3.5.1 Morphology, structure and element analysis

3.5.1.1 Optical microscopy

The optical microscopy was used to observe the morphology and the size of microcapsules roughly. The optical microscope (Leica Microsystems Ltd., the UK) was equipped with the objective lenses having the magnification from ×5 to ×40 and the ocular lenses having the magnification of ×1, ×1.5 and ×1.6.

3.5.1.2 Scanning Electron Microscopy (SEM) and Energy Dispersive Spectroscopy (EDS)

Scanning Electron Microscopy (SEM) was used to characterise the morphology of microcapsules with more precision than the optical microscopy, and Energy Dispersive Spectroscopy (EDS) was used for detecting the surface elements on the samples. SEM was performed in the microscope JSM-6060 (JEOL Ltd., Japan) with Inca EDS (Oxford Instruments plc, UK).

The dry microcapsules were placed and stuck on a specimen stub with the conductive carbon adhesive tabs, and then metallised by gold coating (Polaron Sputter Coater SC7640, Quorum Technology Ltd., UK) to make the microcapsules electrically conductive. The microcapsules containing capsaicin synthetic without metallic compound were characterized at 15kV-20kV, and the microcapsules with metallic particles were scanned at 20kV-30kV for the elements analysis. For observing the inner structure of microcapsules, liquid nitrogen was used to freeze the sample rapidly and the microcapsules were ground immediately by a pestle in a

mortar. The brittle broken microcapsules were obtained after the liquid nitrogen evaporated, and the following procedures were the same as observing those intact microcapsules

3.5.2 Malvern particle sizing

The size and the size distribution of the microcapsules were measured by Malvern Mastersizer 2000 (Malvern Panalytical Ltd., UK). A sample dispersion unit filled with DI-water was connected with the instrument to deliver the samples into the optical bench. The microcapsules were well dispersed in DI-water and dripped into the dispersion unit. The experiments were carried out at 20℃ for three times and the average of the mean size and the size distribution were obtained. The size range of measurements was 0.01-1000μm. The refractive index of CAB was 1.475 and that of water is 1.330 (obtained from the supplier).

3.5.3 UV-VIS spectrophotometry

The UV-VIS spectrophotometry was used to quantify the amount of capsaicin synthetic in the microcapsules, as the capsaicin synthetic contains the aromatic groups which can be analysed by this method (Lewis, 2016). The UV-VIS spectrophotometer (CE 2021, Cecil Instruments Ltd., the UK) covers the wavelength range from 190nm to 900nm with a deuterium lamp for the ultraviolet range and a tungsten lamp for the visible range, and all the measurements took place in the same quartz cuvette with the path length of 10mm.

The UV-VIS spectrophotometry is based on the Beer–Lambert law shown below, which applies on the solutions in low concentration (Lewis, 2016; Perkampus, 1992).

$$A = lg\frac{I_0}{I} = lg\frac{1}{T_l} = \varepsilon \cdot \imath \cdot c \quad (3.1)$$

where A is absorbance; I_0 represents the intensity of the light entering the solution; I represents the intensity of the light emerging from the solution; T_l means the transmittance of the light; ε is the extinction coefficient; ι is the path length of the light through the cuvette and c is the concentration of the component in the solution.

For the dilute solution measured in a specific cuvette, the extinction coefficient ε and the path length l are constants at the given wavelength. Therefore the relation between the absorbance A and the concentration c is linear. The solution must be diluted into an appropriate concentration before the measurements to have the absorbance reading between 0.3 and 0.7. Otherwise, ε is no longer a constant but related to the refractive index of the solution (Perkampus, 1992).

3.5.3.1 Calibration

To obtain the concentration of the component, a calibration curve is needed and can be drawn with a series of concentration and the absorbance values at the specific wavelength. In this case, the solute was capsaicin synthetic and the solvents used were 80% v/v ethanol in water and pure cyclohexane, respectively. First of all, the pure solvent in the quartz cuvette was scanned as the baseline. Then the solution of capsaicin synthetic in one of the solvents was scanned, showing the wavelength of 280nm at the absorption peak (λ_{max}), which was corresponding to the capsaicin's absorption peak (Koleva et al., 2013). All the following measurements were carried out at the wavelength of 280nm. Then the absorbance of 6-8 solutions with different given concentrations were analysed by the UV-VIS

spectrophotometer. At last, the calibration curve was plotted by the absorbance and their corresponding concentration, shown in Fig 3.1.

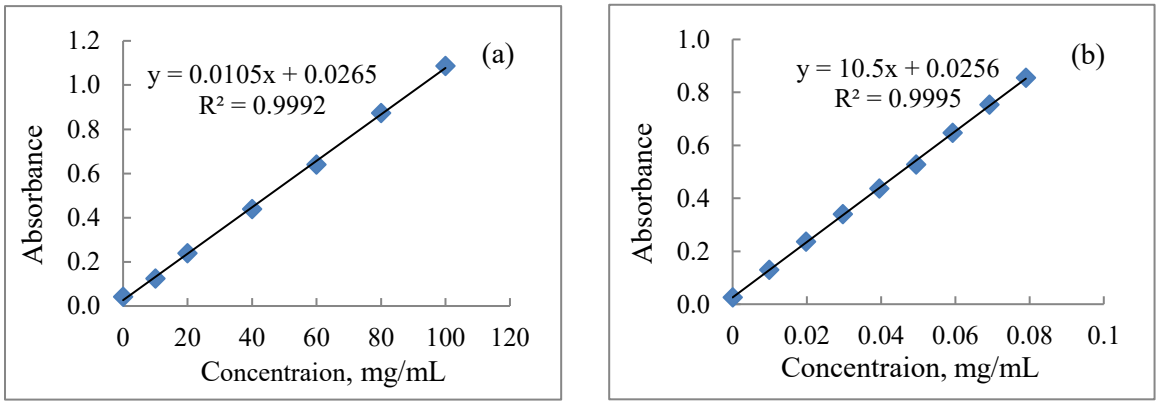

Fig 3.1 Calibration curve of capsaicin synthetic in (a) 80% v/v ethanol and (b) pure cyclohexane

3.5.3.2 Measurement of the encapsulation efficiency

The amount of capsaicin synthetic in the microcapsules was quantified by the UV-VIS spectrophotometry. First of all, the dry microcapsules, weighed in triplicate (15mg for each), were ground in a mortar and dissolved in 15mL ethanol to extract capsaicin synthetic, and the same amount of the blank CAB sample was prepared in the same way. The solution was shaken in an orbital mixer (Denley, UK) at 100rpm for 3h for the full extraction of capsaicin synthetic to ethanol, and the mortars were wrapped and covered by aluminium foil in case of capsaicin synthetic degradation by light and quick evaporation of ethanol. Each solution was diluted to 10 times by 80% v/v aqueous ethanol solution. The absorbance of solution was measured, and the payload and the encapsulation efficiency were calculated as follows (Im et al., 2010). The payload is the amount of core material in the whole capsules, and the

encapsulation efficiency is the ratio of the mass of core material indeed encapsulated to the mass of the total core material added into the preparation. The effect of CAB on the absorbance was eliminated when calculated.

$$Payload\ (\%) = 100 \times \frac{m_{core,samp}}{m_{samp}} \tag{3.2}$$

$$Encapsulation\ efficiency\ (\%) = 100 \times \frac{m_a}{m_o} = 100 \times \frac{Payload}{m_{core}/(m_{core}+m_{shell})} \tag{3.3}$$

where $m_{core,samp}$ is the mass of core material in the microcapsules sample; m_{samp} represents the mass of the sample; m_a represents the actual loading; m_o represents the theoretical loading; m_{core} is the mass of core material used for encapsulation and m_{shell} is the mass of shell material used for encapsulation.

3.5.4 Micromanipulation technique

3.5.4.1 Preparation of force transducer probes

The transducers (Model 403A and 405A, force scale 10mN, Aurora Scientific Inc., Canada) were used to compress the microcapsules to generate the force versus displacement data, and a glass probe with a flat end was connected to the transducer output tube, making the compression. The glass probe was made by heating and pulling a borosilicate glass rod in a puller (Narishige, Japan), and the sharp end was polished to a required diameter by a microgrinder (Narishige, Japan). The probe was glued to a transducer with a required force scale.

3.5.4.2 Calibration of force transducer

The force transducer was calibrated prior to the experiments to obtain the sensitivity which was defined as the force change per unit of voltage. The transducer was placed and fixed on a flat desk by Blu-Tac with the glass probe pointing upward. A few pieces of paper with various mass (0.1g, 0.2g, 0.4g) were cut into small size and weighed accurately by a balance (Secura 124-1S, Sartorius, Germany). The papers with various weights were then placed carefully on the tip of the glass probe, respectively, and the force applied to the probe could be calculated by the weight of the paper and gravitational constant G (9.8 m/s^2). The corresponding voltage change due to adding each piece of paper was recorded after the voltage reading was stable. The voltage of baseline was recorded while there was no paper on the probe. A calibration curve could be plotted by force versus voltage change compared with the baseline, and the slope of the trendline was the sensitivity of the transducer.

3.5.4.3 Compression of single microcapsules

The compression of single microcapsules was made between two flat surfaces which were the glass probe with the required diameter and the glass slide holding the microcapsules. The dry microcapsules were spread on the glass slide to separate single microcapsules, and the glass slide was fixed in the sample stage horizontally. The probe of transducer was positioned vertically above the single microcapsules. The view of compression could be observed from a side-view camera connected with a TV monitor. The diameter of the individual microcapsules was measured on the TV monitor, and 1mm on the TV monitor equals to the actual diameter 1.0758μm. For each sample, 20 microcapsules were selected for compression. The compression on the glass slide without single microcapsules was carried out for three times to

obtain the average compliance of the transducer probe. All the data sampling frequency was 50Hz and the compression velocity applied to single microcapsules was 2μm/s. The graph of force versus displacement was obtained after the measurement.

3.5.4.4 Determination of Young's Modulus

The compression of the microcapsules between two flat rigid surfaces could be described by the Hertz theory below which is applied for the nominal strain less than 10% (Muller et al., 2005; Yan et al., 2009), while the Tatara theory is presented for large elastic deformations such as a rubber sphere (Tatara, 1991).

$$F = \frac{\sqrt{2R}E}{3(1-\nu^2)}\Delta^{\frac{3}{2}} \tag{3.4}$$

$$\Delta = 2\delta \tag{3.5}$$

$$\epsilon = \frac{\Delta}{2R} \tag{3.6}$$

where F is the force applied, mN; R is the radius of the microcapsule, μm; E is Young's Modulus, MPa; ν is the Poisson's ratio which is 0.3 for CAB (Gindl and Keckes, 2004); Δ represents the diametric compressive displacement, μm; δ represents the displacement of local compression at each contact point, μm, and ϵ is the nominal strain, MPa. As R, E and ν were considered as constants for a microcapsule, the relation between F and $\Delta^{\frac{3}{2}}$ is linear, which could be obtained from the obtained data, and the slope $\frac{\sqrt{2R}E}{3(1-\nu^2)}$ could be determined easily using a linear regression. So Young's Modulus E of a single microcapsule was calculated, and the higher value it is, the more rigid the material is.

3.5.5 Thermal conductivity measurement

3.5.5.1 Differential Scanning Calorimetry (DSC)

Heat capacity is defined as the amount of heat required to raise the temperature of a unit quantity of a substance by 1K (Varshneya and Mauro, 2019a). Differential Scanning Calorimetry (DSC) was used for measuring c_p (the molar heat capacity at constant pressure) which was used for the following measurement of LFA. The dry microcapsules were placed in an aluminium crucible with lid sealed by the crucible sealing press (Mettler Toledo, UK). The samples were heated up at a rate of 5℃/min from 5℃ to 85℃. Sapphire was measured as the comparison of the c_p data. The DSC curve was obtained and the c_p value could be analysed and calculated by the baseline of the curve as the rectangle shown in Fig 3.2.

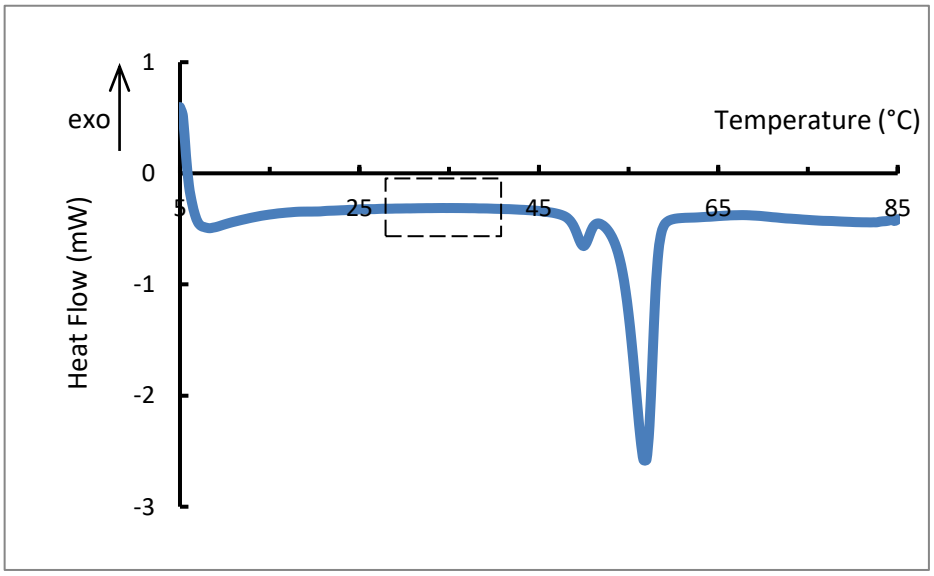

Fig 3.2 DSC curve of the microcapsules of capsaicin synthetic with core/shell ratio 1/2 agitated at 1000 rpm in 0.1% PVA, and the rectangle is used to calculate the heat capacity

3.5.5.2 Laser flash technique

The thermal conductivity was measured by Laser Flash Apparatus (LFA427, Netzsch Instruments, Germany). The dry microcapsules were compressed into tablets in a punch mould with a diameter of 13.0mm by a universal testing machine (LS100, Lloyd Instruments Ltd., UK) prior to the analysis. The tablets were sprayed homogeneously by a thin layer of graphite as the absorber for the heating laser on one side and an emitter for the IR detector on the other side (Ruoho et al., 2015), and left to dry and the thickness of each tablet was measured by a micrometre. Before mounting horizontally on the top of a sample carrier tube in the chamber of LFA, the tablet was trimmed to 12.7mm in diameter to fit in the holder. The liquid nitrogen was used to cool down the furnace, and the flow rate of nitrogen gas was 100mL/min. The measuring temperature was started from 20℃ to 45℃ at a rate of 2℃/min, and 5 shots were carried out for each temperature. The three-layer-model was selected for considering the effect of the layers of graphite. When the predetermined temperature of furnace was stable, a pulsed laser emitted energy under the sample, and an infrared sensor above the sample detected the change of heat. The thermal diffusivity a of each sample was obtained after the measurements based on Equation (3.7), and thermal conductivity λ was calculated from Equation (3.8) with the c_p value from DSC.

$$a = 1.38\frac{l^2}{\pi^2 \cdot t_{0.5}} \tag{3.7}$$

$$\lambda(T) = a(T) \cdot c_p(T) \cdot \rho(T) \tag{3.8}$$

where a represents the thermal diffusivity, mm^2/s; l represents the thickness of the sample, mm; $t_{0.5}$ is the time at 50% of the temperature increase; λ represents the thermal conductivity,

W/(m·K); c_p is the molar heat capacity at constant pressure, J/(g·K) and ρ is the density of the material, g/cm^3.

3.6 Release rate measurement

The continuous release study was carried out at room temperature (20±2°C) in DI-water and cyclohexane, respectively. The release of the capsaicin synthetic in each liquid was under the sink condition (Pal et al., 2018). Each experiment was undertaken duplicate.

For the release in water, the dry microcapsules, weighed in duplicate (20mg for each), were placed in a tea bag and closed firmly by a clip. The release medium of 250mL of DI-water was added into a glass bottle which was wrapped by aluminium foil completely to shade from light. The tea bag with microcapsules was put into the deionised water, which was shaken at 100rpm by an orbital mixer (Denley, UK). An aliquot (3mL) was taken and replaced by the same volume of deionised water at various time intervals from four times a day to once a day (Fundueanu et al., 2005; Wang et al., 2013; Zhu et al., 2015). The samples were extracted by ethanol solution (ethanol/water = 4/1 v/v) and analysed by a UV/VIS spectrophotometer at the wavelength of 280nm. The concentration of capsaicin synthetic in each sample was calculated from the absorbance reading, as described in the section of 3.4.3. The curve of the cumulative versus time was drawn based on the average value of the release data at each sampling time.

Cyclohexane was used as a dissolution liquid to speed up the release of capsaicin synthetic whose solubility in the solvent is much greater than in water in order to shorten the experimental duration. For the release in cyclohexane, the dry microcapsules, weighed in duplicate (20mg for each), were placed in a glass bottle of 100mL wrapped by aluminium foil

tightly to shade from the light. The release started once the release medium which was 100mL cyclohexane was added into the bottle and shaken at 100rpm by the orbital mixer. An aliquot (1mL) was taken and replaced by the same volume of cyclohexane at various time intervals from every hour to once a day gradually. The samples were analysed by a UV/VIS spectrophotometer at the wavelength of 280nm, and the concentration of capsaicin synthetic in each sample was calculated from the absorbance reading, as described previously. The curve of the cumulative versus time was drawn based on the average value of the release data at each sampling time.

CHAPTER 4 PREPARATION AND CHARACTERISATION OF ANTIFOULING MICROCAPSULES BY SOLVENT EVAPORATION

4.1 Introduction

Biofouling is an undesirable accumulation of marine biological organisms on the surface of substratum under seawater (Deng et al., 2016; Kochkodan and Hilal, 2015; Yebra et al., 2004). The phenomenon caused by complex marine environment can influence the state of power generation systems in seawater. Marine biofouling can cause a series of problems to the equipment working under the sea, such as the corrosion of metal, high consumption of energy, low heat transfer efficiency of the equipment in seawater and high cost of maintenance. In order to prevent marine biofouling, it is necessary to apply the coatings with antifouling property on the surface of equipment. Currently there are a few coatings containing antifouling agents in the market, such as hybrid fluorine copolymer, silicone oils, hybrid and hydrogel silicone (Dafforn et al., 2011; Li et al., 2014). Capsaicin can be an alternative of the antifouling agent, which is a non-toxic and environmental-friendly substance (Wang et al., 2014). However, it is not desirable to reapply the coatings frequently, not only increasing the down time of the equipment but also the cost of maintenance. Therefore, it is necessary to achieve sustained release of the antifouling agent from the coatings. Microcapsules to be incorporated into the coatings can be an effective way to prevent the release immediately and maintain a sustained release of the antifouling agent.

The aim of the work presented in this chapter is to achieve the sustained release of the antifouling agent from microcapsules into the marine system. A typical thickness of coatings is approximately 200 μm and the size of microcapsules should be less than 60 μm to prevent change of the morphology of the coatings (Personal communication with Dr Jianfeng Hu,

South China University of Technology, China). In this chapter, the preparation and characterisation of microcapsules containing antifouling agent are demonstrated. The microcapsules are prepared with cellulose acetate butyrate (CAB) as the shell material and capsaicin synthetic as the core material by solvent evaporation based on oil(O)/water(W) emulsification. The effects of different formulation and processing conditions including emulsifier concentration, emulsification time, agitation speed and the ratio of core/shell material on the formation of microcapsules, their morphology, the size distribution, the encapsulation efficiency and payload are studied. In addition, the mechanical properties of the formed microcapsules are characterised. Moreover, the release rates of capsaicin from the microcapsules to two dissolution liquids are measured. The basic experimental details are described in Chapter 3, and specific experimental details are presented in this chapter.

4.2 Experimental

4.2.1 Microencapsulation of capsaicin synthetic by solvent evaporation

The microencapsulation of capsaicin synthetic with CAB as shell material was carried out by solvent evaporation. 1% (w/v) Tween 80 solution, 1% (w/v) hydrophilic Aerosil silica suspension and 0.5% (w/v) polyvinyl alcohol (PVA) solution were used as the emulsifier, and different concentrations of PVA (0.1%, 0.2%, 0.5% and 0.8%, w/v) were used to investigate its effect on the formation of microcapsules. The microcapsules with various ratios of capsaicin synthetic/CAB (1/1, 1/2, 1/4 and 1/8, w/w) were prepared. The emulsification time (5 min, 15 min, 30 min and 60 min) and the agitation speed (400 rpm, 600 rpm, 800 rpm and 1000 rpm) were used to study their effects on the morphology and the size of the formed

microcapsules. The details of the formulation and the processing conditions are described in Section 3.3.

4.2.2 Morphology of microcapsules

The morphology of microcapsules containing capsaicin synthetic was observed by optical microscopy and Scanning Electron Microscopy (SEM). Generally, Transmission Electron Microscopy (TEM) is an useful method to observe the internal structure of microcapsules by getting ultra-thin sections cut by ultramicrotome (Long et al., 2009). However the shell material CAB was not compatible with ethanol during the sampling process. Thus the internal structure of the microcapsules was obtained by freezing the microcapsules with liquid nitrogen and breaking them rapidly (Liu, 2010). The detailed information is provided in Section 3.5.1.

4.2.3 Size and size distribution

The size and size distribution of microcapsules containing capsaicin synthetic were measured by Malvern particle sizing, and the experimental details are described in Section 3.5.2.

4.2.4 Encapsulation efficiency and payload

The amount of capsaicin synthetic in the microcapsules was quantified by the UV-VIS spectrophotometry as described in the section of 3.5.3. Then the encapsulation efficiency and payload were calculated by Equations (3.2) and (3.3).

4.2.5 Determination of the mechanical properties of single microcapsules

The mechanical properties were determined by a micromanipulation technique. Single microcapsules of capsaicin synthetic and microspheres of CAB were compressed, respectively, and the microcapsules with different formulations were analysed. The details of the operation are demonstrated in the section of 3.5.4.

4.2.6 Release of antifouling agent in water and in cyclohexane

The continuous release study was carried out at room temperature (20±2°C) in DI-water and cyclohexane, respectively. The details of the release experiments are described in the section of 3.6. The measurements of the solubility of capsaicin synthetic in DI-water and cyclohexane were undertaken at room temperature as well. Excess capsaicin synthetic in powder was dispersed in water and cyclohexane, respectively. The solution was kept shaking for 7 days in water or 2 days in cyclohexane so that the capsaicin synthetic could fully dissolve in the dissolution liquid. Before the solubility was measured, the solution was placed still in order to allow those capsaicin synthetic particles to settle at the bottom of the container. The

concentration of the upper clear liquid corresponding to its solubility was measured by the UV-VIS spectrophotometry as described in Section 3.5.3.

4.3 Results and discussion

4.3.1 Effect of the emulsifier on the formation of microcapsules

Tween 80, hydrophilic Aerosil silica and polyvinyl alcohol (PVA) were chosen as the emulsifier to investigate the formation of microcapsules of capsaicin synthetic and CAB as shell material. The optical microscope images of the formed microcapsules are shown in Fig 4.1. It can be seen from Fig 4.1(a) that the microcapsules prepared in Tween 80 solution are not spherical and tend to agglomerate, and the size varies from 20μm to 300μm. Fig 4.1(b) shows that the microcapsules prepared in Aerosil silica aqueous suspension are highly in-regular in shape. This may be due to the inadequate dispersion of the silica powder with nano scale in the water so that the suspension could not provide effective coverage on the surface of the droplets. Compared with these two types of microcapsules, those prepared in PVA aqueous solution are more spherical and homogenous. From the images taken under the optical microscope, it is obvious that the microcapsules have a matrix structure rather than the typical core-shell structure with the size range from 10μm to 150μm. With the help of emulsifier, the oil droplets can be produced and stabilised in the emulsion. Based on this preliminary work, therefore, PVA aqueous solution has been selected as the emulsifier for the further experiments.

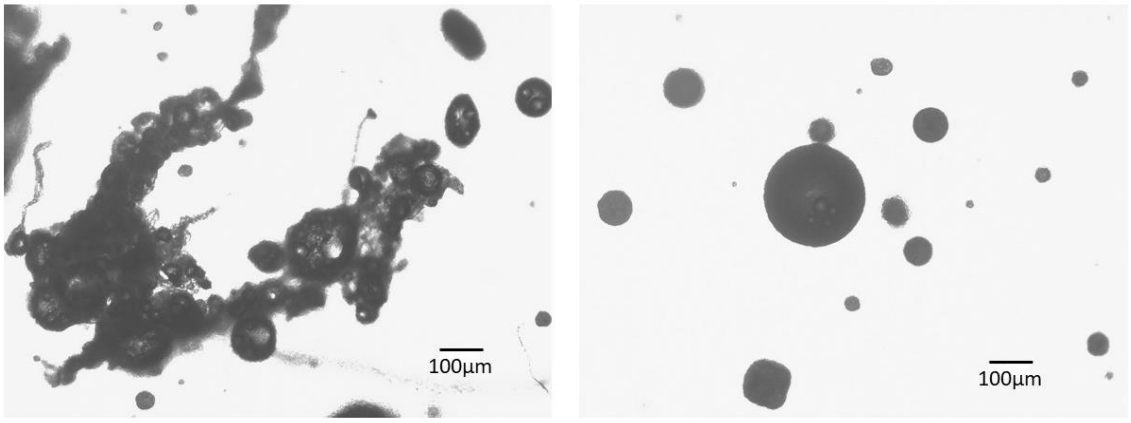

(a) Prepared with 1% (w/v) Tween 80

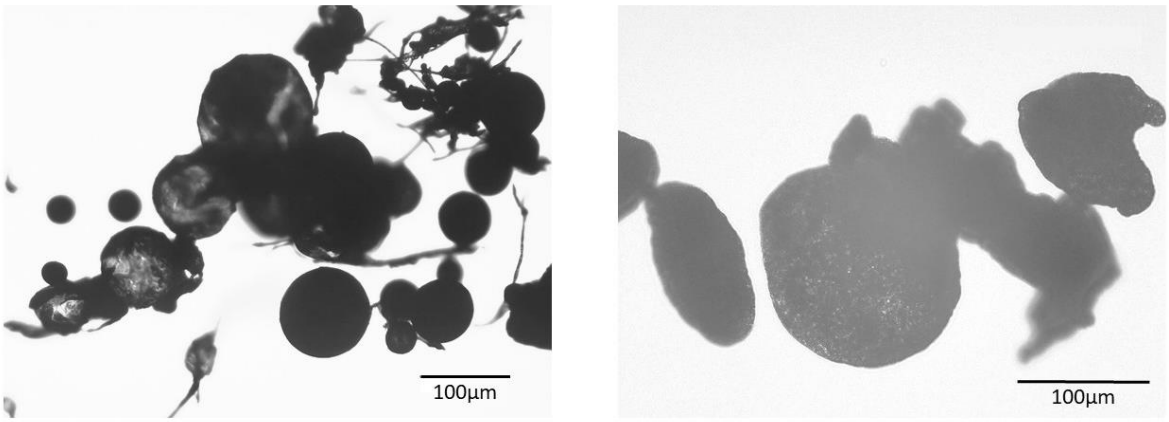

(b) Prepared with 1% (w/v) Aerosil Silica

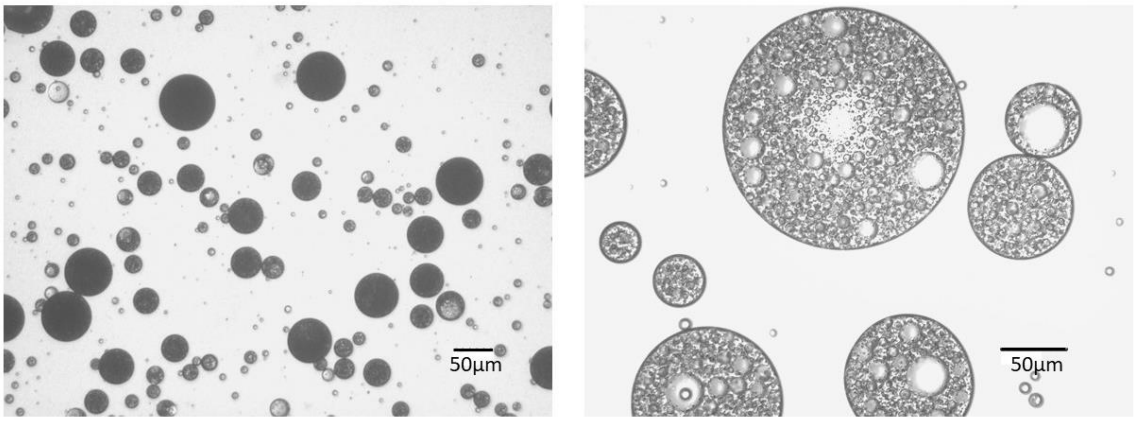

(c) Prepared with (0.5%) PVA

Fig 4.1 Microcapsules prepared with different emulsifiers under optical microscope

Fig 4.2 shows SEM images of the microcapsules containing capsaicin synthetic prepared using PVA aqueous solution, which clearly have a highly porous honeycomb structure with multiple cores. The matrix structure might be caused by solvent evaporation. In general, the solvent evaporation method consists of four steps: (1) dispersion of the oil phase as the dispersed phase containing solvent, core and shell materials; (2) emulsification of the oil phase in the aqueous phase as the continuous phase; (3) evaporation or extraction of the solvent to transform the droplets into solid microcapsules; (4) harvest of the microcapsules (Freitas et al., 2005). In stage of (3) the solvent evaporation or extraction, raising the temperature and continuously adding aqueous phase solution are needed to enhance the removal of the solvent, which could cause the matrix structure with pores inside the microcapsules (Yang et al., 2000). Since the formation of the internal structure could be affected by several parameters such as the temperature gradient during the evaporation, the speed of rising temperature, the extent of diluting the aqueous phase and the speed of diluting

it (Jeyanthi et al., 1996; Jyothi et al., 2010), these conditions were kept consistent in this research to eliminate their effects.

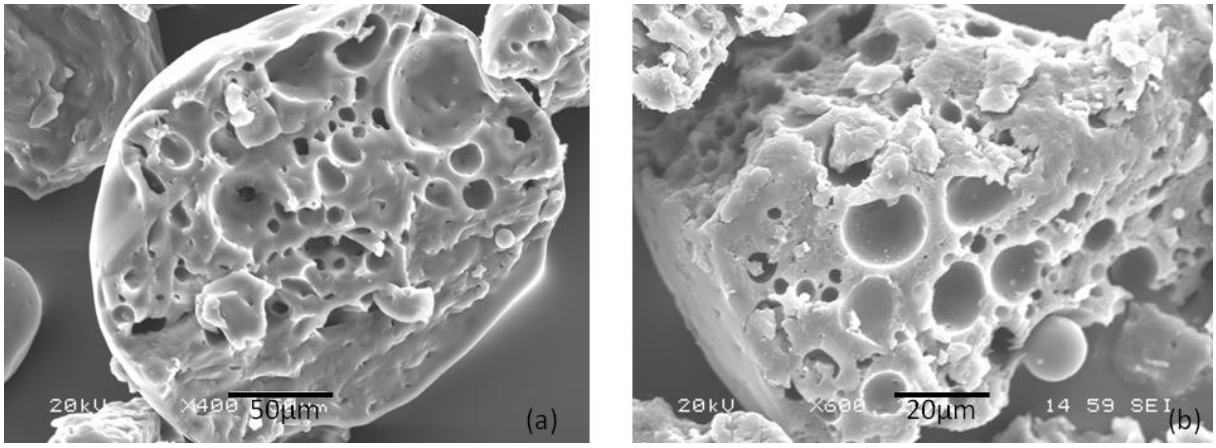

Fig 4.2 SEM images (a: X400 and b: X600) of the internal structure of microcapsules prepared by solvent evaporation

4.3.2 Effect of emulsification time on the formation of microcapsules

The formation of the O/W emulsion is achieved by breaking the oily dispersed phase into small droplets in an aqueous continuous phase by hydrodynamic force which results from a rotating turbine (Wilde, 2009). The stable emulsion is formed after agitation for some time. Fig 4.3 shows the morphology of the microcapsules of capsaicin synthetic prepared for the different lengths of emulsification time (5 min, 15 min, 30 min and 60 min) in the PVA aqueous solution as the continuous phase under the optical microscope. From Fig 4.3(a), it is shown that the microcapsules are coarse and their sizes are large over 200µm. When the emulsification time was increased to 15 min, the microcapsules as shown in Fig 4.3(b) are

more homogeneous, and their sizes are smaller than 200µm. For an emulsification time of 30 min, the microcapsules (shown in Fig 4.3(c)) have even smaller sizes (under 50µm) and their shape looks spherical. When the emulsification time was further increased to 60 min, the sizes of microcapsules (Fig 4.3(d)) are reduced slightly and their shape remains spherical. Even though it affected the size of the microcapsules, the emulsification time of 30 min is chosen for further microencapsulation work since it generated the microcapsules less than 60µm, which can meet the requirement for being incorporated into the antifouling coatings in the end-use.

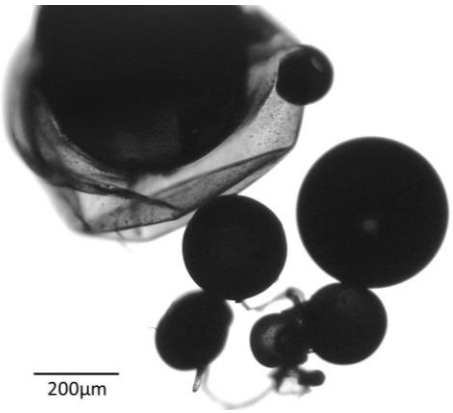

(a) Emulsification for 5 min

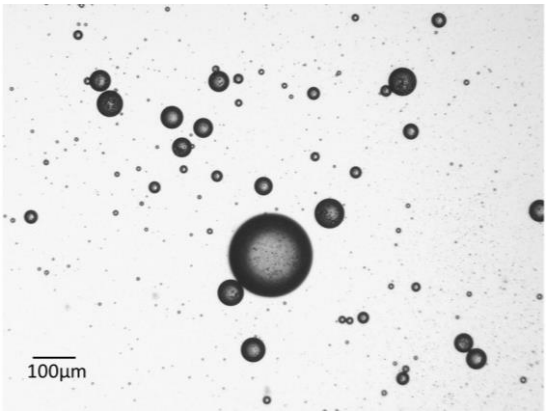

(b) Emulsification for 15 min

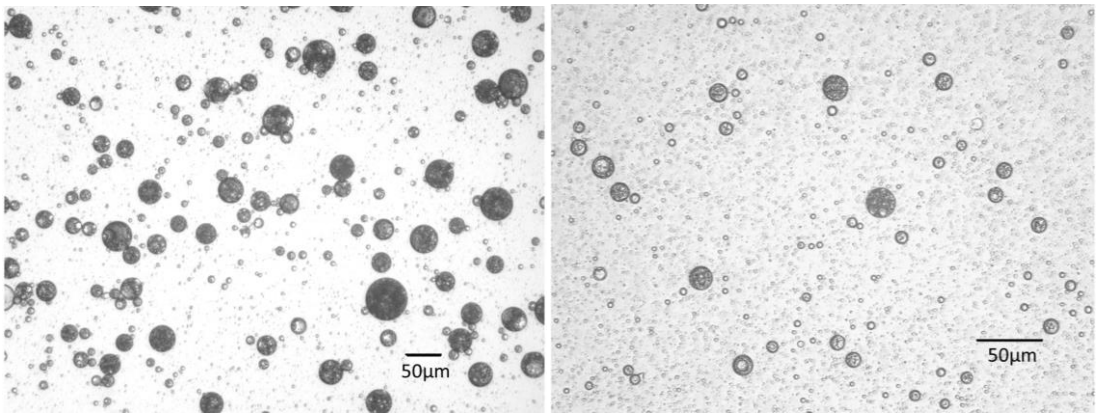

(c) Emulsification for 30 min (d) Emulsification for 60 min

Fig 4.3 Images of microcapsules prepared after emulsification for different lengths of time under optical microscope (the microcapsules were prepared with the core/shell ratio of 1/4 (w/w), agitation speed of 1000 rpm and 0.1% (w/v) PVA solution)

4.3.3 Effect of the concentration of PVA on the morphology, the size distribution and the encapsulation efficiency

The formation of microcapsules is a complicated process with a variety of parameters affecting the results. The effect of the concentration of PVA in the continuous phase was therefore investigated on the morphology, the size distribution and the encapsulation efficiency of the microcapsules containing capsaicin synthetic, which are shown in Fig 4.4 and Table 4.1.

From the images under optical microscope and SEM, the morphologies of microcapsules prepared in 0.1%, 0.2%, 0.5% and 0.8% (w/v) PVA aqueous solution are shown in Fig 4.4. The other preparation conditions remained the same. It is obvious that the microcapsules are becoming less spherical and coarser as the concentration of PVA increases. From the images

taken under SEM in Fig 4.4(a), the microcapsules prepared in 0.1% PVA have a very smooth surface and appear to be spherical, and there is no clear blemish on them. The microcapsules prepared in 0.2% PVA, shown in Fig 4.4(b), also have a smooth surface but are slightly more porous than the ones prepared with 0.1% PVA. There are a few small particles sticking on the larger ones. However, the surface of the microcapsules prepared with 0.5% PVA is coarser than those prepared with lower concentrations, and they are less spherical as shown in Fig 4.4(c). There are also smaller microcapsules sticking on the larger ones. Moreover, compared with the previous three samples of microcapsules prepared with lower concentrations of PVA, those with 0.8% PVA are not spherical as shown in Fig 4.4(d), and there are some indents/holes on the surface. This implies that there may be hollows inside the microcapsules, which tend to agglomerate. The reason for this might be that the viscosity of PVA aqueous solution increases with its concentration. However, without PVA as the emulsifier, the emulsion could not be well formed as the oil droplet could not be stable in the system because of coalescence. The droplets merged to form larger ones, which can be prevented by adding emulsifier (Wilde, 2009). Overall, with the increasing concentration of PVA from 0.1% to 0.8%, the microcapsules became less spherical, coarser and likely to agglomerate.

The concentration of the emulsifier could affect the size of the microcapsules in two different ways. On the one hand, the higher the concentration of emulsifier is, the smaller the mean size of droplet is (Freitas et al., 2005; Jeffery et al., 1993). On the other hand the viscosity of the continuous phase can also affect the size of the droplet (Wilde, 2009). The increasing emulsifier concentration could increase the viscosity of the continuous phase, leading to the larger droplet size. The two effects may explain the initial decrease in the mean diameter d_{32} from 37.5μm (corresponding to PVA concentration of 0.1%) to 19.9 μm (PVA 0.2%), and then increased to 26.3μm (PVA 0.5%).

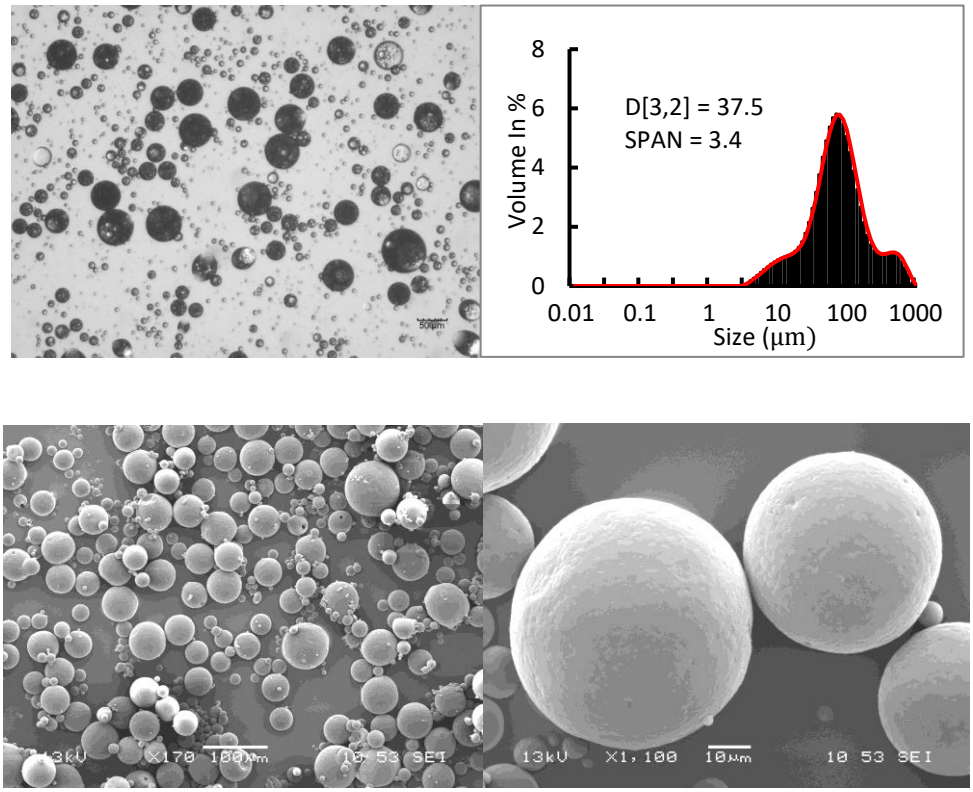

(a) 0.1% PVA (up left: optical microscope; up right: size distribution; down: two different magnifications under SEM)

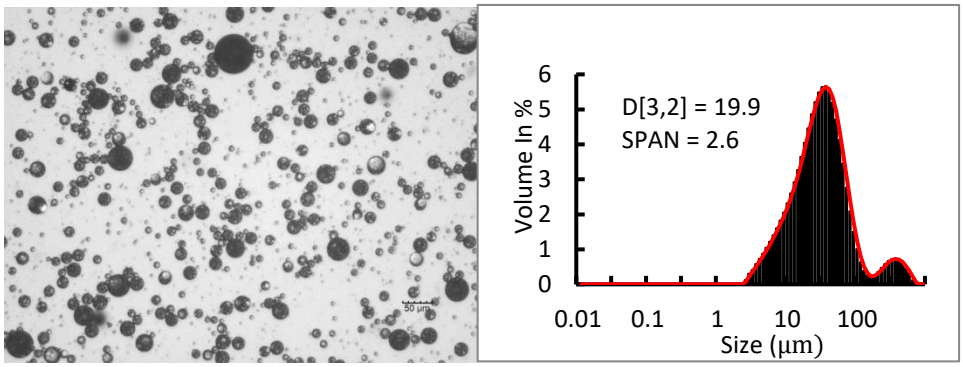

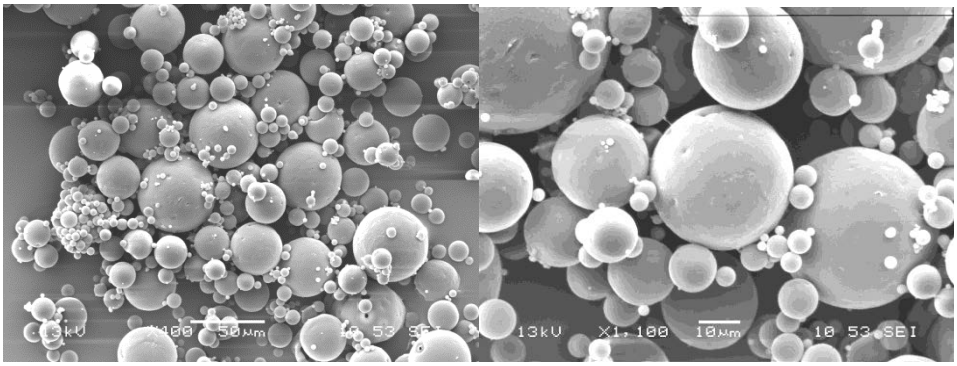

(b) 0.2% PVA (up left: optical microscope; up right: size distribution; down: two different magnifications under SEM)

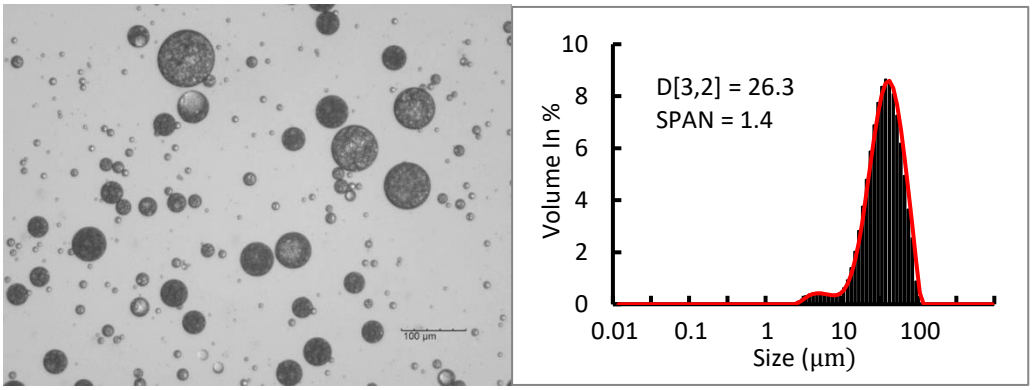

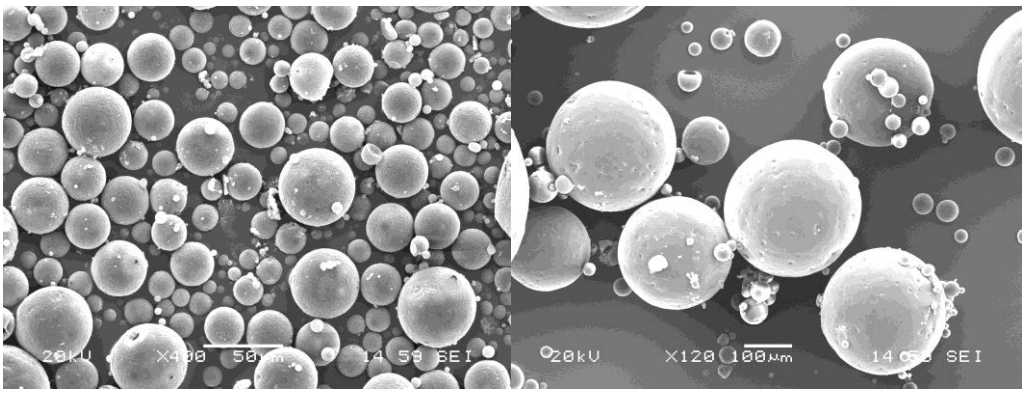

(c) 0.5% PVA (up left: optical microscope; up right: size distribution; down: two different magnifications under SEM)

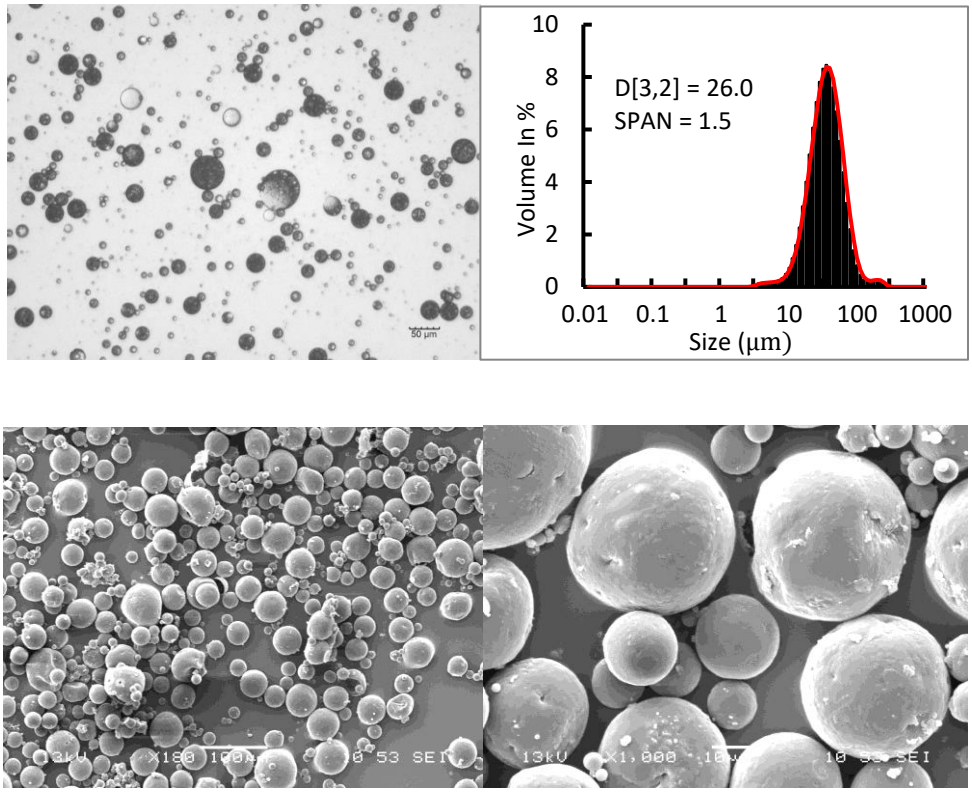

(d) 0.8% PVA (up left: optical microscope; up right: size distribution; down: two different magnifications under SEM)

Fig 4.4 Morphologies and size distributions of microcapsules prepared with different concentrations of PVA aqueous solution

The concentration of PVA may affect the encapsulation efficiency as well. The payload and the encapsulation efficiency of microcapsules containing capsaicin synthetic prepared with different concentrations of PVA aqueous solution are presented in Table 4.1. It is shown that the payloads of capsaicin synthetic are between 13.4% and 17.9% and the encapsulation efficiency varies from 67.0% to 88.9%. The encapsulation efficiency increases as the concentration of PVA varies from 0.1% to 0.5%. When prepared with 0.5% PVA, the microcapsules had the highest encapsulation efficiency of 88.9%, and the corresponding

payload reached 17.9%. This may be due to the stabilisation of the droplets against coalescence by adding more PVA into the continuous phase (Yang et al., 2001). So more capsaicin synthetic could be encapsulated. However, the encapsulation efficiency drops to 79.4% while microcapsules are prepared with 0.8% PVA aqueous solution, which is consistent with the observed indents/holes on their surfaces.

Table 4.1 The payload and the encapsulation efficiency of microcapsules containing capsaicin synthetic prepared with different concentrations of PVA aqueous solution. The figures after ± represents the standard error. The same applies to the following tables.

Concentration of PVA	0.1%	0.2%	0.5%	0.8%
Payload	(13.4±0.5)%	(15.8±0.4)%	(17.9±0.2)%	(15.9±0.3)%
Encapsulation efficiency	(67.0±2.3)%	(79.0±1.9)%	(88.9±0.8)%	(79.4±1.7)%

4.3.4 Effect of agitation speed on the size distribution and the encapsulation efficiency

The emulsification of capsaicin synthetic in an aqueous phase was carried out with a Rushton turbine which had a flat disk with 6 vertical blades. The turbine provides hydrodynamic force in the mixing system while agitation, so the speed of the agitation can be important to the formation of the microcapsules. The size distribution of microcapsules prepared at a series of agitation speed (400 rpm, 600 rpm, 800 rpm and 1000 rpm) is shown in Fig 4.5. It can be seen

that the mean size of the microcapsules is getting smaller as the agitation speed increases, as expected. It is obvious that the SPAN values of all the microcapsules vary from 1.20 to 1.79, which indicates that the widths of the size distribution are all reasonably narrow. While agitated at 400 rpm and 600 rpm, the mean sizes D[3,2] of the microcapsules are 61.7μm and 50.9μm, respectively, and there is a significant amount of microcapsules bigger than 100μm as shown in Fig 4.5(a) and (b), which is much beyond the size requirement (maximum 60μm) of the particles which can be incorporated into the coatings in the end-use. As shown in Fig 4.5(c), the mean size D[3,2] of the microcapsules at 800 rpm is 26.3μm, but there are still some microcapsules larger than 60μm. While agitated at 1000 rpm, all the microcapsules are smaller than 60μm and their mean size D[3,2] is 4.5μm, which is desirable. As for the payload and the encapsulation efficiency of microcapsules prepared with different agitation speeds, Table 4.2 shows that the encapsulation efficiency reached 88.9% and 80.7% respectively while the agitation speed is 800 rpm and 1000 rpm. Therefore in the following study, an agitation speed of 1000 rpm has been chosen and kept constant.

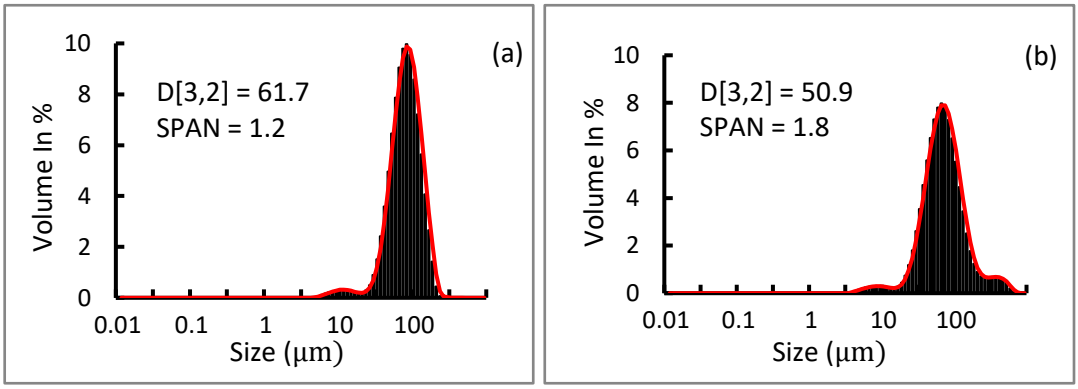

(a) At 400 rpm

(b) At 600 rpm

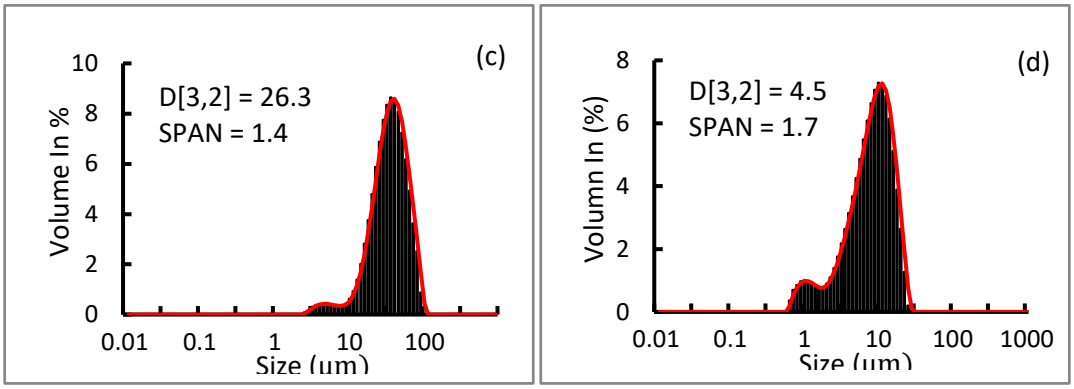

(c) At 800 rpm (d) At 1000 rpm

Fig 4.5 The mean size and the size distribution of microcapsules prepared by mechanical agitation at different speeds

Table 4.2 The payload and the encapsulation efficiency of microcapsules containing capsaicin synthetic prepared with different agitations speeds

Agitation speed (rpm)	400	600	800	1000
Payload	(14.4±0.7)%	(15.1±0.7)%	(17.9±0.2)%	(16.5±0.4)%
Encapsulation efficiency	(72.0±3.5)%	(72.8±3.4)%	(88.9±0.8)%	(80.7±1.8)%
D[3,2]	61.7µm	50.9µm	26.3µm	4.5µm
SPAN	1.2	1.8	1.4	1.7

4.3.5 Effect of the ratio of core/shell material on the encapsulation efficiency and the payload

The mass ratio of capsaicin synthetic/CAB, the corresponding payload and the encapsulation efficiency are presented in Table 4.3. It is shown that the payload increases from 10.1% to 16.5% while the core/shell ratio changes from 1/8 to 1/4 and then to 1/2, as expected, whilst the encapsulation efficiency decreased.

Table 4.3 The payload and the encapsulation efficiency of microcapsules containing capsaicin synthetic and CAB prepared with different ratios of core/shell material

Core/Shell ratio (w/w)	1/8	1/4	1/2
Payload	(10.1±0.4)%	(14.4±0.7)%	(16.5±0.4)%
Encapsulation efficiency	(87.4±3.2)%	(86.8±2.4)%	(80.7±1.8)%

4.3.6 Mechanical properties of microcapsules

The mechanical properties of microcapsules containing capsaicin synthetic were characterised using the micromanipulation technique. Fig 4.6(a) shows a typical curve of force of compression versus probe displacement from compressing single microcapsules of capsaicin synthetic, and Fig 4.6(b) is the corresponding curve of nominal stress versus nominal strain. Clearly, the force of compression gradually rises with the increasing displacement of the

probe compressing the single microcapsule. There appears to be an approximately linear region A-B at the beginning of the curve demonstrating that the nominal stress is proportional to the strain. It was also observed that the microcapsule deformed in this range showed full recovery after the force was released, which indicates the deformation was elastic. And this region A-B could be used to calculate Young's Modulus which describes the elasticity of a material (Roylance, 2008). After that, the curve starts bending from the point B to point C and then to point D, which means the deformation from the point B becomes nonlinear, plastic and unrecoverable. Unlike the microcapsules with a liquid core such as oil (Hu et al., 2018; Pan et al., 2013; Sun and Zhang, 2001) or the cells (Du et al., 2017) having a rupture point while compressed, there is only elastic and plastic deformations observed for the microcapsules of capsaicin synthetic. This is due to the matrix structure of the microcapsules and the solid core of capsaicin synthetic.

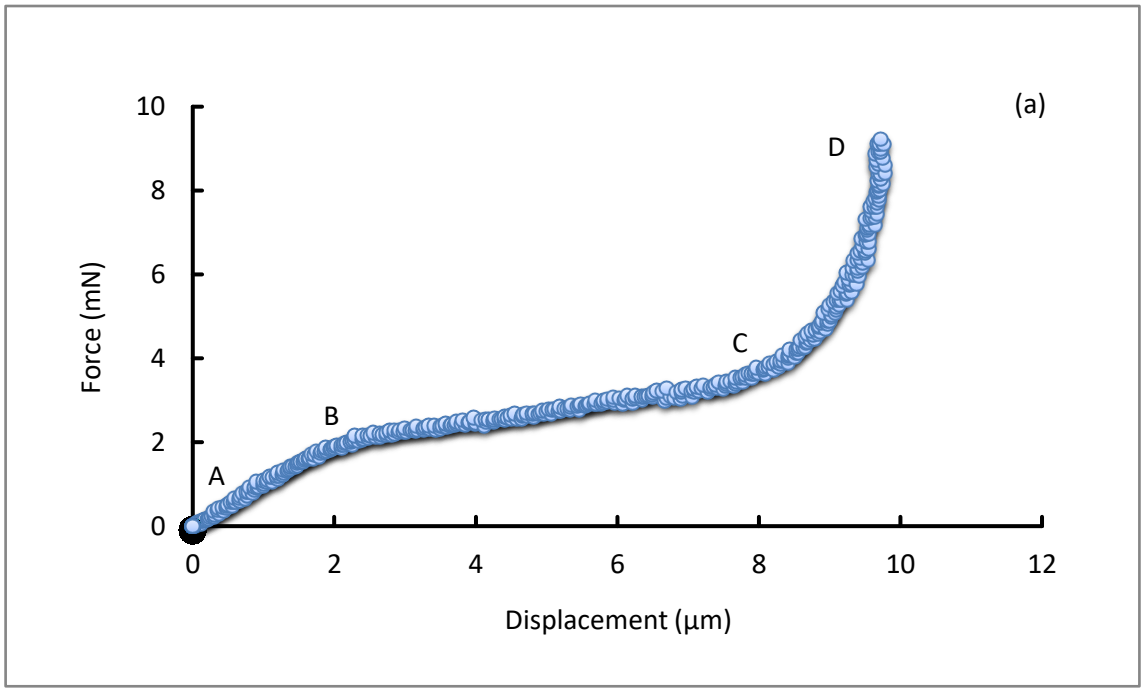

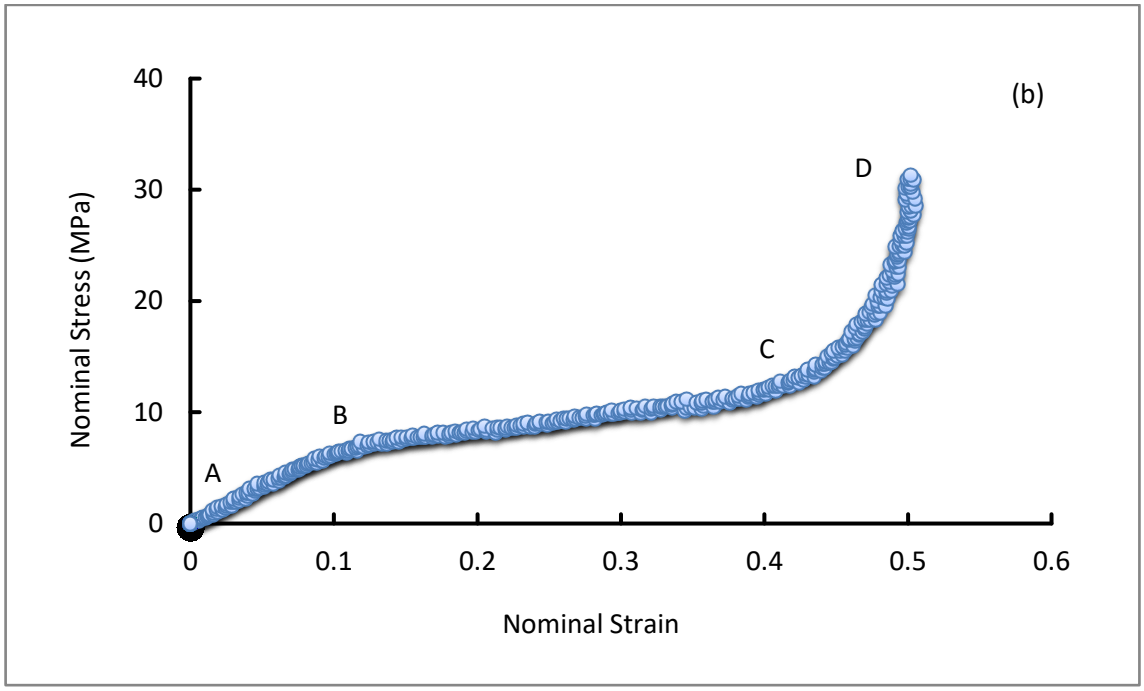

Fig 4.6 A typical curve of (a) force of compression versus probe displacement from compressing a single microcapsule of capsaicin synthetic (diameter 19.4μm); (b) the corresponding nominal stress versus nominal strain from compressing the same microcapsule of capsaicin synthetic.

The compression of the microcapsules between two flat rigid surfaces could be described by Hertz theory which is applied for the nominal strain less than 10% (Ding et al., 2008; Muller et al., 2005; Yan et al., 2009), while Tatara theory is presented for large elastic deformations such as a rubber sphere (Tatara, 1991). Here Hertz theory was used for describing the relationship between the compressive force and displacement up to 10% nominal strain. Fig 4.7 presents a typical Hertz equation fitting curve up to 10% nominal strain of the microcapsule. It is shown that the force applied to the single microcapsule is proportional to $\Delta^{\frac{3}{2}}$. Based on Hertz theory Equation (3.4) to (3.6), the slope of the linear regression equals to

$\frac{\sqrt{2R}E}{3(1-\nu^2)}$ so that Young's Modulus E of a single microcapsule could be calculated by assuming the Poisson ration is 0.3 for the shell material CAB (Gindl and Keckes, 2004).

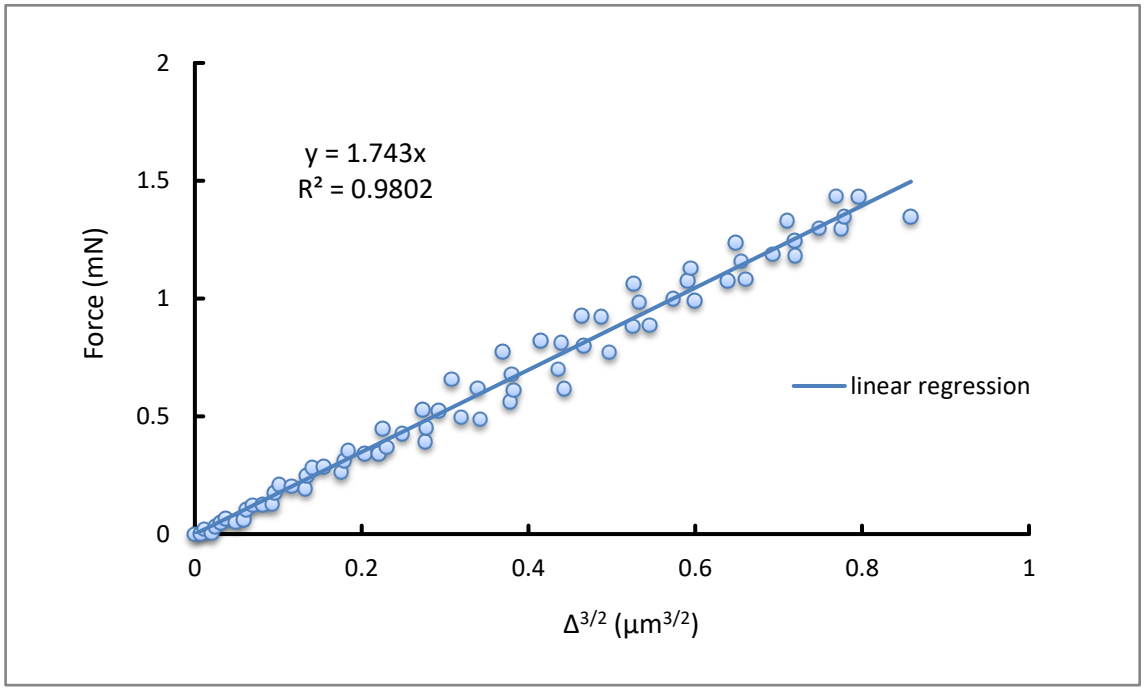

Fig 4.7 A typical curve of Hertz equation fitting data up to 10% nominal strain, where Δ represents the diametric compressive displacement

Young's Modulus can describe the stiffness of a material (Roylance, 2008), and the higher value it has, the more rigid the material is. Fig 4.8 gives the comparison of Young's modulus of microcapsules of capsaicin synthetic prepared with different ratios of core/shell material (1/2, 1/4, 1/8, w/w) and the pure CAB microparticles prepared under the same conditions as other microcapsules. It is obvious that Young's modulus decreases significantly as the ratio of core/shell material increases (0, 1/8, 1/4 to 1/2). In the previous section, it is presented in

Table 4.3 that the payload of capsaicin synthetic drops while the ratio decreases. Therefore, while more capsaicin synthetic was encapsulated, the microcapsules were less rigid. In contrast to Young's modulus values of other microcapsules with core/shell structure varying only from 15kPa up to 700kPa (Du et al., 2019; Wang et al., 2005; Yan et al., 2009), the microcapsules of capsaicin synthetic have Young's values all in Mega Pascal scale, which mean these microcapsules are more stiff than most of other microcapsules. The more rigid they are, the more likely they can survive when mixed into the coatings for the end-use application. In summary, the composition and structure of the microcapsule can significantly affect its stiffness, and the microcapsules of capsaicin synthetic are more rigid compared with others.

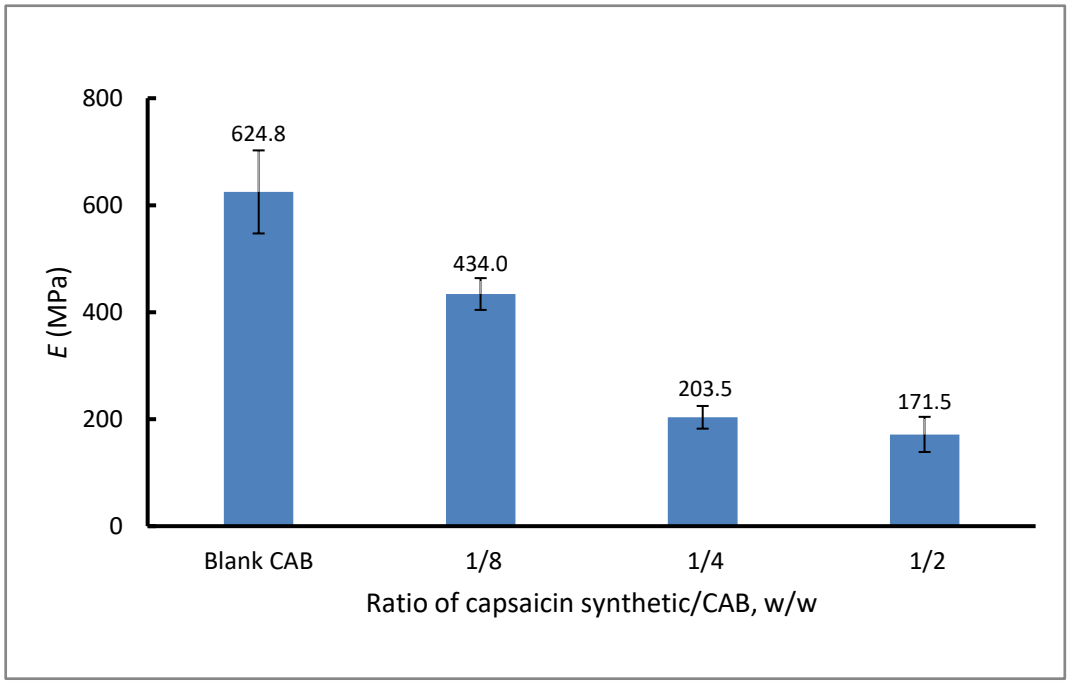

Fig 4.8 The comparison of Young's modulus of microcapsules of capsaicin synthetic prepared with different ratios of core/shell material, where *E* represents the Young's modulus and Blank CAB means the sample is pure CAB microparticles prepared under the same conditions as other microcapsules

4.3.7 Release study

The continuous release study of capsaicin synthetic was carried out in DI-water and cyclohexane, respectively. As the release rate of capsaicin synthetic in water can be very slow which is desirable for the application, the release in cyclohexane was used as the dissolution liquid for accelerating the release rate of capsaicin synthetic by increasing the solubility of the active ingredient in the liquid. The cumulative amount of capsaicin synthetic released in water and cyclohexane each is shown in Fig 4.9(a) and (b), respectively. It is obvious that the release rate in cyclohexane is much faster than that in water. As shown in Fig 4.9(a), the release in water can be sustained over 300 days with approximately a cumulative release of 25%, while in Fig 4.9(b) the capsaicin synthetic takes only 22 hours to reach 80% amount released from the microcapsules. As seen from the graph, the maximum release amount is around 82% as the dissolution equilibrium. This might be due to the incomplete release of capsaicin synthetic from the deep pores of the matrix structure. Therefore it was difficult for the capsaicin synthetic to fully release from the microcapsules into the dissolution liquid, which has also been reported in other researchers' work (Junyaprasert and Manwiwattanakul, 2008). The initial accumulative release of capsaicin synthetic from the microcapsules is plotted in Fig 4.10, and both of them show good linear regression. By comparing the solubility of capsaicin synthetic in both of the dissolution liquids with the slope of the linear regression of their initial release, the ratios of the value of cyclohexane to water could match as indicated in Table 4.4. It could be implied that the release is mainly driven by diffusivity, and the release rate in water could be predicted by releasing capsaicin synthetic in cyclohexane and calculating with the proportion of their solubility. As for the intercept of the

linear regression equation, it might be caused by the burst release at the beginning of the release. Since the microcapsules had matrix structure, there might be some capsaicin synthetic molecules on the surface of the microcapsules. Once the microcapsules were immersed in the dissolution liquid, those capsaicin synthetic molecules on the surface were likely to diffuse into the liquid very quickly. The intercepts of the linear regressions are different, which indicates the different amount of burst release. The reason might be that capsaicin synthetic takes longer time to dissolve into water than into cyclohexane, so the burst release in water is 8 times slower than in cyclohexane.

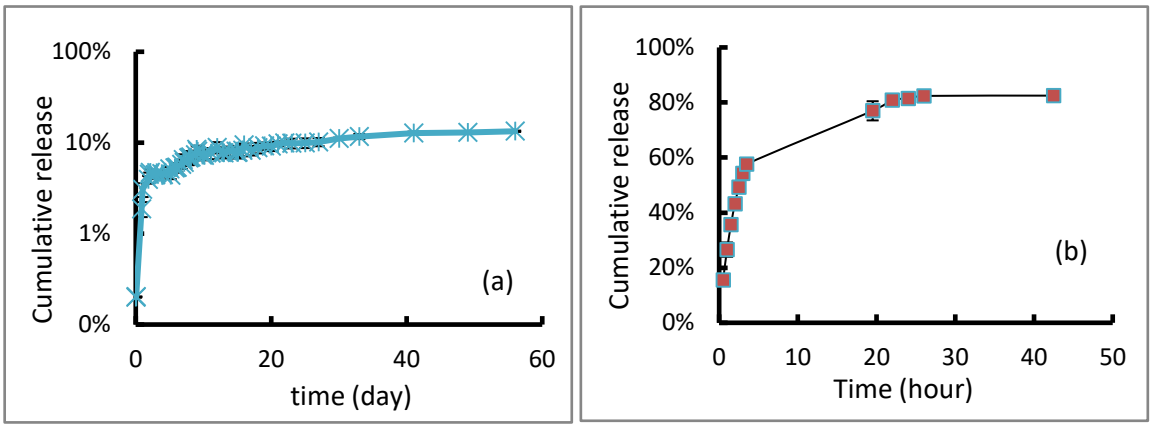

Fig 4.9 Cumulative amount of capsaicin synthetic released (a) in water and (b) in cyclohexane. The microcapsules were prepared with the core/shell ratio 1/4 agitated at 800 rpm in 0.5% PVA solution. The same conditions apply to the microcapsules below.

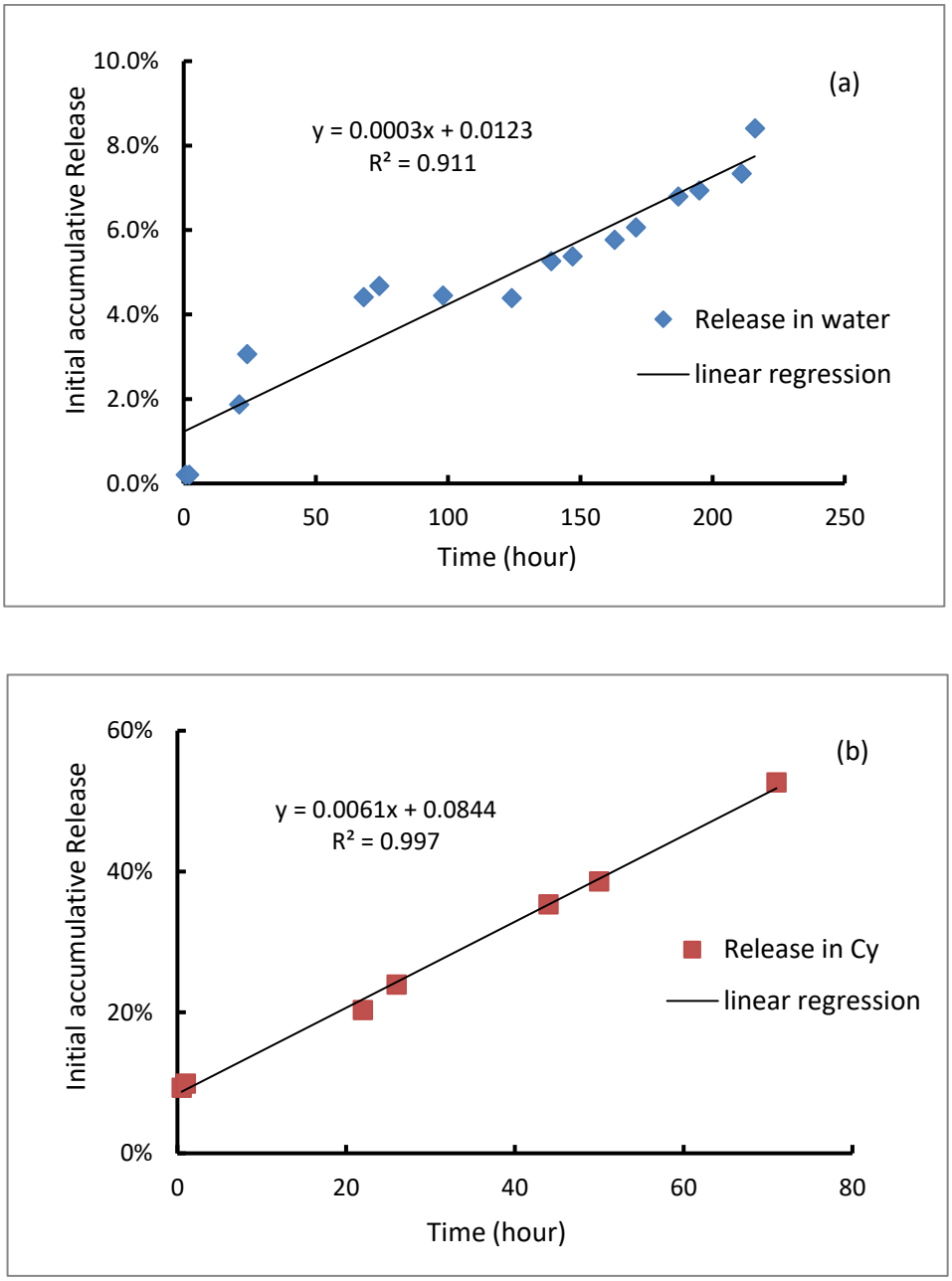

Fig 4.10 Initial accumulative release of capsaicin synthetic from the microcapsules in (a) water and (b) cyclohexane

Table 4.4 Summary of the initial release rate and the solubility values of capsaicin synthetic in water and cyclohexane

	Slope of the linear regression	Solubility (mg/L)
In cyclohexane	0.0061	220±0.014
In water	0.0003	8.7±1.7
The ratio of the value of cyclohexane to water	20.3	25.3

In order to predict the release profile for a long-term release, it is necessary to know the mechanism of the release and study the release kinetics. There are a large number of mathematical models describing the release kinetics. As introduced in Section 2.4.3.2, the Zero-order Model, First-order Model, Higuchi Model, Hixson-Crowell Model and Ritger-Peppas Model were investigated to find the most suitable model to predict the release profile of capsaicin synthetic from the microcapsules.

The release constants K of each model and their values of R^2 are calculated as shown in Table 4.5. It is found that the release for all the microcapsules prepared with three different concentrations of PVA is best described by Ritger-Peppas Model with the release exponent n = 0.43, with R^2 values all higher than 97%. Ritger-Peppas Model is a semi-empirical model specifically for the drug release from a polymeric matrix (Bruschi, 2015). This model can be used to investigate the release mechanism unknown or driven by more than one type. Based on its theory and the fact that the release took place from spheres instead of thin films or cylinders, as shown in Table 2.1, n = 0.43, 0.65, 0.85 and 1.20 are selected for the study.

When n = 0.43, the model shows a better linear regression. So it can be implied that the release of capsaicin synthetic from the matrix microcapsules was driven by Fickian diffusion. The rate of the dissolution liquid diffusing into the microcapsules was much faster than the swelling or the relaxation of the polymeric chain, resulting in the time-dependent release. Thus, the Ritger-Peppas Model could be used to describe the release kinetics of capsaicin synthetic from the microcapsules with n = 0.43. The value of K could indicate the release rate of capsaicin synthetic from the microcapsules. It is shown that the release from microcapsules prepared in 0.2% PVA was faster than the ones prepared in 0.5% PVA, while those prepared in 0.1% PVA shows the slowest release rate. The release rate is related to the surface area, the larger it is, the faster the release is. This means the microcapsules prepared in 0.2% PVA have larger surface area than those prepared in 0.1% PVA and in 0.5% PVA, which is consistent with the results of their mean sizes shown in the previous section. The comparison between the experimental data and the modelling fittings is shown in Fig 4.11. It is obvious that the experimental data and the corresponding modelling are fitting well.

Table 4.5 Release kinetics of microcapsules containing capsaicin synthetic, where K is the release constant of each model, R^2 is the coefficient of determination, and the microcapsules were samples prepared in different concentrations of PVA as shown in the previous section (i: 0.1%, ii: 0.2% and iii: 0.5%)

Microcapsules	Zero-order Model		First-order Model		Higuchi Model		Hixson-Crowell Model	
	K_0	R^2	K_1	R^2	K_H	R^2	K_{HC}	R^2
i	0.008	0.346	0.042	0.546	0.076	0.920	0.003	0.558
ii	0.010	0.458	0.058	0.483	0.106	0.945	0.005	0.669
iii	0.007	0.075	0.028	0.552	0.099	0.835	0.003	0.364
Microcapsules	Ritger-Peppas Model							
	n=0.43		n=0.65		n=0.85		n=1.20	
	K_{RP}	R^2	K_{RP}	R^2	K_{RP}	R^2	K_{RP}	R^2
i	0.092	0.976	0.035	0.943	0.017	0.913	0.003	0.765
ii	0.128	0.977	0.052	0.939	0.024	0.898	0.006	0.817
iii	0.107	0.972	0.040	0.918	0.018	0.864	0.004	0.774

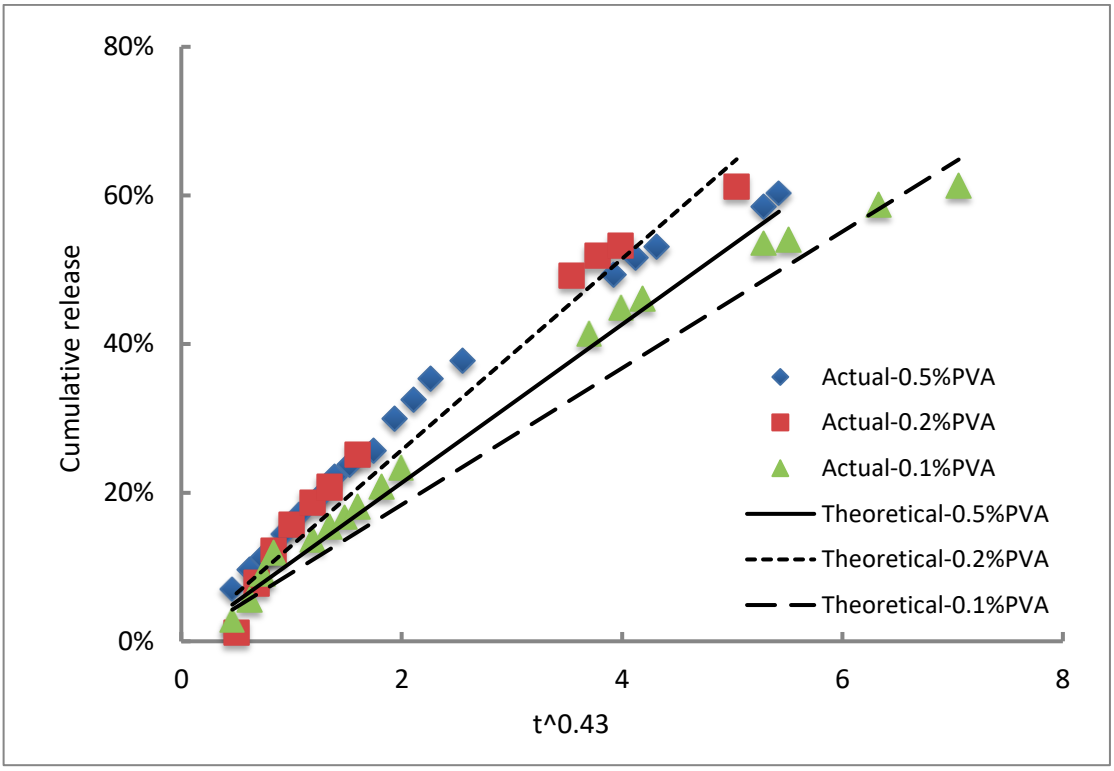

Fig 4.11 The comparison between the experimental data and the modelling fittings of Ritger-Peppas Model with n = 0.43

4.4 Conclusions

In this chapter, the preparation and characterisation of microcapsules containing antifouling agent are demonstrated. The microcapsules were prepared with cellulose acetate butyrate (CAB) as the shell material and capsaicin synthetic as the core material by solvent evaporation based on O/W emulsification. Initially, the effects of 3 emulsifiers: 1% (w/v) Tween 80 solution, 1% (w/v) hydrophilic Aerosil silica suspension and (0.5%, w/v) polyvinyl alcohol (PVA) solution were investigated. It was found that the microcapsules of capsaicin synthetic prepared using PVA were more spherical and smooth compared with the other two emulsifiers. The microcapsules prepared by solvent evaporation had a matrix structure with

multiple cores. The emulsification taking place for 30 min produced spherical and smooth microcapsules. Various concentrations (0.1%, 0.2%, 0.5% and 0.8%, w/v) of PVA in aqueous phase were then used to prepare microcapsules. As the concentration was increased, the microcapsules became less spherical, coarser and more likely to agglomerate, and the encapsulation efficiency reached the highest (88.9%) at a PVA concentration of 0.5%, and the corresponding payload was 17.9%. The effect of agitation speed was also studied. While agitated at 1000 rpm, all the microcapsules were smaller than 60μm, and the encapsulation efficiency and the payload reached 80.7% and 16.5%, respectively. It was found that the payload increased while the core/shell ratio was changed from 1/8 to 1/4 and then to 1/2, as expected. In addition, the mechanical properties of the microcapsules with different ratios of core/shell material (1/2, 1/4, 1/8, w/w) and the pure CAB microparticles were also characterised. There were only elastic and plastic deformations observed for the microcapsules of capsaicin synthetic due to their matrix structure. Hertz theory was used for determining the Young's modulus of the microcapsules. While the ratio of core/shell material was increased (0, 1/8, 1/4 to 1/2), the Young's modulus value decreased significantly, and the microcapsules became less rigid. The microcapsules of capsaicin synthetic were all in Mega Pascal scale and more rigid compared with the different microcapsules prepared by other researchers. Moreover, the release of capsaicin synthetic from microcapsules prepared using three different concentrations of PVA were studied using DI-water and cyclohexane as dissolution liquid, respectively. It was found that cyclohexane could be used for shortening the release duration and predicting the release profile in water by considering the solubility of capsaicin synthetic in each liquid. The release the mechanism and kinetics are discussed as well. Ritger-Peppas Model with n = 0.43 was demonstrated to describe the release kinetics of

capsaicin synthetic from the microcapsules well, and it is concluded that the release from the matrix microcapsules was driven by Fickian diffusion.

CHAPTER 5 METALLIC COATING OF MICROCAPSULES CONTAINING ANTIFOULING AGENT BY ELECTROLESS PLATING

5.1 Introduction

Coatings in marine equipment have been widely used to protect corrosion and fouling on steel surfaces, the bottoms of ships, marine power generators and marine platforms (Carteau et al., 2014; Gittens et al., 2013). It is desirable to apply the coatings with not only antifouling property but also good thermal conductivity so that the coatings would not affect the heat transfer efficiency, which otherwise can cause additional problems such as increase in heat transfer area for a given capacity. As concluded in the previous chapter, the microcapsules with antifouling property have been prepared with cellulose acetate butyrate (CAB) as the shell material by solvent evaporation. With the microcapsules incorporated into the coatings, the thermal property should also be enhanced. It is well known that metals are thermally conductive, so the thermal conductivity of the microcapsules may be promoted by incorporating metal in them. Electroless plating is a widespread method to produce a coating of metal on substrate, and copper has been widely used in a large variety of industries due to its high electrical and thermal conductivities (Sharma et al., 2016). The aim of this chapter is to incorporate metal onto the microcapsules of antifouling agent prepared in the previous chapter with enhanced thermal conductivity.

In this chapter, the preparation and characterisation of microcapsules of capsaicin synthetic containing metal are introduced. The microcapsules containing metallic particles were prepared by three different methods: emulsification with alumina, coating with copper oxide by spray drying and electroless plating of copper. The morphology, the size and size distribution were measured for the microcapsules containing alumina. The morphology of the

microcapsules with copper oxide coated by spray drying is presented and discussed. The electroless plating of copper on the microcapsules have been undertaken, and their morphology, mechanical properties and thermal conductivities were analysed, respectively. The basic experimental details are described in Chapter 3, and the specific experimental details are presented in this chapter.

5.2 Experimental

5.2.1 Preparation of microcapsules of capsaicin containing metallic particles

The microcapsules of capsaicin synthetic with CAB as shell material were prepared by solvent evaporation as described in the previous chapter. The microcapsules with the core/shell ratio 1/4 (w/w), agitation speed of 1000 rpm and the 0.1% (w/v) PVA solution were chosen for the following experiments of metallic coating.

5.2.1.1 Emulsification with Alumina

For the microcapsules containing alumina nano-particles (AEROXIDE® Alu 130 with BET Surface Area 110-150 m^2/g, Evonik, Germany), the preparation of primary CAB microcapsules was also based on the emulsification of oil in water phase. Aluminium oxide (alumina) powders (5%, 10% and 20% of the microcapsules, w/w) were suspended in the solvent, and an ultrasonic tank (45kHz, VWR, Germany) was used for 2 hours for their dispersion. Then the suspension was mixed with the solution of CAB/ethyl acetate, and capsaicin synthetic was subsequently added to form the oil phase. The following procedure

was the same as preparing microcapsules without metallic particles as described in Section 3.3.

5.2.1.2 Coated with copper oxide by spray drying method

The microcapsules were coated with copper oxide by the spray dryer (B290, Buchi, Switzerland). 2g of the microcapsules of capsaicin synthetic and 1g of copper oxide powder (particle size<50nm, Sigma-Aldrich, UK) were suspended in 250mL aqueous solution of acrylic resin (Macpherson Trade Paints, UK) as the binding material, stirred by a magnetic stirrer plate (Stuart, UK) continuously. After the spray dryer was warmed up to 140℃, the suspension was injected into a nozzle (diameter 2.00mm) with feed flow rate of 9mL/min continuously. The dry powders were collected from the sample chamber.

5.2.1.3 Coated with copper by electroless plating

The microcapsules were coated with copper by electroless plating at room temperature. 1g of the microcapsules without polydopamine (PDA) involved were sensitised in 10g/L $SnCl_2$ aqueous solution for 2 hours, subsequently activated in 2mM $NaPdCl_4$ aqueous solution for another 2 hours, and then suspended in Cu^{2+} bath for electroless plating. For the microcapsules with PDA involved, the sensitisation process was excluded. Before the activation process, the microcapsules were suspended in TRIS solution with PDA self-polymerising to introduce the amines on their surfaces, which could help copper grow during the electroless plating. Subsequently, the microcapsules modified by PDA were activated in

2mM $NaPdCl_4$ solution and then suspended in Cu^{2+} bath for electroless plating. The details of the experiments are described in Section 3.4.

5.2.2 Morphology and element analysis of microcapsules

The morphology of microcapsules containing metal was observed by optical microscopy and Scanning Electron Microscopy (SEM) with Energy Dispersive Spectroscopy (EDS), and the samples were all sputtered by gold for electrical conducting. The detailed protocol is provided in Section 3.5.1.

5.2.3 Size and size distribution

The size and size distribution of microcapsules containing metal were measured by Malvern particle sizing, and the experimental details are presented in Section 3.5.2.

5.2.4 Determination of mechanical properties

The mechanical properties of the prepared microcapsules were determined by a micromanipulation technique. For the spherical microcapsules, the compression was carried out using the same protocol as those without metal. For the non-spherical microcapsules which were deformed like a cake, they were placed horizontally on the glass slide and the heights of each flat microcapsules were recorded instead of their diameters. The details of the operation are provided in Section 3.5.4.

5.2.5 Thermal analysis

The thermal conductivity of the metallic microcapsules was measured by Laser Flash Analysing with the value of c_p measured by Differential Scanning Calorimetry (DSC). The microcapsules containing copper prepared under various conditions by electroless plating were analysed, respectively. The details of the experimental conditions are described in Section 3.5.5.

5.3 Results and discussion

5.3.1 Morphology and size distribution of microcapsules containing alumina

For the microcapsules containing alumina nano-particles, the preparation of primary CAB microcapsules was also based on the emulsification of oil in water phase. Fig 5.1 shows the morphologies of microcapsules containing alumina in various amounts (0, 5%, 10% and 20%, w/w). The other preparation conditions remained the same. It is obvious that the microcapsules without alumina have a very spherical morphology and smooth surfaces as shown in Fig 5.1(a). When 5% alumina was added into the emulsification, shown in Fig 5.1(b), the microcapsules appear to be less spherical and oval. However, the microcapsules show irregular shapes with 10% alumina added as shown in Fig 5.1(c). Moreover, when prepared with 20% alumina added into the preparation, none of the spherical microcapsules can be observed in Fig 5.1(d). As the amounts of alumina added into the emulsification increase, the morphology of the microcapsules tends to be less spherical and more irregular. While agitated in the emulsification process, the oil droplets containing alumina generated by

the hydrodynamic force tend to break into irregular shape due to the alumina with higher density. Fig 5.2 shows the size distributions of microcapsules prepared with different amounts of alumina. From Fig 5.2(a), the curve of the size distribution looks relatively narrow with a span value of 1.2. For the microcapsules with 5% alumina as shown in Fig 5.2(b), their size distribution appears to be similar to that without alumina in Fig 5.2(a). While the microcapsules were prepared with 10% alumina, the size distribution is obviously much wider and multi-peaks are observed in Fig 5.2(c). In addition, the microcapsules with 20% as shown in Fig 5.2(d) have a much wider size range (the minimum to maximum) than those with lower amounts of alumina. Overall, the size distribution tends to be wider as the amount of alumina increases due to the irregular morphology measured by laser diffraction of the Mastersizer.

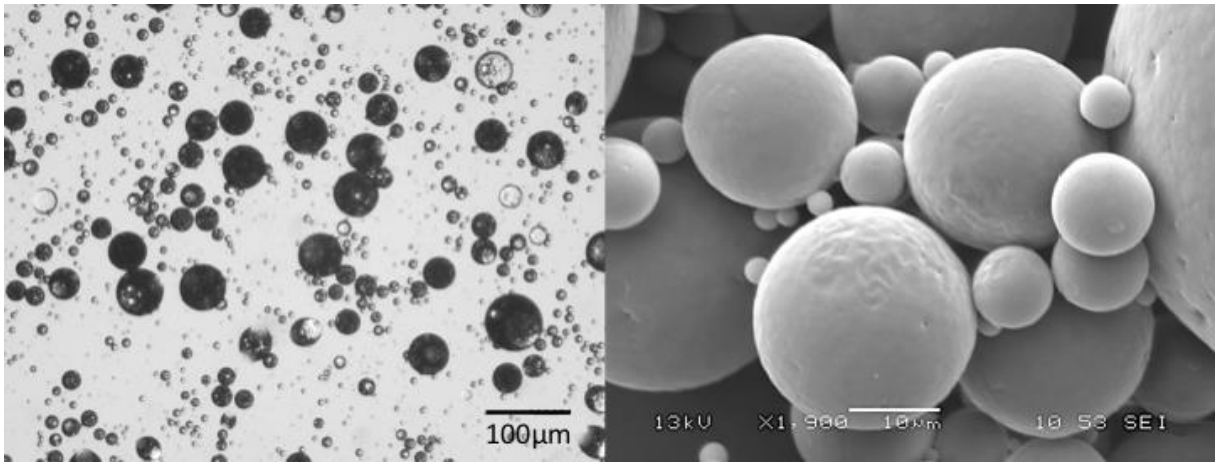

(a) Microcapsules without alumina

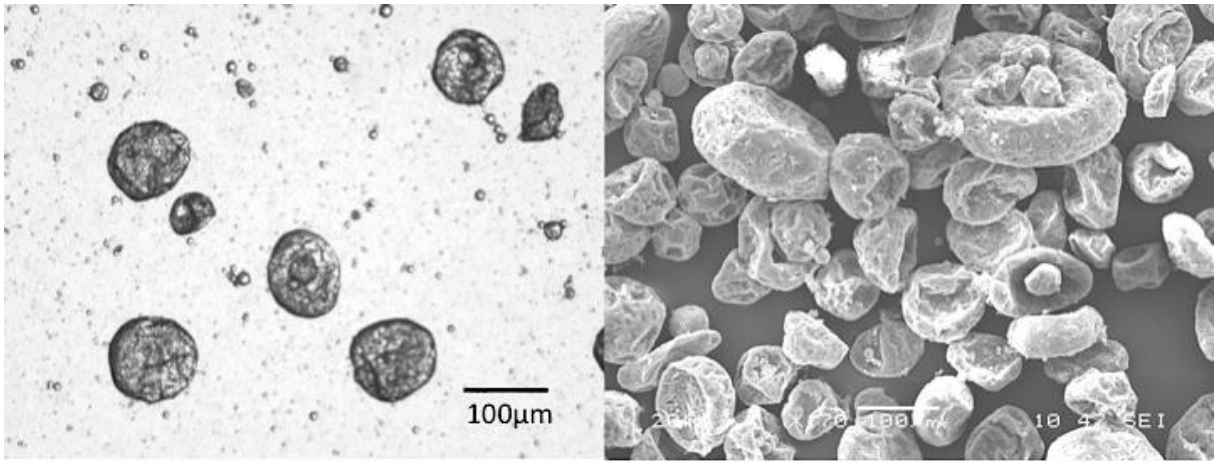

(b) Microcapsules with 5% (w/w) alumina

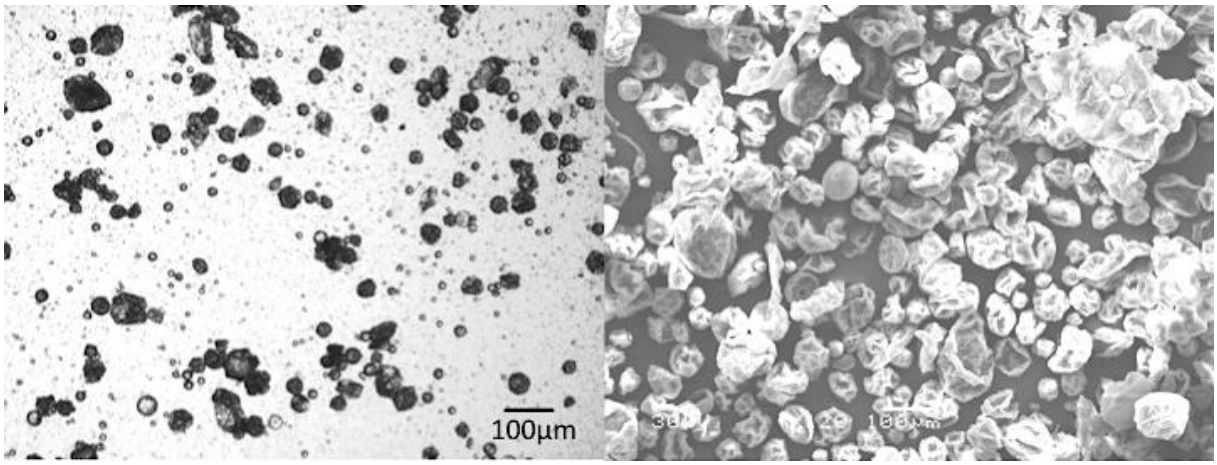

(c) Microcapsules with 10% (w/w) alumina

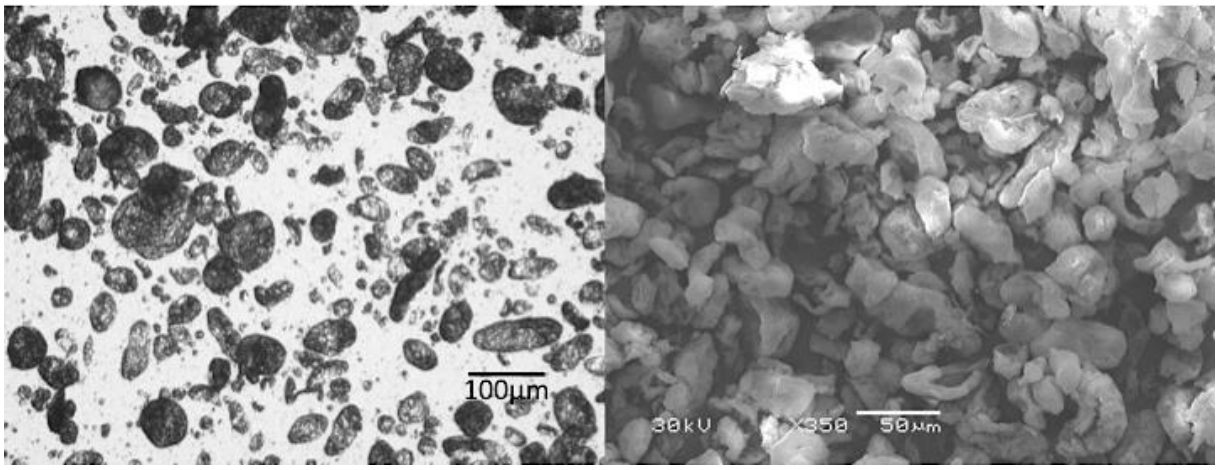

(d) Microcapsules with 20% (w/w) alumina

Fig 5.1 Morphology of microcapsules containing different amount of alumina under optical microscope (left) and SEM (right), the microcapsules were prepared with the core/shell ratio 1/4 (w/w), agitation speed of 1000 rpm and 0.1% (w/v) PVA solution. The same applies to the following microcapsules

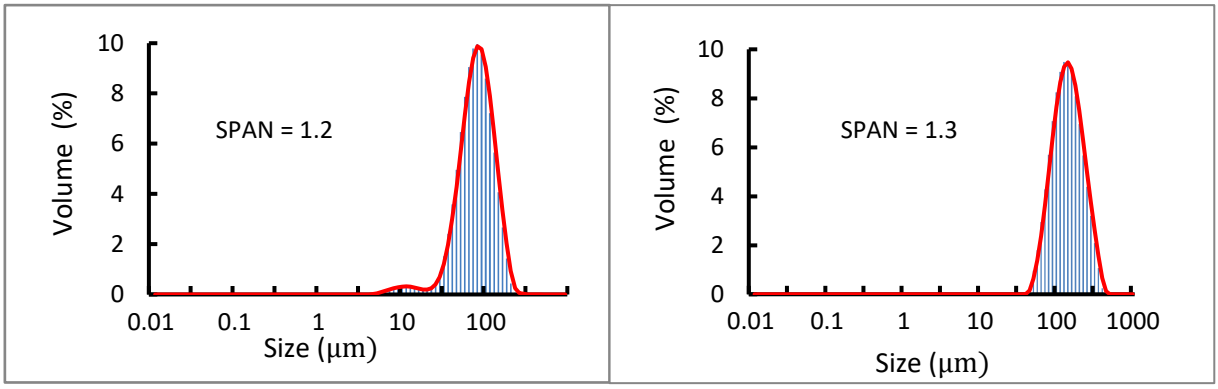

(a) Without alumina

(b) With 5% alumina

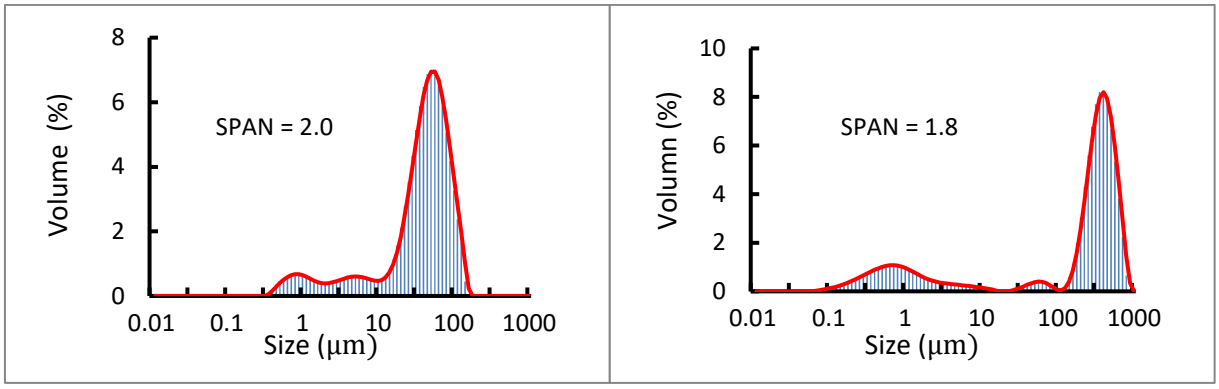

(c) With 10% alumina (d) With 20% alumina

Fig 5.2 Size distributions of microcapsules containing alumina in different amounts prepared with the same other conditions

5.3.2 Morphology of microcapsules coated with copper oxide by spray drying method

The microcapsules coated with copper oxide were prepared by spray drying. Fig 5.3 shows the morphology of the microcapsules under optical microscope and SEM. It is found that the microcapsules appear to be broken into pieces. Spherical and intact microcapsules are hardly observable under the microscope. This may be due to the high operating temperature of the spray drying close to the melting point of CAB. Although the melting temperature range of CAB varies broadly from 127℃ to 240℃ depending on its composition, the spray drying carried out at 140℃even in short time could damage the structure of the CAB microcapsules so that capsaicin synthetic could be released immediately from the microcapsules, which is not desirable.

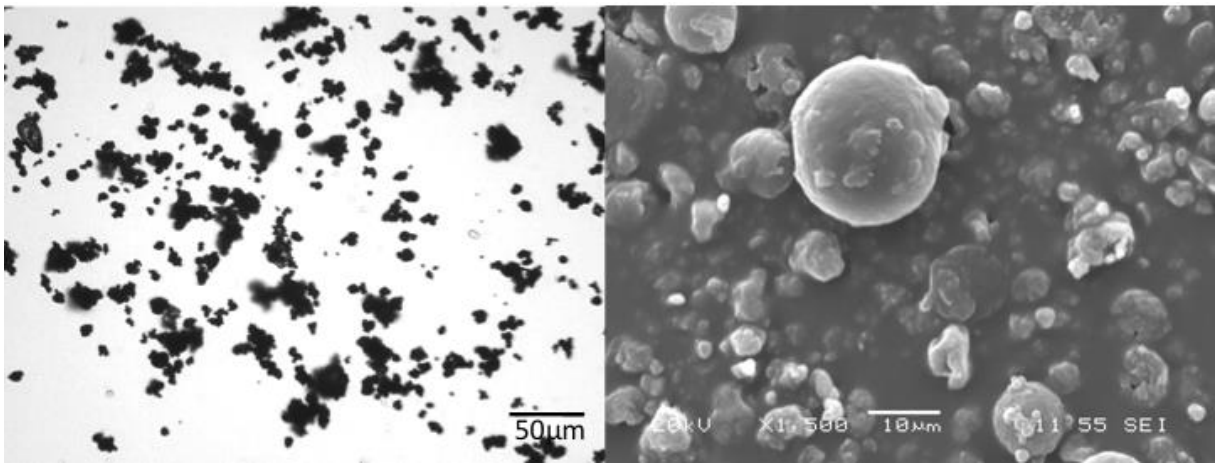

Fig 5.3 Morphology of capsules coated with CuO (2:1, w:w) by spray drying under optical microscope (left) and SEM (right)

5.3.3 Morphology of microcapsules coated with copper by electroless plating

5.3.3.1 Effect of PDA on electroless plating of copper

The microcapsules were further prepared by electroless plating of copper on their surfaces. However, as shown in Fig 5.4(a), no trace of copper was detected by EDS in the microcapsules without PDA involved before the electroless plating. It is difficult to plate copper following the standard procedures of sensitisation and activation (Al-Shannaq et al., 2016). It has been reported that polydopamine (PDA) can be formed as a thin layer on a large variety of substances including microcapsules (Al-Shannaq et al., 2016). Subsequently the surface-modified microcapsules could have metal coated easily on their surfaces by electroless plating because of the amine group (Wang et al., 2011b; Wang et al., 2012; Wu et al., 2015). In contrast to Fig 5.4(a), the microcapsules suspended in the PDA solution before the electroless plating show an obvious amount of copper as displayed in Fig 5.4(b). This means PDA can successfully help the copper deposit on the microcapsules.

Instead of the sensitisation in $SnCl_2$ solution, the microcapsules with PDA as a thin layer on their surface could realise electroless plating easily after the activation in Pd^{2+} solution. It is known that PDA contains amino groups in the molecules (Liu et al., 2014), and Pd^{2+} could bind with the amino groups as shown in Fig 5.5 (Kind et al., 1998). With Pd^{2+} reduced to Pd^0 which is the catalyst of the electroless plating, copper could be subsequently deposited on the surface of microcapsules. Thus, it is necessary to introduce PDA into the process of coating metal on the microcapsules.

However, both dopamine and TRIS have amines as parts of their molecules, which could react with the carbonyl group of CAB as shown in Fig 5.6 and Fig 5.7. Dopamine and TRIS have a primary amine $–RNH_2$ in the molecule and it can react with the carbonyl group to produce imine by addition and dehydration reactions. The intermediates of PDA produced during the reaction may contain secondary amines $–R_2NH$ with which the carbonyl group can react and dehydrate to enamine (Carey, 2000). So far, the formation of PDA and its mechanism are not fully clear, so it is difficult to fully figure out the pathway of the PDA self-polymerisation and the intermediates during the complex redox process (Liebscher et al., 2013; Liu et al., 2014). In order to reduce the negative effects of the amines, it is necessary to control the reacting time of the CAB microcapsules in the PDA solution.

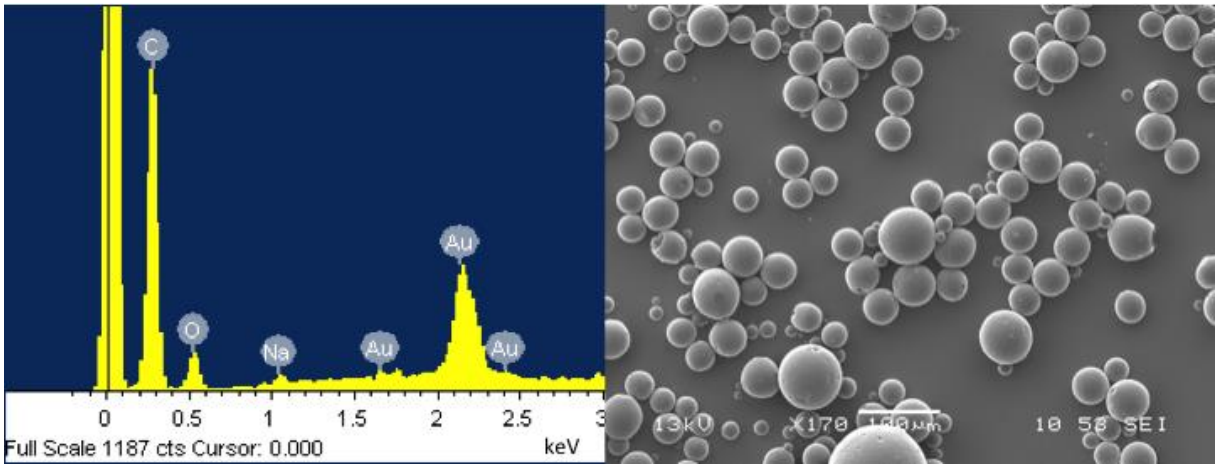

(a) Without PDA

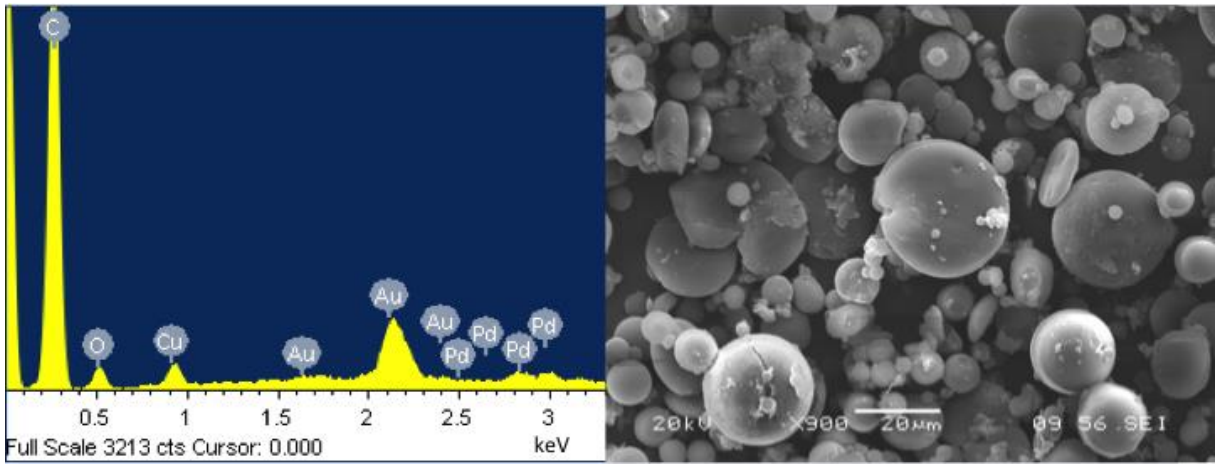

(b) With PDA

Fig 5.4 The EDS results of microcapsules prepared by electroless plating copper without and with PDA involved (left side: EDS spectrum, right side: SEM image), all the samples were sputtered by gold for electrical conduction on the stage of SEM sample preparation

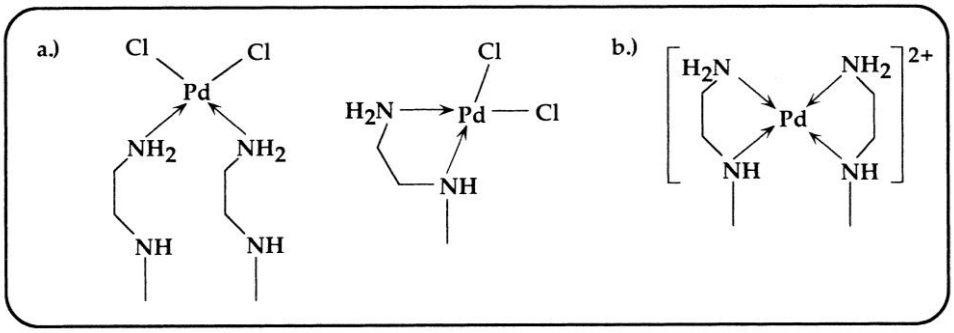

Fig 5.5 Scheme of Pd^{2+} binding with the amine group (Kind et al., 1998)

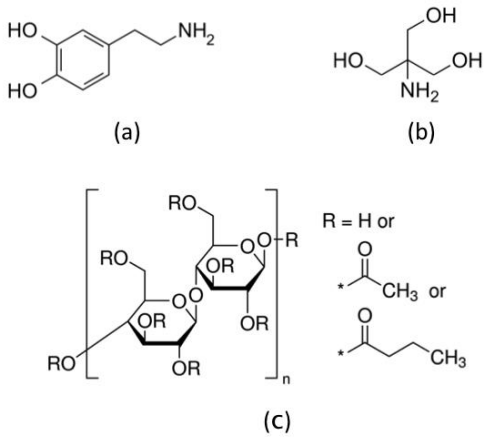

Fig 5.6 Chemical structures of (a) dopamine, (b) tris(hydroxymethyl)aminomethane (TRIS) and (c) cellulose acetate butyrate (CAB)

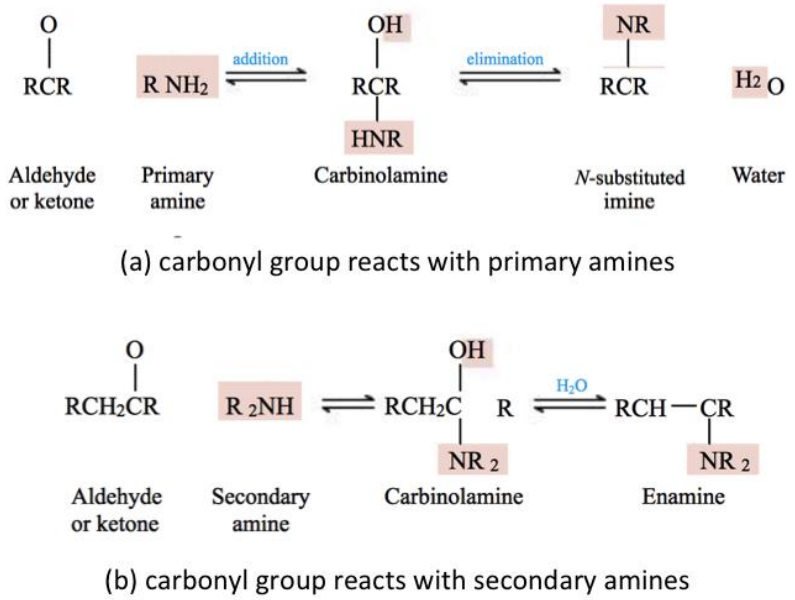

Fig 5.7 Reactions of the carbonyl group with amines (Carey, 2000)

5.3.3.2 Effect of different time of self-polymerising PDA on the morphology of microcapsules

It was carried out to polymerise dopamine before suspending microcapsules in the polydopamine (PDA) solution, as the compositions in the PDA solution could react with the CAB microcapsules during its self-polymerisation. Dopamine hydrochloride was dissolved in TRIS solution to reach the concentration of 2mg/mL and kept stirring for 30 min, 1 hour, 2 hours and 24 hours, respectively, and then the microcapsules were suspended in the PDA-TRIS solution all for 2 hours, followed by electroless plating of copper. Fig 5.8 shows the morphology of microcapsules coated by copper prepared for different time of PDA self-polymerisation. When PDA was self-polymerised for 30 min in Fig 5.8(a), the microcapsules suspended in the PDA solution look still spherical and no crack can be observed under SEM.

For the microcapsules suspended in the pre-formed PDA solution for 1 hour as shown in Fig 5.8(b), there are some cracks observed on the surface but most of them appear to be spherical. While PDA was self-polymerised for 2 hours, as shown in Fig 5.8(c), the microcapsules suspended in the PDA solution look less spherical and flatter with some scars seen on the surface. As for the microcapsules suspended in the pre-formed PDA solution for 24 hours, the spherical morphology of the microcapsules in Fig 5.8(d) was destroyed severely, which may result in the immediate release of capsaicin synthetic from the microcapsules. It can be seen from Fig 5.8(a) to (d) that the microcapsules became less intact and spherical as the time of PDA self-polymerisation was increased from 30min to 24 hours. This may be due to the reaction of the functional groups between CAB microcapsules and a series of intermediates during the complex redox process of PDA as explained previously. The longer they were suspended in the solution, the more contents could react with the compositions in the solution. So shortening the time of pre-forming PDA is more desirable to maintain the morphology of the CAB microcapsules but it may cause a low amount of copper coated on the microcapsules in the following processes. Therefore, 1 hour has been chosen to pre-form PDA for the subsequent electroless copper plating.

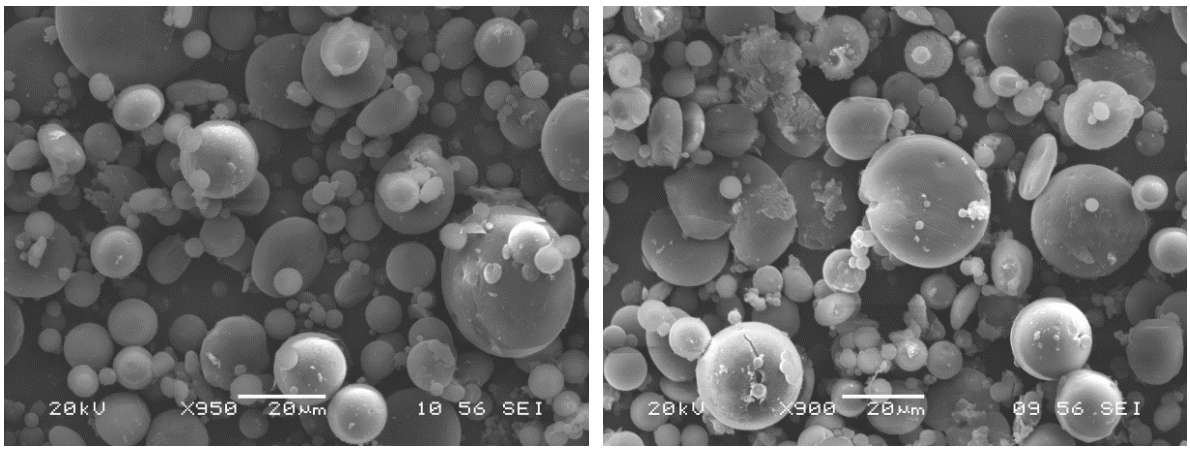

(a) 30 min (b) 1 hour

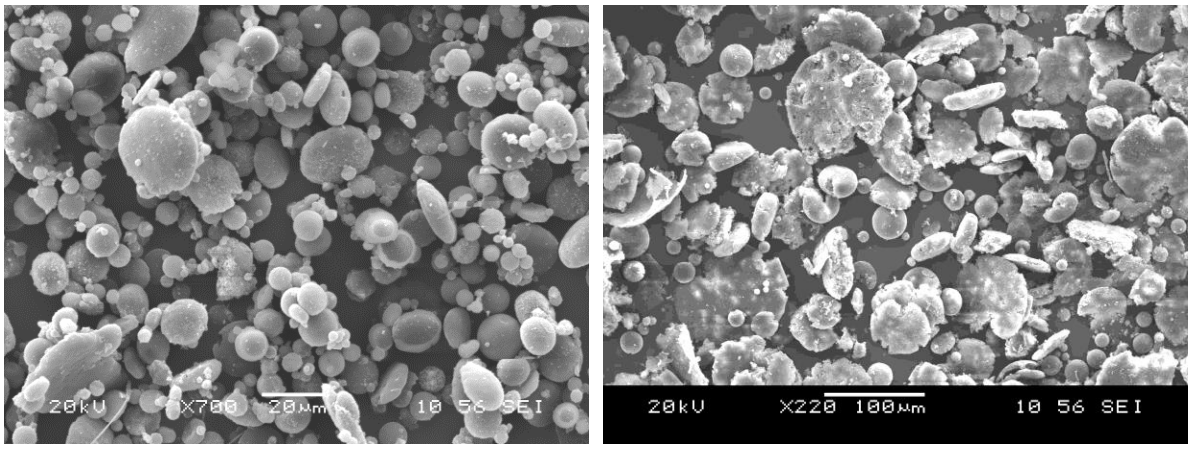

(c) 2 hours (d) 24 hours

Fig 5.8 Morphology of microcapsules coated by Cu with pre-forming PDA for various time under SEM, followed by suspending capsules in PDA for 2 hours and the electroless plating of copper

5.3.3.3 Effect of different suspending time of microcapsules in the pre-formed PDA solution (1h) on the morphology and the relative amount of Cu plated

Based on the effect of different PDA pre-forming time on the morphology above, 1 hour was chosen to investigate the effect of different suspending time of microcapsules on the morphology and the relative amount of copper plated. Dopamine hydrochloride was dissolved in TRIS solution and kept stirring for 1 hour, and then the microcapsules were suspended in the PDA-TRIS solution for 30 min, 1 hour, 2 hours and 3 hours, respectively, followed by electroless plating of copper. Fig 5.9 shows the morphology of the microcapsules coated by copper prepared after suspended in the pre-formed PDA solution for different lengths of time. As can be seen in (a) and (b), the morphologies of the microcapsules suspended for 30 min and 1 hour are almost spherical. For the microcapsules suspended in the PDA solution for 2

hours as shown in (c), most of them are still spherical, but some are flatter and a few cracks can be observed on their surface. As for the microcapsules suspended in PDA solution for 3 hours, it is very obvious in (d) that their spheres were completely damaged into pieces. It is obvious that the microcapsules became less intact and less spherical as the suspending time in the PDA solution was prolonged from 30 min to 3 hours, due to the reaction between the carbonyl group and amines. Fig 5.10 shows the comparison of the relative amounts of copper plated on the microcapsules prepared for different suspending time in the PDA solution. The relative amounts of copper detected from the microcapsules with 30-min and 1-hour suspending time are only 0.9% and 1.0% (w%), respectively. This may be due to the insufficient time for the intermediates of PDA attaching on the microcapsules. When the suspending time was increased from 1 hour to 2 hours, the relative amount of copper rose rapidly to 5.4%. It can be considered that the dopamine is self-polymerising and adhering gradually on the microcapsules. For the microcapsules suspended for 3 hours, the relative amount of copper reached 6.4%. As the structure of the microcapsules was damaged progressively after two-hour suspending, the inner structure was gradually exposed to the solution where the intermediates of PDA might not have sufficient time to deposit. So the amount of copper still increased but the increasing rate was slower than before. By considering both the morphology of the microcapsules and the amount of copper plated on the surface, therefore, it is suggested that the desirable condition was to suspend the CAB microcapsules for 2 hours after the self-polymerisation of PDA for 1 hour.

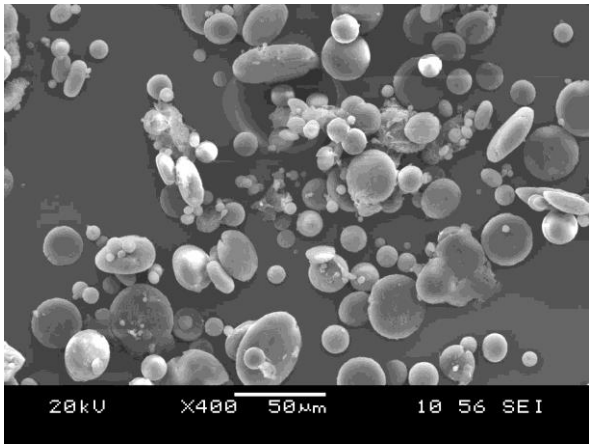

(a) 30 min

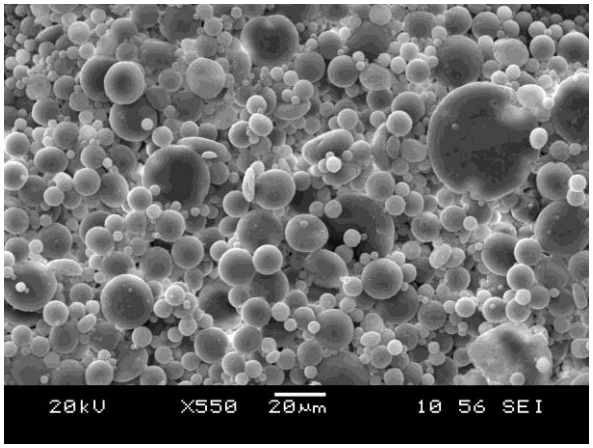

(b) 1 hour

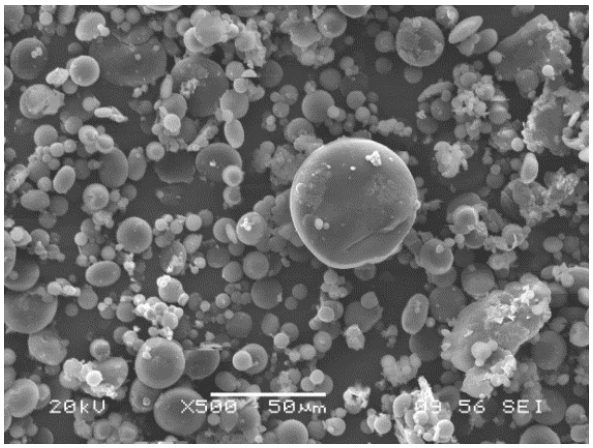

(c) 2 hours

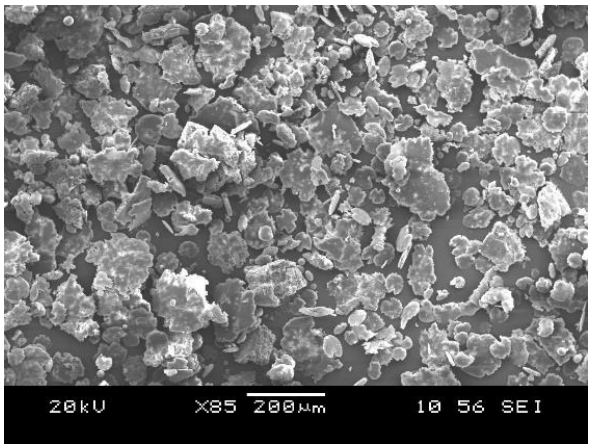

(d) 3 hours

Fig 5.9 Morphology of microcapsules coated by Cu suspending in the pre-forming PDA for 1 hour and various lengths of suspending time in PDA under SEM, followed by the electroless plating of copper

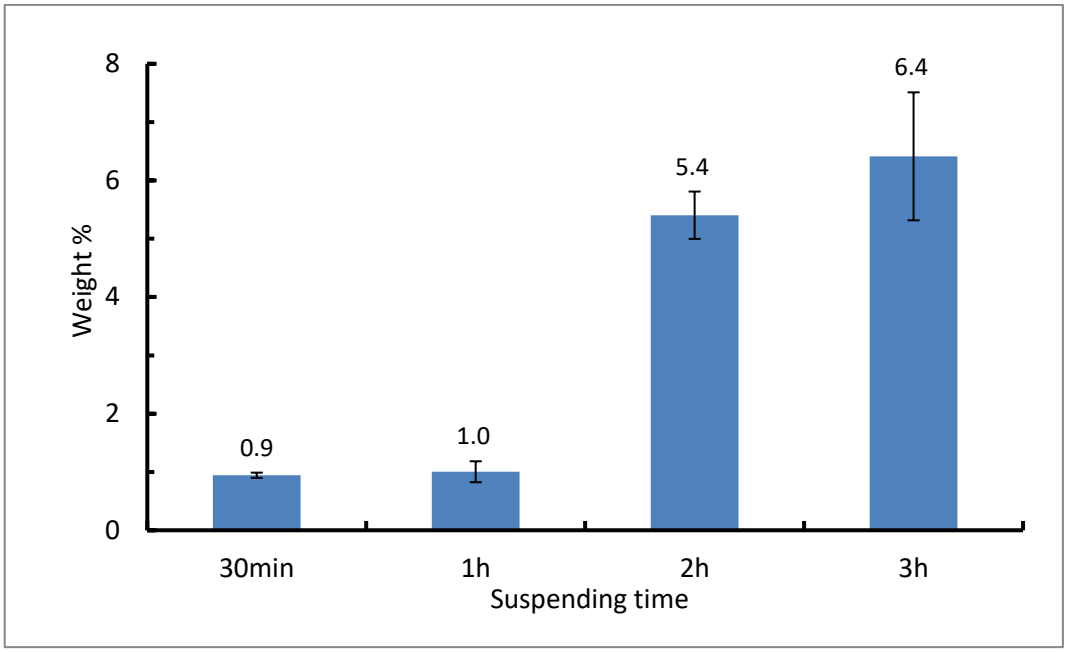

Fig 5.10 Relative amount of copper plated on the microcapsules for different suspending time in the pre-formed PDA solution for 1 hour (detected by EDS, error bars represent the standard error)

5.3.4 Mechanical properties of microcapsules containing copper prepared by electroless plating

The mechanical properties of the microcapsules containing copper prepared by electroless plating were characterised by the micromanipulation technique, and the Young's modulus values of microcapsules in each sample were calculated by Hertz model as described in Section 3.5.4. As known that Young's modulus can indicate the stiffness of the material, the high value it has, the more rigid it is (Roylance, 2008). The mean Young's modulus value of the microcapsules containing copper prepared by electroless plating under different conditions are presented in Fig 5.11 and Fig 5.12.

Fig 5.11 shows the Young's modulus of microcapsules containing copper prepared by electroless plating with different lengths of time of PDA self-polymerising from 30 min to 2 hours. The dopamine was self-polymerised for various lengths of time and then all the microcapsules were suspended in the pre-formed PDA solution for 2 hours. As can be seen from the graph, when PDA was self-polymerising for 30 min, the mean Young's modulus of microcapsules suspended in the PDA solution is 502MPa. When the time of PDA self-polymerisation was increased to 1 hour, the Young's modulus reaches 723MPa. With the self-polymerisation of PDA for 2 hours, the microcapsules suspended in the PDA solution have a higher value of Young's modulus 876MPa. It is obvious that the value of Young's modulus increased significantly and the microcapsules became stiffer, while the dopamine was self-polymerised for longer time (from 30 min up to 2 hours) before suspending the microcapsules in the PDA solution.

Fig 5.12 presents the Young's modulus of microcapsules containing copper with different suspending time in the PDA solution. The dopamine was self-polymerised for 1 hour and then the microcapsules were suspended in the pre-formed PDA solution for 30 min to 3 hours. When suspending the microcapsules in the PDA solution for 30 min, the Young's modulus is 661MPa. When the suspending time was increased to 1 hour, the Young's modulus reaches 705MPa. After the microcapsules were suspended in the PDA solution for 2 hours, the Young's modulus rises to 723MPa. While suspending the microcapsules for 3 hours, the Young's modulus of the microcapsules becomes 997MPa. Clearly, the Young's modulus increased as the suspending time of microcapsules in the pre-formed PDA solution was prolonged from 30 min to 3 hours, which helped to enhance their stiffness.

Thus, it is clear that prolonging the time of both self-polymerising PDA and suspending microcapsules in the PDA solution could make the microcapsules become stiffer. In addition, by comparing with the Young's modulus value of 204MPa for the microcapsules without metal prepared in the same other conditions (data presented in Chapter 4), all the microcapsules containing copper had much higher values of Young's modulus. Similarly, no rupture of the metallic microcapsules was shown under compression. Therefore it can be implied that the microcapsules with copper were much more rigid than those without any metallic composition. From this point of view, the electroless plating of copper on the microcapsules could significantly enhance their mechanical stiffness.

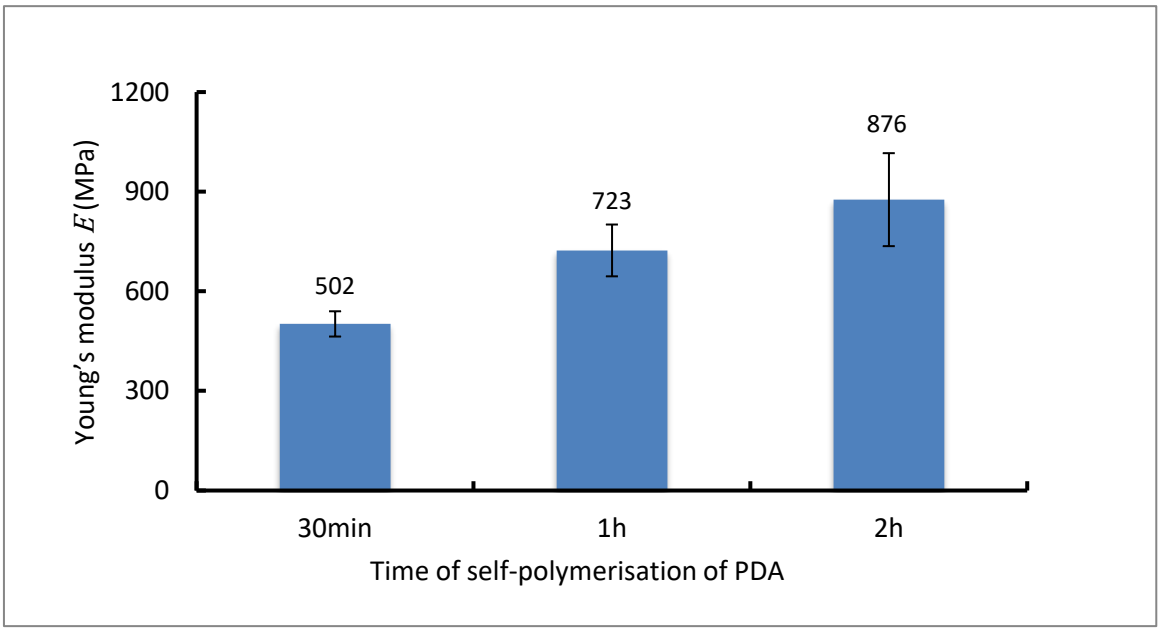

Fig 5.11 Young's modulus of microcapsules containing Cu prepared by electroless plating with different lengths of time for PDA self-polymerisation before microcapsules were suspended in the PDA solution for 2 hours (error bars represent the standard error)

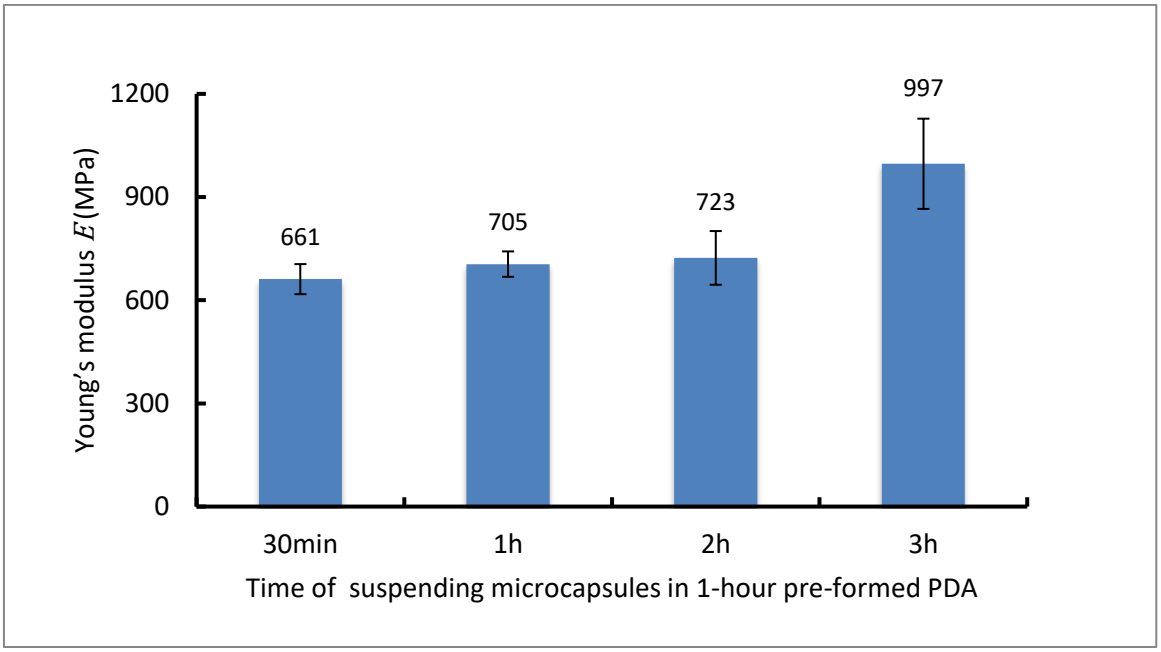

Fig 5.12 Young's modulus of microcapsules containing Cu prepared by electroless plating with different lengths of suspending time in the PDA solution pre-formed for 1 hour (error bars represent the standard error)

5.3.5 Thermal conductivity of microcapsules containing copper prepared by electroless plating

The thermal properties of the microcapsules containing copper prepared by electroless plating were characterised by laser flash technique, and the thermal conductivity data was obtained. The microcapsules without metallic coating prepared with the same other conditions had a value of thermal conductivity 0.07 W/(m·K). A typical example of the original data of the thermal diffusivity and the thermal conductivity analysed by Laser Flash Apparatus (LFA) is shown in Fig 5.13. The thermal conductivities of the microcapsules containing copper prepared by electroless plating under different conditions are shown in Fig 5.14 and Fig 5.15.

Fig 5.14 shows the thermal conductivities of microcapsules containing copper prepared by electroless plating with different lengths of time for PDA self-polymerising from 30 min to 2 hours. The dopamine was self-polymerised for various lengths of time and then all the microcapsules were suspended in the pre-formed PDA solution for 2 hours. As shown in the figure, the thermal conductivity of the microcapsules suspended in the 30-minute pre-formed PDA solution is only 0.078±0.001 W/(m·K), which is close to the value of the microcapsules prepared without copper. When the PDA was self-polymerised for 1 hour, the microcapsules suspended in it have a value of thermal conductivity 0.143±0.002 W/(m·K). When suspended in the 2-hour pre-formed PDA solution, the microcapsules have the thermal conductivity 0.212±0.003 W/(m·K). Compared with the thermal conductivity of microcapsules without copper, these microcapsules all showed enhanced thermal property. As the PDA self-polymerisation time was prolonged, the thermal conductivity of the microcapsules suspended in PDA and coated by copper increased.

Fig 5.15 presents the thermal conductivities of microcapsules containing copper with different lengths of suspending time in the PDA solution. The dopamine was self-polymerised for 1 hour and then the microcapsules were suspended in the pre-formed PDA solution from 1 hour to 3 hours. When suspending the microcapsules in the PDA solution for 1 hour, the thermal conductivity is only 0.072±0.001 W/(m·K). When the suspending time was increased to 2 hours, the thermal conductivity reaches 0.143±0.002 W/(m·K). While suspending the microcapsules for 3 hours, the thermal conductivity of the microcapsules increases to 0.492±0.002 W/(m·K), which is 7 times as high as that of the microcapsules without metal. It is obvious that the thermal conductivity increased while the suspending time of microcapsules in the 1-hour pre-formed PDA solution was extended from 1 hour to 3 hours.

Therefore, it has been demonstrated that the thermal conductivity was enhanced by incorporating metal on the microcapsules by electroless plating. And prolonging the time of both PDA self-polymerisation and suspending microcapsules was beneficial to promote their thermal conductivities so that the microcapsules with metal could conduct heat more easily when incorporated into the marine coatings in the end-use.

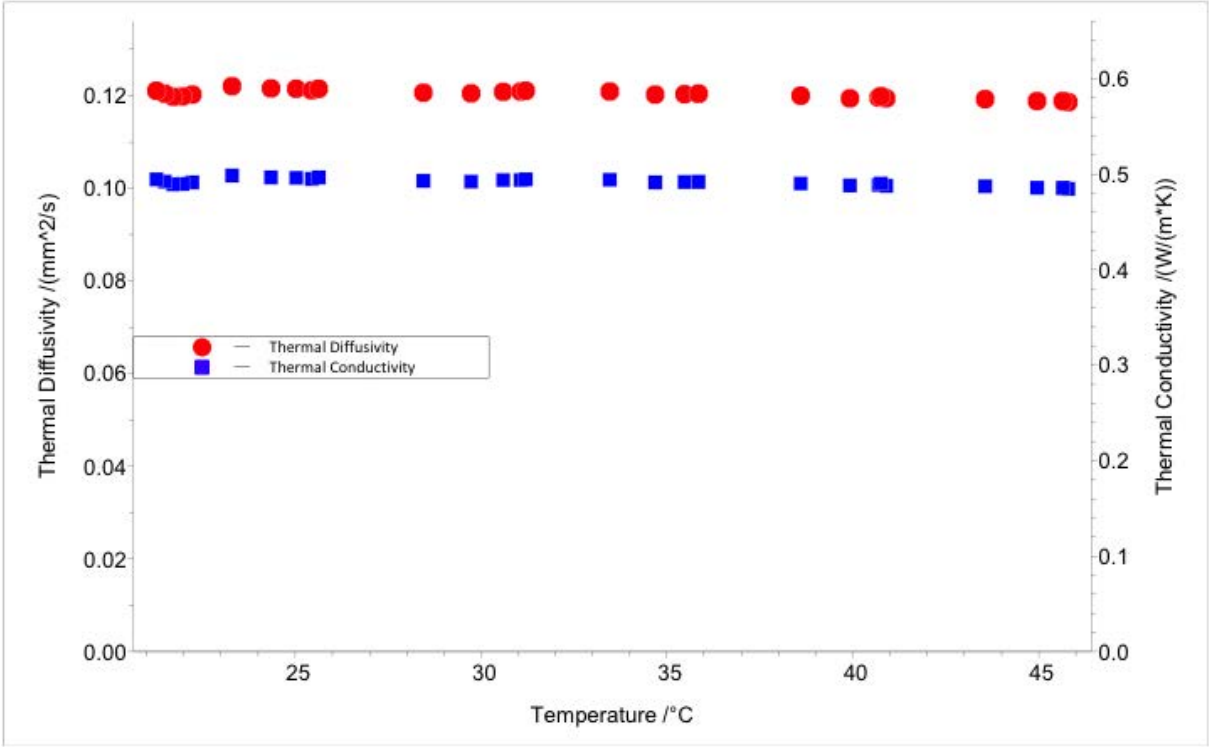

Fig 5.13 A typical example of the original data of the thermal diffusivity and the thermal conductivity analysed by Laser Flash Apparatus (LFA) (the sample was the microcapsules suspended in the 1-hour pre-formed PDA solution for 3 hours before the electroless plating)

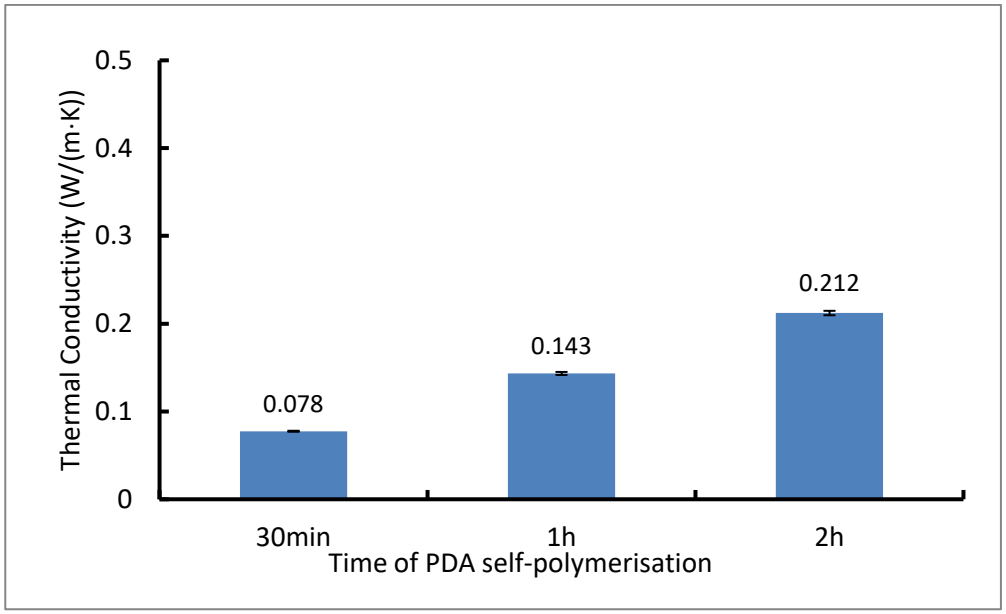

Fig 5.14 Thermal conductivities of microcapsules containing Cu prepared by electroless plating with different lengths of time for PDA self-polymerisation before microcapsules were suspended in the PDA solution for 2 hours

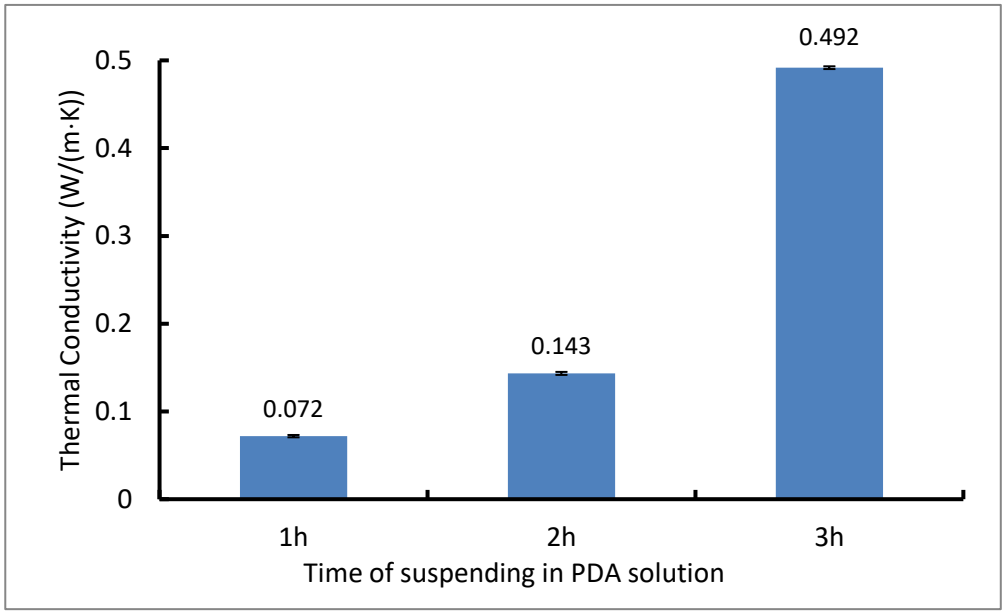

Fig 5.15 Thermal conductivities of microcapsules containing Cu prepared by electroless plating with different lengths of time for suspending microcapsules in the PDA solution pre-formed for 1 hour

5.4 Conclusion

In this chapter, the preparation methods and characterisation results of microcapsules of capsaicin synthetic containing metal are presented. The microcapsules of capsaicin synthetic with CAB as shell material were prepared by solvent evaporation as described in the previous chapter. The microcapsules with the core/shell ratio 1/4 (w/w), agitation speed of 1000 rpm and 0.1% (w/v) PVA solution were chosen for the following experiments of metallic coating. The microcapsules containing metallic particles were prepared by three different methods: emulsification with alumina, coating with copper oxide by spray drying and electroless plating of copper. The morphology of the microcapsules prepared with alumina in the O/W emulsification tended to be less spherical and more irregular and their size distribution was wider as the amounts of alumina was increased from 5% to 20% (w/w). The microcapsules with copper oxide prepared by spray drying appeared to be broken into pieces, and spherical and intact microcapsules were hardly observable under the microscope due to the high operating temperature required for the spray drying process. The microcapsules were then prepared by electroless plating of copper on their surfaces. However, following the standard procedures of sensitisation and activation did not lead to successful outcomes. Instead of the sensitisation in $SnCl_2$ solution, the microcapsules were suspended in the polydopamine (PDA) solution to form a thin layer of PDA with the amine group on their surfaces before the activation and the electroless plating of copper were undertaken. As the compositions in the PDA solution could react with the CAB microcapsules during its self-polymerisation, it was carried out to polymerise dopamine before suspending microcapsules in the polydopamine (PDA) solution. The microcapsules became less intact and spherical as the time of PDA self-

polymerisation was increased from 30 minutes to 24 hours due to the possible reaction of the functional groups between CAB microcapsules and a series of intermediates during the complex redox process. Therefore pre-forming PDA for 1 hour was chosen in the following experiments for investigating the effect of microcapsules suspending time in the PDA solution. The microcapsules were found to be less intact and less spherical while the suspending time in the PDA solution was prolonged from 30 minutes to 3 hours, but the relative amount of copper plated on the microcapsules increased. Besides, the mechanical properties of the microcapsules containing copper prepared by electroless plating were characterised. Prolonging the time of both self-polymerising PDA and suspending microcapsules obviously increased the value of Young's modulus, which made the microcapsules become stiffer. And the microcapsules with copper were proved much more rigid than those without any metallic composition, based on the higher values of Young's modulus of the former. In addition, the thermal conductivities were also characterised for the microcapsules containing copper. The thermal conductivities were enhanced up to 7 times by incorporating copper and prolonging the time of both self-polymerising PDA and suspending microcapsules. Thus, the electroless plating of copper with the help of PDA on the antifouling microcapsules could achieve the enhanced mechanical properties and thermal properties.

CHAPTER 6 OVERALL CONCLUSIONS AND RECOMMENDATIONS FOR FUTURE WORK

6.1 Overall conclusions

The aim of this project was to prepare microcapsules with enhanced thermal properties for potential applications in coatings to achieve its sustained release of an antifouling agent in marine environment, which can prevent the adhesion of the microbial organisms to the surface of equipment. The specific objectives were to encapsulate capsaicin as an antifouling agent in microcapsules with high payload, sufficient mechanical stability, sustainable release rate in water environment and high heat conductivity.

Capsaicin synthetic (n-vanillylnonanamide) was selected as the active ingredient of the antifouling microcapsules, and cellulose acetate butyrate (CAB) was selected as the shell material due to its outstanding properties. Solvent evaporation method was used to prepare microcapsules, based on oil in water (O/W) emulsification in a stirred vessel with a Rushton turbine. Initially, the effects of 3 emulsifiers: 1% (w/v) Tween 80 solution, 1% (w/v) hydrophilic Aerosil silica suspension and (0.5%, w/v) polyvinyl alcohol (PVA) solution were investigated. It was found that the microcapsules of capsaicin synthetic prepared using PVA were more spherical and had more smooth surface compared with the other two emulsifiers. The microcapsules prepared by solvent evaporation had a matrix structure with multiple cores. The emulsification taking place for 30 min produced spherical microcapsules with smooth surface. Various concentrations (0.1%, 0.2%, 0.5% and 0.8%, w/v) of PVA in aqueous phase were then used to prepare microcapsules. As the concentration was increased, the microcapsules became less spherical, coarser and more likely to agglomerate, and the encapsulation efficiency reached the highest (88.9%) at a PVA concentration of 0.5%, and the

corresponding payload was 17.9%. The effect of agitation speed was also studied. While agitated at 1000 rpm, all the microcapsules were smaller than 60μm, and the encapsulation efficiency and the payload reached 80.7% and 16.5%, respectively. It was found that the payload increased while the core/shell ratio (w/w) was changed from 1/8 to 1/4 and then to 1/2, as expected. In addition, the mechanical properties of the microcapsules with different ratios of core/shell material (1/2, 1/4, 1/8, w/w) and the pure CAB microparticles were also characterised. The microcapsules of capsaicin synthetic showed elastic and plastic deformations under compression, but not rupture for the experimental conditions investigated due to their matrix structure. Hertz model was used for determining the Young's modulus of the microcapsules. While the ratio of core/shell material was increased (0, 1/8, 1/4 to 1/2, w/w), the Young's modulus value decreased significantly, and the microcapsules became less rigid. The Young's modulus values of all the microcapsules were all in Mega Pascal scale and stiffer compared with many different microcapsules prepared by other researchers. Moreover, the release of capsaicin synthetic from microcapsules prepared using 3 different concentrations of PVA were studied using DI-water and cyclohexane as dissolution liquid, respectively. It was found that cyclohexane could be used for shortening the release duration and predicting the release profile in water by considering the solubility of capsaicin synthetic in each liquid. The release mechanism and kinetics are discussed as well. Ritger-Peppas Model with n = 0.43 was demonstrated to describe the release kinetics of capsaicin synthetic from the microcapsules well, and it is concluded that the release from the matrix microcapsules was driven by Fickian diffusion.

The microcapsules with metal on their surface were prepared by electroless plating copper after generating a layer of polydopamine based on its self-polymerisation of dopamine. The microcapsules of capsaicin synthetic with CAB as shell material were prepared by solvent

evaporation as described in the previous chapter. The microcapsules with the core/shell ratio 1/4 (w/w), agitation speed of 1000 rpm and 0.1% (w/v) PVA solution were chosen for the following experiments of metallic coating. The microcapsules containing metallic particles were prepared by three different methods: emulsification with alumina, coating with copper oxide by spray drying and electroless plating of copper. The morphology of the microcapsules prepared with alumina in the O/W emulsification tended to be less spherical and more irregular and their size distribution was wider as the amounts of alumina was increased from 5% to 20% (w/w). The microcapsules with copper oxide prepared by spray drying appeared to be broken into pieces, and spherical and intact microcapsules were hardly observable under the microscope due to the high operating temperature required for the spray drying process. The microcapsules were then prepared by electroless plating of copper on their surfaces. However, following the standard procedures of sensitisation and activation did not lead to successful outcomes. Instead of the sensitisation in $SnCl_2$ solution, the microcapsules were suspended in the polydopamine (PDA) solution to form a thin layer of PDA with the amine group on their surfaces before the activation and the electroless plating of copper were undertaken. As the compositions in the PDA solution could react with the CAB microcapsules during its self-polymerisation, it was carried out to polymerise dopamine before suspending microcapsules in the PDA solution. The microcapsules became less intact and spherical as the time of PDA self-polymerisation was increased from 30 minutes to 24 hours due to the possible reaction of the functional groups between CAB microcapsules and a series of intermediates during the complex redox process. Therefore pre-forming PDA for 1 hour was chosen in the following experiments for investigating the effect of microcapsules suspending time in the PDA solution. The microcapsules were found to be less intact and less spherical while the suspending time in the PDA solution was prolonged from 30 minutes to 3 hours, but the relative amount of

copper plated on the microcapsules increased. Besides, the mechanical properties of the microcapsules containing copper prepared by electroless plating were characterised. Prolonging the time of both self-polymerising PDA and suspending microcapsules obviously increased the value of Young's modulus, which made the microcapsules stiffer. And the microcapsules with copper were proved much stiffer than those without any metallic composition, based on the higher values of Young's modulus of the former. In addition, the thermal conductivities were also characterised for the microcapsules containing copper. The thermal conductivities were enhanced up to 7 times by incorporating copper and prolonging the time of both self-polymerising PDA and suspending microcapsules. Thus, the electroless plating of copper with the help of PDA on the antifouling microcapsules could achieve the enhanced mechanical properties and thermal properties.

6.2 Future work

Based on the results obtained from the current work, in the future the research could focus not only on the improvement of the preparation of microcapsules with metal but also on the performance of the antifouling microcapsules in the coatings in the end-use.

In the work presented in Chapter 4, the microcapsules with the antifouling agent were prepared by solvent evaporation, which demonstrated to achieve sustained release over a few months. The process was based on lab scale, therefore the further work could include the scale up of the process for preparation of antifouling microcapsules.

In Chapter 5, coating of the microcapsules on their surface were prepared by electroless plating copper after generating a layer of polydopamine based on its self-polymerisation of

dopamine, achieving the aim of enhancing thermal conductivity of the antifouling microcapsules. However, the morphology of the microcapsules was affected due to the reaction with polydopamine. It is desirable to investigate the milder conditions of the polymerisation of dopamine on the CAB microcapsules so that more metal could be deposited by electroless plating to further enhance the thermal conductivity.

In addition, after the mechanical and thermal properties of the microcapsules are enhanced, they should be incorporated into marine coatings that will then be applied to metal surfaces. The mechanical stability of the microcapsules in the coating on metal surfaces and their thermal conductivity should be studied. The release rate of the active ingredient from the microcapsules to be incorporated into the coatings on metal surfaces in marine environment will be determined, and their antifouling performances be validated, which has not been realised due to the time limit of this project.

APPENDIX

List of Publications:

[1] Zhang, Y., Mustapha, A., Zhang, X., Baiocco, D., Davies, T., Wellio, G., Zhang, Z., Li, Y., 2020. Improved volatile cargo retention and mechanical properties of capsules via sediment-free in situ polymerization with cross-linked poly(vinyl alcohol) as an emulsifier. Journal of Colloid and Interface Science (submitted).

XZ's Contributions: synthesis of capsules, and measurements of their size distribution, mechanical properties and structure.

[2] Zhang, Y., Baiocco, D., Mustapha, A., Zhang, X., Yu, Q., Wellio, G., Zhang, Z., Li, Y., 2020. Hydrocolloids: nova materials assisting encapsulation of volatile phase change materials for cryogenic energy transport and storage. Chemical Engineering Journal 382: 123028.

XZ's contribution: measurement of the mechanical properties of the microcapsules including data analysis.

[3] Zhou, J., Zhang, X., Yan, Y., Hu, J., Wang, H., Cai, Y., Qu, J., 2019. Preparation and characterization of a novel antibacterial acrylate polymer composite modified with capsaicin. Chinese Journal of Chemical Engineering (in press), https://doi.org/10.1016/j.cjche.2019.03.024.

XZ's contribution: design of some experiments.

[4] Hu, J., Zhang, X., Qu, J., 2018. Investigation on the mechanical properties of polyurea (PU)/melamine formaldehyde (MF) microcapsules prepared with different chain extenders. Journal of Microencapsulation 35: 219-228.

XZ's contribution: measurement of the mechanical properties of some microcapsule samples.

[5] Wang, H., Zhang, X., Zhu, W., Jiang, Y., Zhang, Z., 2018. Facile fabrication of biodegradable Zein-based microcarrier system for colon-targeted oral drug delivery. Industrial & Engineering Chemistry Research 57: 12689−12699.

XZ's contribution: measurement of the mechanical properties of some microcapsule samples.

[6] Hu, J., Zhang, X., Qu, J., Wen, Y., Sun, W., 2018. Synthesis, characterizations and mechanical properties of microcapsules with dual shell of polyurethane (PU)/melamine formaldehyde (MF): effect of different chain extenders. Industrial & Engineering Chemistry Research 57: 3591-3601.

XZ's contribution: measurement of the mechanical properties of some microcapsule samples.

[7] Lu, Z., Zhang, X., Hu, J., Wen, Y., Zhang, Z., Qu, J., 2018. Preparation of environmental-friendly microcapsules with antifouling property. CN108753012A.

XZ's contributions: preparation and characterisation of the microcapsules.

[8] Zhang, X., 2017. Microencapsulation of an antifouling agent by solvent evaporation. New Frontiers in Colloid Science, Birmingham, UK.

[9] Zhang, X., Hu, J., Zhang, Z., 2017. Preparation and characterisation of antifouling and antiseptic microcapsules. ChemEngDayUK, Birmingham, UK.

BIBLIOGRAPHY

Abad, B., Borca-Tasciuc, D.A., Martin-Gonzalez, M.S., 2017. Non-contact methods for thermal properties measurement. Renew Sust Energ Rev 76, 1348-1370.

Aguiar, J., Estevinho, B.N., Santos, L., 2016. Microencapsulation of natural antioxidants for food application – The specific case of coffee antioxidants – A review. Trends Food Sci Technol 58, 21-39.

Al-Shannaq, R., Kurdi, J., Al-Muhtaseb, S., Farid, M., 2016. Innovative method of metal coating of microcapsules containing phase change materials. J Sol 129, 54-64.

Altshuller, A.P., Everson, H.E., 1953. The Solubility of Ethyl Acetate in Water. J Am Chem Soc 75, 1727-1727.

Ang, L.M., Hor, T.S.A., Xu, G.Q., Tung, C.H., Zhao, S.P., Wang, J.L.S., 2000. Decoration of activated carbon nanotubes with copper and nickel. Carbon 38, 363-372.

Badmeier, R., Chen, H., 1993. Hydrolysis of Cellulose Acetate and Cellulose Acetate Butyrate Pseudolatexes Prepared by a Solvent Evaporation-Microfluidization Method. Drug Dev Ind Pharm 19, 521-530.

Bahaj, A.S., 2011. Generating electricity from the oceans. Renew Sustain Energy Rev 15, 3399-3416.

Bakry, A.M., Abbas, S., Ali, B., Majeed, H., Abouelwafa, M.Y., Mousa, A., Liang, L., 2016. Microencapsulation of Oils: A Comprehensive Review of Benefits, Techniques, and Applications. Compr Rev Food Sci F 15, 143-182.

Ball, V., Del Frari, D., Toniazzo, V., Ruch, D., 2012. Kinetics of polydopamine film deposition as a function of pH and dopamine concentration: insights in the polydopamine deposition mechanism. J Colloid Interface Sci 386, 366-372.

Barbier, E., 2002. Geothermal energy technology and current status an overview. Renew Sustain Energy Rev 6, 3-65.

Barton, J.P., Infield, D.G., 2004. Energy storage and its use with intermittent renewable energy. IEEE T Energy Conver 19, 441-448.

Bengston, J., 2005. Stabilizer for electroless copper plating solution, C23C18/40 ed, US.

Berke, T.G., Shieh, S.C., 2012. Capsicum cultivars, Handbook of Herbs and Spices, pp. 116-130.

Bernsmann, F., Ball, V., Addiego, F., Ponche, A., Michel, M., Gracio, J.J., Toniazzo, V., Ruch, D., 2011. Dopamine-melanin film deposition depends on the used oxidant and buffer solution. Langmuir 27, 2819-2825.

Bile, J., Bolzinger, M.A., Vigne, C., Boyron, O., Valour, J.P., Fessi, H., Chevalier, Y., 2015. The parameters influencing the morphology of poly(varepsilon-caprolactone) microspheres and the resulting release of encapsulated drugs. Int J Pharm 494, 152-166.

Bruschi, M.L., 2015. 5 - Mathematical models of drug release, in: Bruschi, M.L. (Ed.), Strategies to Modify the Drug Release from Pharmaceutical Systems. Woodhead Publishing, pp. 63-86.

Buck, W., Rudtsch, S., 2011. Thermal Properties, in: Czichos, H., Saito, T., Smith, L. (Eds.), Springer Handbook of Metrology and Testing. Springer Berlin Heidelberg, Berlin, Heidelberg, pp. 453-483.

Carey, F.A., 2000. Aldehydes and Ketones: Nucleophilic Addition to the Carbonyl Group, in: Kane, K.T. (Ed.), Organic chemistry, 4th ed. The McGraw-Hill Companies, Inc, United States of America, pp. 654-700.

Carteau, D., Vallée-Réhel, K., Linossier, I., Quiniou, F., Davy, R., Compère, C., Delbury, M., Faÿ, F., 2014. Development of environmentally friendly antifouling paints using biodegradable polymer and lower toxic substances. Prog Org Coat 77, 485-493.

Champ, M.A., 2000. A review of organotin regulatory strategies, pending actions, related costs and benefits. Sci Total Environ 258, 21-71.

Cichewicz, R.H., Thorpe, P.A., 1996. The antimicrobial properties of chile peppers (Capsicum species) and their uses in Mayan medicine. J Ethnopharmacol 52, 61-70.

Collins, N.A., Flint, K., Ghosh, K., Goodrich, J.D., Islam, S.B., Seiler, B.D., Wilson, S.A., 2017. Cellulose Ester Materials with Tunable Degradation Characteristics. Eastman Chemical Company (Kingsport, TN, US), United States.

Cui, X., Hutt, D.A., Scurr, D.J., Conway, P.P., 2011. The Evolution of Pd⁄Sn Catalytic Surfaces in Electroless Copper Deposition. J Electrochem Soc 158.

Dafforn, K.A., Lewis, J.A., Johnston, E.L., 2011. Antifouling strategies: history and regulation, ecological impacts and mitigation. Mar Pollut Bull 62, 453-465.

Della Vecchia, N.F., Avolio, R., Alfè, M., Errico, M.E., Napolitano, A., d'Ischia, M., 2013. Building-Block Diversity in Polydopamine Underpins a Multifunctional Eumelanin-Type Platform Tunable Through a Quinone Control Point. Adv Funct Mater 23, 1331-1340.

Deng, L., Guo, W., Ngo, H.H., Zhang, H., Wang, J., Li, J., Xia, S., Wu, Y., 2016. Biofouling and control approaches in membrane bioreactors. Bioresour Technol 221, 656-665.

Dinderman, M.A., Dressick, W.J., Kostelansky, C.N., Price, R.R., Qadri, S.B., Schoen, P.E., 2006. Electroless Plating of Iron onto Cellulose Fibers. Chem Mater 18, 4361-4368.

Ding, P., Norton, I.T., Zhang, Z., Pacek, A.W., 2008. Mechanical properties of gelatin-rich micro-particles. J Food Eng 86, 307-314.

Dreyer, D.R., Miller, D.J., Freeman, B.D., Paul, D.R., Bielawski, C.W., 2012. Elucidating the structure of poly(dopamine). Langmuir 28, 6428-6435.

Du, M., Kalia, N., Frumento, G., Chen, F., Zhang, Z., 2017. Biomechanical properties of human T cells in the process of activation based on diametric compression by micromanipulation. Med Eng Phys 40, 20-27.

Du, M., Kavanagh, D., Kalia, N., Zhang, Z., 2019. Characterising the mechanical properties of haematopoietic and mesenchymal stem cells using micromanipulation and atomic force microscopy. Med Eng Phys https://doi.org/10.1016/j.medengphy.2019.07.013 (in press).

Freitas, S., Merkle, H.P., Gander, B., 2005. Microencapsulation by solvent extraction/evaporation: reviewing the state of the art of microsphere preparation process technology. J Control Release 102, 313-332.

Fu, Y., Kao, W.J., 2010. Drug release kinetics and transport mechanisms of non-degradable and degradable polymeric delivery systems. Expert Opin Drug Deliv 7, 429-444.

Fundueanu, G., Constantin, M., Esposito, E., Cortesi, R., Nastruzzi, C., Menegatti, E., 2005. Cellulose acetate butyrate microcapsules containing dextran ion-exchange resins as self-propelled drug release system. Biomaterials 26, 4337-4347.

Gindl, W., Keckes, J., 2004. Tensile properties of cellulose acetate butyrate composites reinforced with bacterial cellulose. Compos Sci Technol 64, 2407-2413.

Gittens, J.E., Smith, T.J., Suleiman, R., Akid, R., 2013. Current and emerging environmentally-friendly systems for fouling control in the marine environment. Biotechnol Adv 31, 1738-1753.

Gray, A., Egan, S., Bakalis, S., Zhang, Z., 2016. Determination of microcapsule physicochemical, structural, and mechanical properties. Particuology 24, 32-43.

Gudeczaukas, D., 2007. Electroless Plating. Ceramic Industry 157, 14-16.

Hong, S., Na, Y.S., Choi, S., Song, I.T., Kim, W.Y., Lee, H., 2012. Non-Covalent Self-Assembly and Covalent Polymerization Co-Contribute to Polydopamine Formation. Adv Funct Mater 22, 4711-4717.

Hu, J., Zhang, X., Qu, J., 2018. Investigation on the mechanical properties of polyurea (PU)/melamine formaldehyde (MF) microcapsules prepared with different chain extenders. J Microencapsul 35, 219-228.

Huang, X., Brazel, C.S., 2001. On the importance and mechanisms of burst release in matrix-controlled drug delivery systems. J Control Release 73, 121-136.

Huang, Y., Peng, Q., 2004. The Prevention Method and Research Development of Marine Fouling. Total Corrosion Control 18, 3-5.

Im, H.Y., Kim, J., Sah, H., 2010. Another paradigm in solvent extraction-based microencapsulation. Biomacromolecules 11, 776-786.

Jämsä, S., Mahlberg, R., Holopainen, U., Ropponen, J., Savolainen, A., Ritschkoff, A.C., 2013. Slow release of a biocidal agent from polymeric microcapsules for preventing biodeterioration. Prog Org Coat 76, 269-276.

Jamekhorshid, A., Sadrameli, S.M., Farid, M., 2014. A review of microencapsulation methods of phase change materials (PCMs) as a thermal energy storage (TES) medium. Renewable Sustainable Energy Rev 31, 531-542.

Jeffery, H., Davis, S.S., O'Hagan, D.T.J.P.R., 1993. The Preparation and Characterization of Poly(lactide-co-glycolide) Microparticles. II. The Entrapment of a Model Protein Using a (Water-in-Oil)-in-Water Emulsion Solvent Evaporation Technique. Pharm Res 10, 362-368.

Jeyanthi, R., Thanoo, B.C., Metha, R.C., Deluca, P.P., 1996. Effect of solvent removal technique on the matrix characteristics of polylactide/glycolide microspheres for peptide delivery. J Control Release 38, 235-244.

Jiang, J., Zhu, L., Zhu, L., Zhu, B., Xu, Y., 2011. Surface characteristics of a self-polymerized dopamine coating deposited on hydrophobic polymer films. Langmuir 27, 14180-14187.

Junyaprasert, V.B., Manwiwattanakul, G., 2008. Release profile comparison and stability of diltiazem-resin microcapsules in sustained release suspensions. Int J Pharm 352, 81-91.

Jyothi, N.V., Prasanna, P.M., Sakarkar, S.N., Prabha, K.S., Ramaiah, P.S., Srawan, G.Y., 2010. Microencapsulation techniques, factors influencing encapsulation efficiency. J Microencapsul 27, 187-197.

Kaushik, P., Dowling, K., Barrow, C.J., Adhikari, B., 2015. Microencapsulation of omega-3 fatty acids: A review of microencapsulation and characterization methods. J Funct Foods 19, 868-881.

Kempton, W., Firestone, J., Lilley, J., Rouleau, T., Whitaker, P., 2005. The Offshore Wind Power Debate: Views from Cape Cod. Coast Management 33, 119-149.

Kind, H., Bittner, A.M., Cavalleri, O., Kern, K., Greber, T., 1998. Electroless Deposition of Metal Nanoislands on Aminothiolate-Functionalized Au(111) Electrodes. J Phys Chem B 102, 7582-7589.

Kochkodan, V., Hilal, N., 2015. A comprehensive review on surface modified polymer membranes for biofouling mitigation. Desalination 356, 187-207.

Koleva, G.L., Maksimova, V., Serafimovska, D.M., Gulabovski, R., Ivanovska, J.E., 2013. The effect of different methods of extractions of capsaicin on its content in the capsicum oleoresins, Scientific Works: Food Science, Engineering and Technology, Plovdiv, pp. 18-19.

Kumanek, B., Janas, D., 2019. Thermal conductivity of carbon nanotube networks: a review. J Mater Sci 54, 7397-7427.

Lam, P.L., Gambari, R., 2014. Advanced progress of microencapsulation technologies: in vivo and in vitro models for studying oral and transdermal drug deliveries. J Control Release 178, 25-45.

Langer, R., 1990. New methods of drug delivery. Science 249, 1527.

Lee, C.-L., Wan, C.-C., Wang, Y.-Y., 2003. Pd Nanoparticles as a New Activator for Electroless Copper Deposition. J Electrochem Soc 150.

Lee, H., Dellatore, S.M., Miller, W.M., Messersmith, P.B., 2007. Mussel-Inspired Surface Chemistry for Multifunctional Coatings. Science 318, 426-430.

Lewis, P.R., 2016. Chapter 2 - Sample Examination and Analysis, in: Lewis, P.R. (Ed.), Forensic Polymer Engineering (Second Edition). Woodhead Publishing, pp. 33-69.

Li, J., Wang, G., Ding, C., Jiang, H., Wang, P., 2014. Synthesis and evaluation of polystyrene-polybutadiene-polystyrene-dodecafluoroheptyl methacrylate/polystyrene-polybutadiene-polystyrene hybrid antifouling coating. J Colloid Interface Sci 434, 71-76.

Li, M., Rouaud, O., Poncelet, D., 2008. Microencapsulation by solvent evaporation: state of the art for process engineering approaches. Int J Pharm 363, 26-39.

Liebscher, J., Mrowczynski, R., Scheidt, H.A., Filip, C., Hadade, N.D., Turcu, R., Bende, A., Beck, S., 2013. Structure of polydopamine: a never-ending story? Langmuir 29, 10539-10548.

Liu, K., Wei, W.Z., Zeng, J.X., Liu, X.Y., Gao, Y.P., 2006. Application of a novel electrosynthesized polydopamine-imprinted film to the capacitive sensing of nicotine. Anal Bioanal Chem 385, 724-729.

Liu, M., 2010. Understanding the mechanical strength of microcapsules and their adhesion on fabric surface. The University of Birmingham, UK.

Liu, P.S., Chen, G.F., 2014. Chapter Ten - Characterization Methods: Physical Properties, in: Liu, P.S., Chen, G.F. (Eds.), Porous Materials. Butterworth-Heinemann, Boston, pp. 493-532.

Liu, Y., Ai, K., Lu, L., 2014. Polydopamine and its derivative materials: synthesis and promising applications in energy, environmental, and biomedical fields. Chem Rev 114, 5057-5115.

Long, Y., York, D., Zhang, Z., Preece, J.A., 2009. Microcapsules with low content of formaldehyde: preparation and characterization. J Mater Chem 19, 6882- 6887.

Ma, C., Yang, H., Zhou, X., Wu, B., Zhang, G., 2012. Polymeric material for anti-biofouling. Colloids Surf B Biointerfaces 100, 31-35.

Mercade-Prieto, R., Zhang, Z., 2012. Mechanical characterization of microspheres - capsules, cells and beads: a review. J Microencapsul 29, 277-285.

Miladi, K., Ibraheem, D., Iqbal, M., Sfar, S., Fessi, H., Elaissari, A., 2014. Particles from preformed polymers as carriers for drug delivery. EXCLI Journal 13, 28-57.

Mondin, G., Lohe, M.R., Wisser, F.M., Grothe, J., Mohamed-Noriega, N., Leifert, A., Dörfler, S., Bachmatiuk, A., Rümmeli, M.H., Kaskel, S., 2013. Electroless copper deposition on (3-mercaptopropyl)triethoxysilane-coated silica and alumina nanoparticles. Electrochimica Acta 114, 521-526.

Muller, E., Chung, J.T., Zhang, Z., Sprauer, A., 2005. Characterization of the mechanical properties of polymeric chromatographic particles by micromanipulation. J Chromatogr A 1097, 116-123.

Nguyen, V.B., Wang, C.X., Thomas, C.R., Zhang, Z., 2009. Mechanical properties of single alginate microspheres determined by microcompression and finite element modelling. Chem Eng Sci 64, 821-829.

Olsen, S.M., Kristensen, J.B., Laursen, B.S., Pedersen, L.T., Dam-Johansen, K., Kiil, S., 2010. Antifouling effect of hydrogen peroxide release from enzymatic marine coatings: Exposure testing under equatorial and Mediterranean conditions. Prog Org Coat 68, 248-257.

Pal, Y., Deb, P.K., Bandopadhyay, S., Bandyopadhyay, N., Tekade, R.K., 2018. Chapter 3 - Role of Physicochemical Parameters on Drug Absorption and Their Implications in Pharmaceutical Product Development, in: Tekade, R.K. (Ed.), Dosage Form Design Considerations. Academic Press, pp. 85-116.

Pan, X., Mercadé-Prieto, R., York, D., Preece, J.A., Zhang, Z., 2013. Structure and Mechanical Properties of Consumer-Friendly PMMA Microcapsules. Ind Eng Chem Res 52, 11253-11265.

Parker, W.J., Jenkins, R.J., Butler, C.P., Abbott, G.L., 1961. Flash Method of Determining Thermal Diffusivity, Heat Capacity, and Thermal Conductivity. J Appl Phys 32, 1679-1684.

Peppas, N.A., Narasimhan, B., 2014. Mathematical models in drug delivery: how modeling has shaped the way we design new drug delivery systems. J Control Release 190, 75-81.

Perkampus, H.-H., 1992. Principles, UV-VIS Spectroscopy and Its Applications. Springer Berlin Heidelberg, Berlin, Heidelberg, pp. 3-9.

Ranjha, N.M., Khan, I.U., Naseem, S., 2009. Encapsulation and characterization of flurbiprofen loaded poly(ϵ-caprolactone)–poly(vinylpyrrolidone) blend micropheres by solvent evaporation method. J Solgel Sci Technol 50, 281-289.

Rathore, S., Desai, P.M., Liew, C.V., Chan, L.W., Heng, P.W.S., 2013. Microencapsulation of microbial cells. J Food Eng 116, 369-381.

Ritger, P.L., Peppas, N.A., 1987. A simple equation for description of solute release I. Fickian and non-fickian release from non-swellable devices in the form of slabs, spheres, cylinders or discs. J Control Release 5, 23-36.

Rosca, I.D., Watari, F., Uo, M., 2004. Microparticle formation and its mechanism in single and double emulsion solvent evaporation. J Control Release 99, 271-280.

Roylance, D., 2008. Mechanical Properties of Materials. Massachusetts Institute of Technology.

Ruoho, M., Valset, K., Finstad, T., Tittonen, I., 2015. Measurement of thin film thermal conductivity using the laser flash method. Nanotechnology 26, 195706.

Scoville, W.L., 1912. Note on Capsicums. J Am Pharm Assoc 1, 453-454.

Shacham-Diamand, Y., Dubin, V.M., 1997. Copper electroless deposition technology for ultra-large-scale-integration (ULSI) metallization. Microelectron Eng 33, 47-58.

Shardor, S.A., 2013. An overview: Matrix tablets as sustained release.

Sharma, A., Cheon, C.-S., Jung, J.P., 2016. Recent Progress in Electroless Plating of Copper. J Microelectron Packag Soc 23, 1-6.

Sharma, R., Agarwala, R.C., Agarwala, V., 2006. Development of copper coatings on ceramic powder by electroless technique. Appl Surf Sci 252, 8487-8493.

Sherif, S.A., Barbir, F., Veziroglu, T.N., 2005. Wind energy and the hydrogen economy—review of the technology. Sol Energy 78, 647-660.

Shi, H., Wang, L., 2006. Nontoxic Marine Anti-fouling Coating Containing Capsaicin. Marine Science Bulletin 8, 92-96.

Siepmann, J., Peppas, N.A., 2011. Higuchi equation: derivation, applications, use and misuse. Int J Pharm 418, 6-12.

Siepmann, J., Siepmann, F., 2013. Mathematical modeling of drug dissolution. Int J Pharm 453, 12-24.

Singh, N., Turner, A., 2009. Leaching of copper and zinc from spent antifouling paint particles. Environ Pollut 157, 371-376.

Sun, G., Zhang, Z., 2001. Mechanical properties of melamine-formaldehyde microcapsules. J Microencapsul 18, 593-602.

Tachibana, Y., Giang, N.T.T., Ninomiya, F., Funabashi, M., Kunioka, M., 2010. Cellulose acetate butyrate as multifunctional additive for poly(butylene succinate) by melt blending: Mechanical properties, biomass carbon ratio, and control of biodegradability. Polym Degrad Stabil 95, 1406-1413.

Tan, Y., Deng, W., Li, Y., Huang, Z., Meng, Y., Xie, Q., Ma, M., Yao, S., 2010. Polymeric Bionanocomposite Cast Thin Films with In Situ Laccase-Catalyzed Polymerization of Dopamine for Biosensing and Biofuel Cell Applications. J Phy Chem B 114, 5016-5024.

Tatara, Y., 1991. On Compression of Rubber Elastic Sphere Over a Large Range of Displacements—Part 1: Theoretical Study. J Eng Mater Technol 113, 285-291.

Tsuneyoshi, T., Ono, T., 2017. Metal-coated microcapsules with tunable magnetic properties synthesized via electroless plating. Mater Sci Eng B 222, 49-54.

Turgud, C., Newby, B.-m., Cutright, T.J., 2004. Determination of optimal water solubility of capsaicin for its usage as a non-toxic antifoulant. Environ Sci & Pollut Res 11, 7-10.

Varshneya, A.K., Mauro, J.C., 2019a. Chapter 11 - Heat capacity of glass, in: Varshneya, A.K., Mauro, J.C. (Eds.), Fundamentals of Inorganic Glasses (Third Edition). Elsevier, pp. 273-281.

Varshneya, A.K., Mauro, J.C., 2019b. Chapter 12 - Thermal conductivity and acoustic properties of glass, in: Varshneya, A.K., Mauro, J.C. (Eds.), Fundamentals of Inorganic Glasses (Third Edition). Elsevier, pp. 283-291.

Vengatesan, M.R., Varghese, A.M., Mittal, V., 2018. Thermal properties of thermoset polymers, Thermosets, pp. 69-114.

Wallick, D., 2014. Cellulose Polymers in Microencapsulation of Food Additives, Microencapsulation in the Food Industry, US, pp. 181-193.

Wang, B., Tang, Q., Hong, N., Song, L., Wang, L., Shi, Y., Hu, Y., 2011a. Effect of cellulose acetate butyrate microencapsulated ammonium polyphosphate on the flame retardancy,

mechanical, electrical, and thermal properties of intumescent flame-retardant ethylene-vinyl acetate copolymer/microencapsulated ammonium polyphosphate/polyamide-6 blends. ACS Appl Mater Interfaces 3, 3754-3761.

Wang, C.X., Cowen, C., Zhang, Z., Thomas, C.R., 2005. High-speed compression of single alginate microspheres. Chem Eng Sci 60, 6649-6657.

Wang, J., Dong, X., Chen, S., Lou, J., 2013. Microencapsulation of capsaicin by solvent evaporation method and thermal stability study of microcapsules. Colloid J 75, 26-33.

Wang, J., Shi, T., Yang, X., Han, W., Zhou, Y., 2014. Environmental risk assessment on capsaicin used as active substance for antifouling system on ships. Chemosphere 104, 85-90.

Wang, W., Jiang, Y., Liao, Y., Tian, M., Zou, H., Zhang, L., 2011b. Fabrication of silver-coated silica microspheres through mussel-inspired surface functionalization. J Colloid Interface Sci 358, 567-574.

Wang, W., Jiang, Y., Wen, S., Liu, L., Zhang, L., 2012. Preparation and characterization of polystyrene/Ag core-shell microspheres--a bio-inspired poly(dopamine) approach. J Colloid Interface Sci 368, 241-249.

Watts, J.L., 1995. Anti-fouling coating composition containing capsaicin, US.

Wei, X., Roper, D.K., 2014. Tin Sensitization for Electroless Plating Review. J Electrochem Soc 161, D235-D242.

Weisman, G.R., Sundberg, D.C., Cimini, R.A., Brown, M.G., Beno, B.R., Eighmy, T.T., 1992. Controlled release antifouling coatings. I. approaches for controlled release of 2,4-dinitrophenolate and benzoate into seawater. Biofouling 6, 123-146.

Wilde, P.J., 2009. 21 - Emulsions and nanoemulsions using dairy ingredients, in: Corredig, M. (Ed.), Dairy-Derived Ingredients. Woodhead Publishing, pp. 539-564.

Wu, C., Zhang, G., Xia, T., Li, Z., Zhao, K., Deng, Z., Guo, D., Peng, B., 2015. Bioinspired synthesis of polydopamine/Ag nanocomposite particles with antibacterial activities. Mater Sci Eng C Mater Biol Appl 55, 155-165.

Xing, C., Wang, H., Hu, Q., Xu, F., Cao, X., You, J., Li, Y., 2013. Mechanical and thermal properties of eco-friendly poly(propylene carbonate)/cellulose acetate butyrate blends. Carbohydr Polym 92, 1921-1927.

Xu, C., Wu, G., Liu, Z., Wu, D., Meek, T.T., Han, Q., 2004. Preparation of copper nanoparticles on carbon nanotubes by electroless plating method. Mater Res Bull 39, 1499-1505.

Xu, J., Feng, X., Hou, J., Wang, X., Shan, B., Yu, L., Gao, C., 2013. Preparation and characterization of a novel polysulfone UF membrane using a copolymer with capsaicin-mimic moieties for improved anti-fouling properties. J Membrane Sci 446, 171-180.

Yan, Y., Zhang, Z., Stokes, J.R., Zhou, Q.-Z., Ma, G.-H., Adams, M.J., 2009. Mechanical characterization of agarose micro-particles with a narrow size distribution. Powder Technol 192, 122-130.

Yang, Y.-Y., Chung, T.-S., Bai, X.-L., Chan, W.-K., 2000. Effect of preparation conditions on morphology and release profiles of biodegradable polymeric microspheres containing protein fabricated by double-emulsion method. Chem Eng Sci 55, 2223-2236.

Yang, Y.-Y., Chung, T.-S., Ng, N.P., 2001. Morphology, drug distribution, and in vitro release profiles of biodegradable polymeric microspheres containing protein fabricated by double-emulsion solvent extraction evaporation method. Biomaterials 22, 231-241.

Yebra, D.M., Kiil, S., Dam-Johansen, K., 2004. Antifouling technology—past, present and future steps towards efficient and environmentally friendly antifouling coatings. Prog Org Coat 50, 75-104.

Zhang, Z., 1999. Mechanical strength of single microcapsules determined by a novel micromanipulation technique. J Microencapsul 16, 117-124.

Zhang, Z., Ferenczi, M.A., Lush, A.C., Thomas, C.R., 1991. A novel micromanipulation technique for measuring the bursting strength of single mammalian cells. Appl Microbiol Biotechnol 36, 208-210.

Zhang, Z.L., Kristiansen, H., Liu, J., 2007. A method for determining elastic properties of micron-sized polymer particles by using flat punch test. Comput Mater Sci 39, 305-314.

Zhou, P., Deng, Y., Lyu, B., Zhang, R., Zhang, H., Ma, H., Lyu, Y., Wei, S., 2014. Rapidly-deposited polydopamine coating via high temperature and vigorous stirring: formation, characterization and biofunctional evaluation. PLoS One 9, e113087.

Zhou, S.-w., Yang, C.-y., Xia, C.-h., 2011. The Prevention of Marine Fouling Organisms by Natural Antifoulants: a Review. Natural Product Research and Development 23, 186-192, 197.

Zhou, X., Mao, J., Qiao, Z., 2016. Electroless plating of copper layer on surfaces of urea–formaldehyde microcapsule particles containing paraffin for low infrared emissivity. Particuology 24, 159-163.

Zhu, Y., Zhang, J., Zheng, Q., Wang, M., Deng, W., Li, Q., Firempong, C.K., Wang, S., Tong, S., Xu, X., Yu, J., 2015. In vitro and in vivo evaluation of capsaicin-loaded microemulsion for enhanced oral bioavailability. J Sci Food Agric 95, 2678-2685.

Zuidam, N., Shimoni, E., 2010. Overview of Microencapsulates for Use in Food Products or Processes and Methods to Make Them, Encapsulation Technologies for Active Food Ingredients and Food Processing. Springer-Verlag, New York, pp. 3-29.